Self-Assembly and Gelation Behaviour of Pyridyl Urea Complexes

BYRNE, PETER

Self-Assembly and Gelation Behaviour of Pyridyl Urea Complexes

Peter Byrne

Submitted for the degree of Doctor of Philosophy

December 2009

Abstract

Bis(3-pyridyl)ureas with ethylene, propylene, butylene, phenylene and napthylene spacer groups were synthesised by the reaction of 3-isocyanato-pyridine, prepared *in situ* from nicotinoyl azide, with the appropriate diamine. Each ligand was crystallised and their structures were solved using X-ray crystallography. The urea groups of the napthylene-spaced ligand adopt a bifurcated hydrogen-bonding mode, thereby forming an α-tape whereas in the the propylene-, butylene- and phenylene-spaced ligands, every other bifurcated interaction is replaced with a NH$\cdots$O$_{\text{urea}}$ and a NH$\cdots$N$_{\text{pyridyl}}$, caused by the presence of a single competing intramolecular CH$\cdots$O$_{\text{urea}}$ set-up by the electron-withdrawing pyridyl nitrogen. With the ethylene-spaced urea, the bifurcated hydrogen-bonding motif is absent. These differences in the intermolecular bonding may be only be due to the packing requirements of the spacer group: as these interactions become stronger, either by greater van der Waals attraction in a longer oliomethylene chain or the greater π-π stacking interactions of the napthylene ring, adjacent urea groups become closer and bind preferentially to form the bifurcated interaction.

The bis(3-pyridyl)ureas were subsequently tested for their ability to form gels, and in some cases, crystallised in the presence of selected silver(I) salts. Compound **2.1** formed five pseudo-polymorphs of a Borromean-type structure upon slow crystallisation in various solvent mixtures with silver(I) nitrate. Within each structure, there are layers made up of paired Borromean weaves and the mechanism by which these layers stack, though unclear, must ultimately be driven by the interactions of the solvent molecules incorporated into the structures. When the counteranion in the crystallisation was replaced by either acetate, tetrafluoroborate or hexafluorophosphate, several coordination polymers were synthesised but the Borromean structure was not reproduced. A similar dependency on counteranion was observed with *N,N″*-pentylene-1,5-diylbis(*N′*-pyridin-3-ylurea) which was similarly crystallised with silver(I) nitrate, acetate and tetrafluoroborate. In the presence of the latter, a quintuple helix formed.

Several bis(3-pyridylureas) with ethylene, pyridine, methylenebisphenylene and cyclohexylene spacer groups were shown to form gels and crystals in the presence of silver(I) nitrate. Two macrocyclic structures were grown from gel states which may be further indication as to how the same molecules aggregate in the gel fibres with silver(I) nitrate promoting aggregation of the molecules along one direction.

Self-Assembly and Gelation Behaviour of Pyridyl Urea Complexes

Peter Byrne

A Thesis presented for the degree of
Doctor of Philosophy

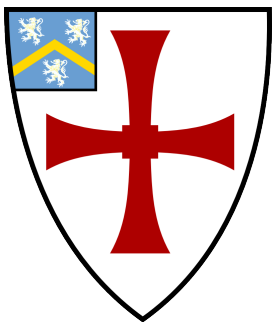

Inorganic Supramolecular Chemistry Group
Department of Chemistry
University of Durham
England

December 2009

Contents

List of Figures

List of Schemes

Abbreviations

br (NMR,IR)	broad
d (NMR)	doublet
dd (NMR)	doublet of doublets
dt (NMR)	doublet of triplets
DMF	*N,N*-dimethylformamide
DMSO	Dimethyl sulfoxide
DNA	Deoxyribonucleic acid
EI	Electron ionisation
FT-IR	Fourier Transform Infra-Red
M.p.	Melting point
MeCN	Acetonitrile
MS	Mass Spectrometry
NMR	Nuclear Magnetic Resonance
OH	Hydroxyl
T_{gel}	Gel to solution transition temperature
TEM	Transmission Electron Microscopy
TGA	Thermogravimetric analysis
THF	Tetrahydrofuran
UV	Ultra-violet
w/v	Weight / Volume
Z'	The number of molecules per asymmetric unit

Declaration

The work in this thesis is based on research carried out within the Inorganic Supramolecular Chemistry Group, the Department of Chemistry, the University of Durham, England. No part of this thesis has been submitted elsewhere for any other degree or qualification and is all my own work unless referenced to the contrary in the text.

Acknowledgements

I could not have completed or indeed started this project without the support and inspiration from countless individuals; I thank you all and I shall be forever grateful.

More specifically, for both offering me the opportunity to work on, and his support both during and after a project that gave so many interesting results, I thank Prof. Jonathan Steed. I also thank Dr Nigel Clarke for his support and helpful discussions. My thanks also go to the departmental staff who maintained the analytical services so necessary for my work and in particular, Jaroslava Dostal and Judith Magee.

On a more personal note, I thank my group colleagues for their friendship and support, in particular Naseem Qureshi and Laura Soriano without whom the late nights and weekends would have been a much lonelier experience. I thank Gareth Lloyd for his enthusiasm in determining the structures of the compounds that crystalised, including those of a dubious quality.

Outside the group and in college, I thank all those who offered me their friendship, especially Amjad Abu-El-Ezz, Amr Gaber, Angie Chen, Anne Soleilhavoup, Bader Obeidat, Damian Moxham, Daniel Tomé, Diana Abu-Ghunmi, Elizabeth New, Guy Siviour, Jamie Carlstone, Javier Velasquez, Justin Orenstein, Karel Aelvoet, Linda Hui Yang, Liz Ellis, Meghan Glass, Milena Trmčić, Mohammad Tayeh, Sabrina Lam, Samantha Highsmith, Una McGahern, Zilia Iskoujina and Zu'bi Al-Zu'bi. I wish you all a long life and success.

I also thank Prudence Knight and Dr Helen Aspinall for both their support and encouragement.

Finally, I thank my parents and my brother for their continuous support.

Dedicated to

my grandparents

Chapter 1

Introduction

1.1 Background

The investigation of gelators and the gels they form has been proceeding for over one hundred years. In the 1860s, Graham reported that certain substances such as hydrated alumina, hydrated silicic acid and gelatin formed gelatinous hydrates and had an inability to crystallise. By making use of their 'low diffusibility' he proposed that they could be used as another way of performing a separation experiment and designed an apparatus to perform this task: the dialyser was a precursor of the modern dialysis machine.[1,2] Since these initial investigations, knowledge of the structural requirements for a molecule to be a gelator, the understanding of how molecules aggregate and gel chemistry has advanced significantly. Jordan Lloyd said that the gel state is easier to recognize than define[3] but in 1974, Flory proposed that for a system to be regarded as a gel, it must both behave rheologically like a solid and possess a continuous, macroscopic structure, sufficiently permanent to be analysed.[4] Both of these requirements are met by the jelly dessert, the essential ingredient of which is gelatin, derived from collagen found in animal hide and bones. Jellies are prepared by dissolving powdered gelatin in hot water and allowing the solution to cool; the mixture steadily becomes more viscous until eventually it can be inverted in its container and not fall out. Ideally, gelatin in the solid state would exist in a triple helix conformation with three polypeptide chains coiled around each

other, held in place by hydrogen-bonding between the amino acid groups, much like DNA. In forming the gel, these three polypeptides separate when the solution is hot and as it cools, they come together again and the triple helix starts to reform. In the rewinding, previously unconnected helices intertwine and a web of polypeptide chains forms. This polypeptide web traps the water by surface tension, solidifying it and giving the jelly its characteristic solid-like elasticity or 'wobble'.[5]

Gelatin is an example of a high molecular weight gelator where the individual monomer units, in this case the peptides, are bonded covalently to each other forming long polymer chains. These chains can then eventually form a fibrous network by cross-linking and gelling the liquid. Alongside high molecular weight gelators are low molecular weights gelators in which the 'monomers' aggregate into chains *via* interactions which are non-covalent, such as π-π stacking and hydrogen-bonding. These weak interactions which are very dependent on molecular structure, are easily overcome at high temperature: the so-called sol-gel transition temperature. However, if one could bring about a molecular change, such as in conformation, then one would have a gel in that, in addition to showing a reversible gel to sol transition, could show electro-, mechano-, sono- and chemo-responsiveness and examples of these multi-responsive gels have already been developed.[6–26]

1.2 Gelators

Within supramolecular chemistry, low molecular weight gelators is an area of research which has been extensively reviewed.[7,27–33] The structural diversity of molecules which are known to form gels is wide, shown by the examples in Figure 1.1 and those discussed in this chapter. While this project focuses on the design of those which include a 3-pyridyl-urea motif, a general overview of the subject may prove useful.

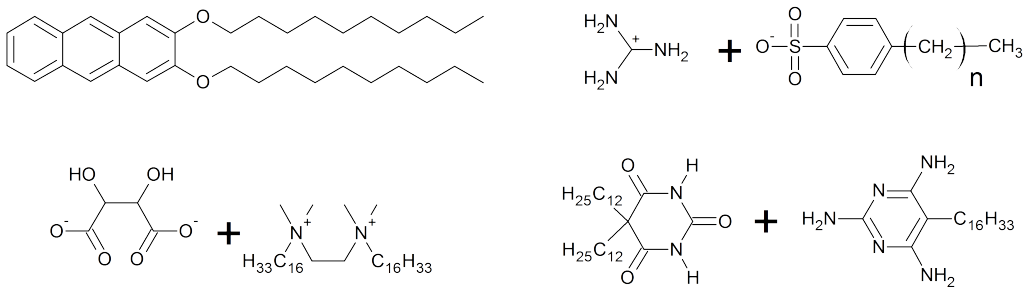

Figure 1.1: A selection of molecules known to act as gelators. [27]

1.2.1 Sugars

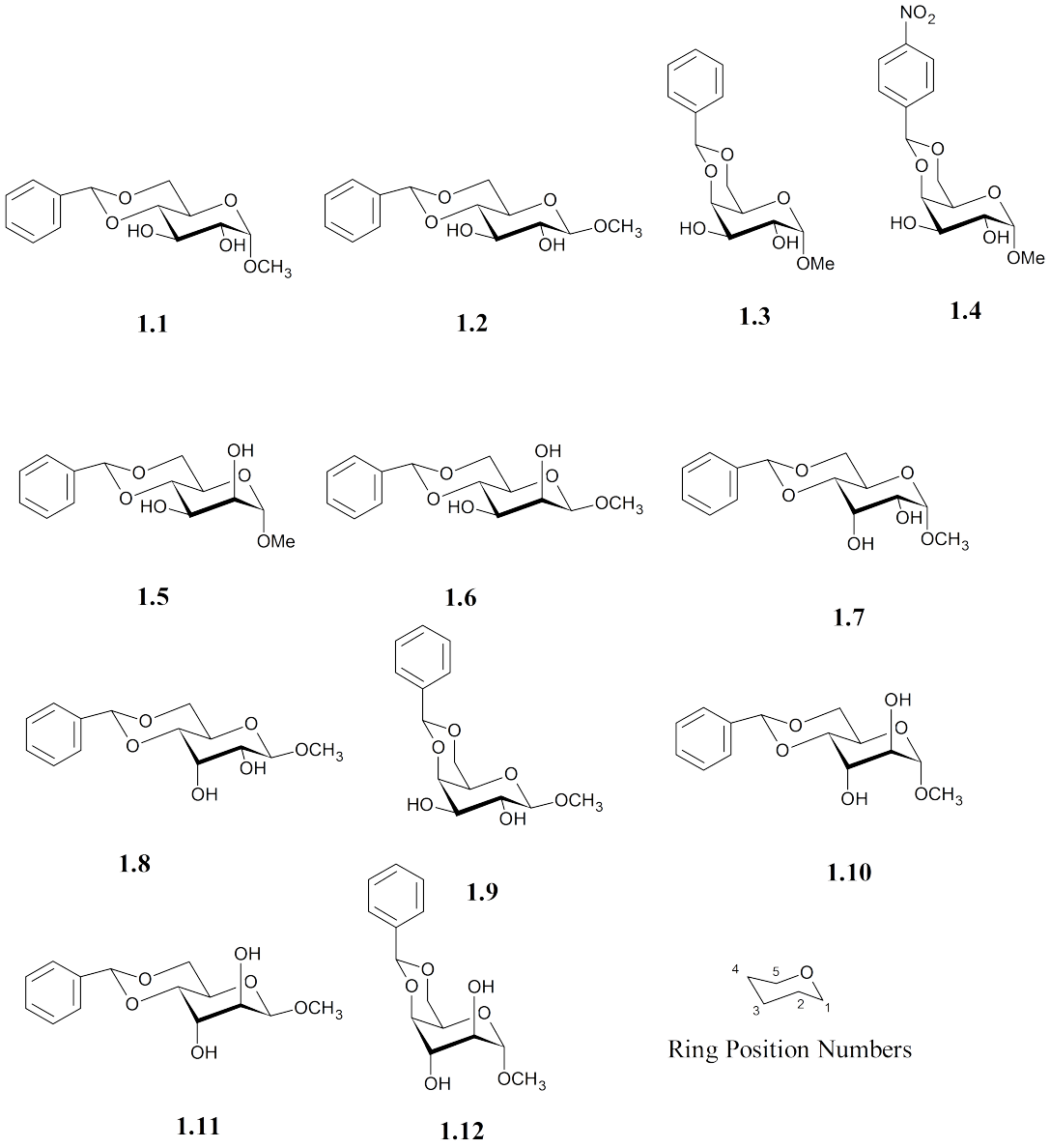

The gelling ability of a set of sugar derivatives has been studied.[34–39] Compounds **1.1**, **1.5**, **1.6**, **1.3** and **1.9** all show gelation ability in a variety of solvents as opposed to the rest in the set, which do not. Among the α-isomers, **1.3** is able to gel the widest range of solvents, followed by **1.5** and then **1.1**: all three are able to gel toluene, *p*-xylene diphenyl ether whilst **1.3** can also gel, amongst others, *n*-hexane, cyclohexane, carbon tetrachloride, carbon disulfide *n*-octanol and triethylamine. Between the β-isomer gelators, **1.9** can gel the widest range, including nitrobenzene, ethyl formate and methylcyclohexane. The mode of aggregation in the gel state is evidenced by variable temperature FT-IR spectroscopy and X-ray crystallography. In the solid state, the IR spectra of the sugars do not show a free OH peak due to intra- and inter-molecular hydrogen-bonding interactions. In the gel state however, the signals are broader and peaks corresponding to the OH appear in two groups between 3220–3475 cm^{-1} and 3573–3588 cm^{-1} which can be assigned to the hydrogen-bonding and free OH groups, respectively. As the temperature of the sample is increased and passes through the gel-sol transition temperature, the peak intensity ratio of hydrogen-bonded OH to free OH abruptly decreases, showing that the network is stabilised by intermolecular hydrogen-bonding. Several of the sugars have been crystallised,[40] including compound **1.1** which formed crystals in ethyl acetate. In the solid state, **1.1** forms one-dimensional zig-zag chains between the OH groups at positions 2 and 3 of the pyranose ring, compared to the non-gelating **1.12** whose hydroxyl groups both take part in intramolecular hydrogen-bonds and therefore there is no significant intermolecular hydrogen-bonds in the crystal.

1.2.2 Steroids

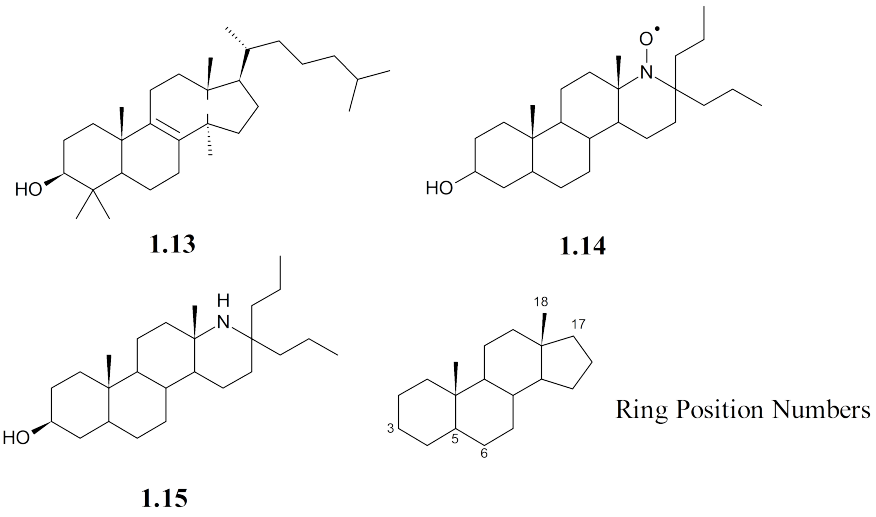

1.13 **1.14** **1.15**

Several steroids and selected derivatives have been shown to act as gelators,[41] among these is dihydrolanosterol (**1.13**) which forms gels at concentrations between 1 and 10 wt % in various mineral oils. Both compounds **1.14** and **1.15** form gels in non-polar, non-aromatic hydrocarbons.[42] A hydroxyl group at position C_3 and an amine or nitroxide free radical functionality at the C_{18} position both work to enhance the gelling ability. The position of a double bond in the molecule can have a detrimental effect depending on where it is placed: replacing the propyl groups with allyl groups at position C_{17} works to inhibit gelation, while a double bond at $C_{5,6}$ does not.[32]

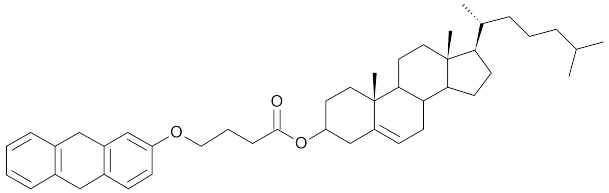

1.16

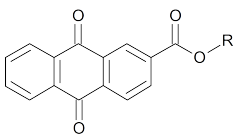

1.17

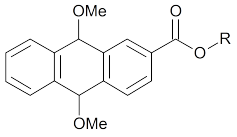

1.18

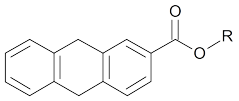

1.19

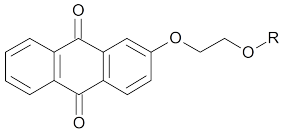

1.20

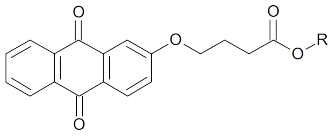

1.21

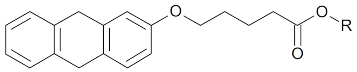

1.22

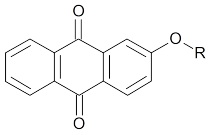

1.23

R = 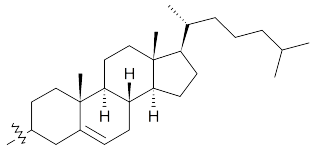

After compound **1.16** was shown to be a versatile gelator,[43] many derivatives including **1.17**–**1.23** have been synthesised to investigate the relationship between the molecular structure and the gelation ability.[28,44,45] This series of compounds again show that small changes in structure can have a profound effect on the bulk properties in solution. Compound **1.17** is a gelator whilst its more electron rich and more sterically hindered counterpart **1.18** is not. It is presumed that the increase in steric bulk leads to less π-π stacking of the aromatic moiety.[28] Changing the 2-anthryl moiety in **1.19** to phenanthyl, pyrenyl and 9-anthryl results in the loss of gelation[46] as does replacing the aromatic moiety in **1.16** with naphthyl or phenyl presumably again due to less π-π stacking interactions.[45]

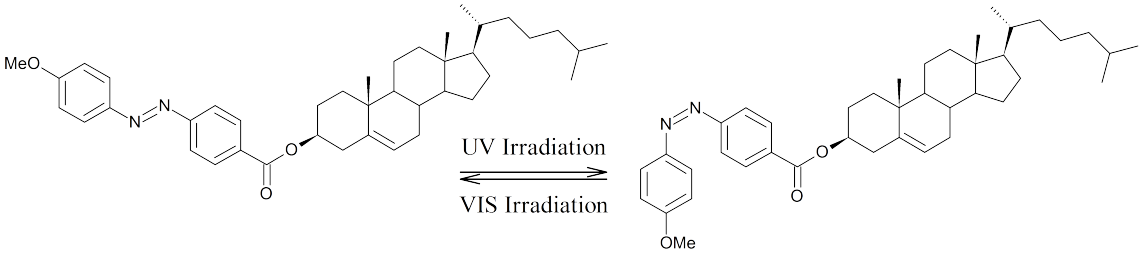

1.24

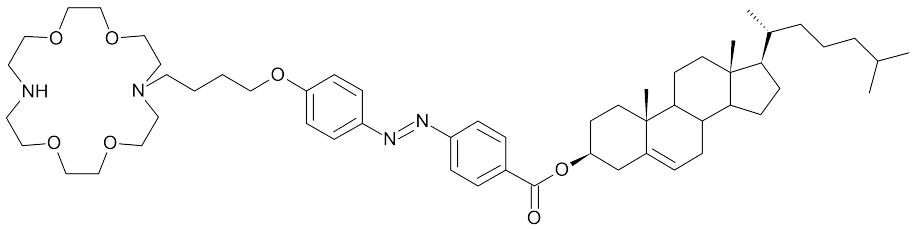

1.25

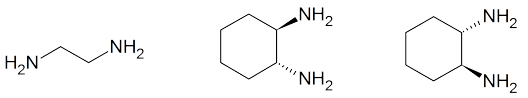

1.26 **1.27** **1.28**

Several ALS (Aromatic-Linker-Steroid) compounds with an azobenzene moiety have been shown to act as gelators.[14] Compound **1.24** gels various solvents including 1-butanol. By switching between the gelating *trans* and non-gelating *cis* forms, the gel can be induced to flow by ultraviolet irradiation and then re-solidified by visible light irradiation.[47] Gels of compound **1.25** are stabilised by the presence of diamines **1.26**, **1.27**, or **1.28**: on the addition of **1.28** to a 1-hexanol gel of **1.25**, the T_{gel} increases when [**1.28**]/[**1.25**] < 0.5, rising to a maximum at [**1.28**]/[**1.25**] $= 0.5$ and decreasing past [**1.28**]/[**1.25**] > 0.5. The diamine may stabilise the gel state by acting as a bridge between two stacked azacrown rings through intermolecular hydrogen-bonds.[14,48]

1.2.3 Peptides

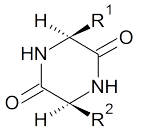

1.29

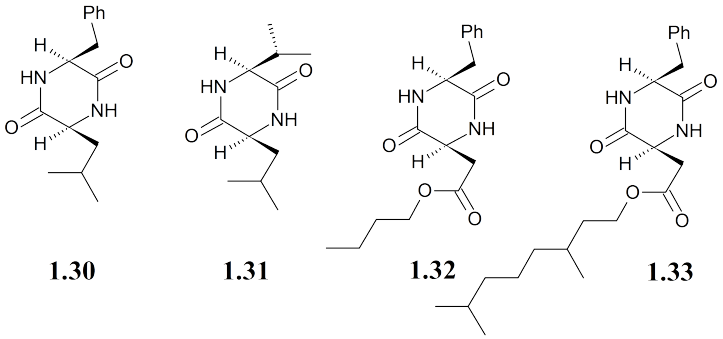

1.30 **1.31** **1.32** **1.33**

There are several examples of amino acid-based organogelators.[49,50] A series of cyclic dipeptides based on compound **1.29** has been synthesised with various groups attached and their gelating ability investigated.[51–53] Compounds **1.30**–**1.33** are those that form gels.

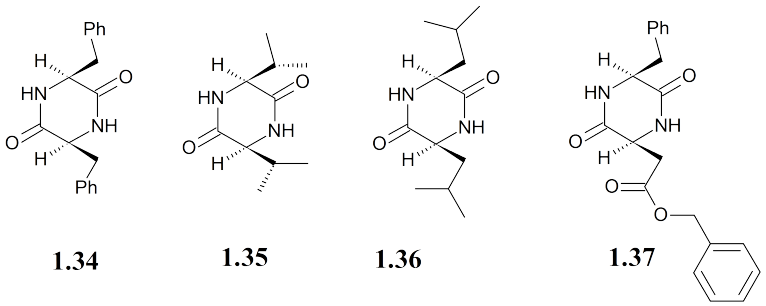

1.34 **1.35** **1.36** **1.37**

For comparison, compounds **1.34**–**1.37** do not form gels. Cyclodipeptide **1.29** (when R = H) gels nitrobenzene, chlorobenzene and methoxybenzene; crystallizes in ethanol and chloroform; is insoluble in acetone and ethyl acetate, and forms a high viscosity fluid in toluene and benzene. When R = $CH_2CH_2CH_2CHMe_2$, the behaviour changes drastically: gels are formed in ethanol, acetone, ethyl acetate and benzene, but crystallization is observed in methoxybenzene and nitrobenzene. Comparing **1.31**, **1.34** and **1.35**, the symmetry of the molecule must be an important factor in determining if it will gel: out of the nine gelators reported, none have R^1 =

R^2. Introduction of a branched chain to produce **1.33** improved the gelling ability inhibiting crystallization. FT-IR spectroscopy of a chloroform gel of **1.31** shows two peaks that correspond to the N–H and C=O stretching vibrations as 3320 and 1640 cm^{-1} respectively, but below the minimum concentration of gelator required to form the gel, these vibrations appear at 3400 and 1690 cm^{-1}. A weakening of these bonds in the gelled state indicates that aggregation may take place by hydrogen-bonding between the N–H and C=O of adjacent cyclodipeptides.

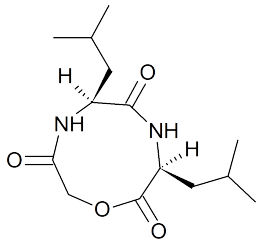

1.38

Compound **1.38** forms gels in a range of polar and non-polar solvents.[54] When the solubilising $–CH_2CHMe_2$ groups are replaced by hydrogen atoms, the compound is no longer a gelator. In order for compound **1.38** to form gels, it is first dissolved in either a drop of methanol or DMSO to bring it into solution and then the solvent under investigation is added using a Pasteur pipette. Without a drop of methanol, **1.38** fails to dissolve in acetone alone even if heated or sonicated. On the addition of the solvent, virtually instantaneous gelation is observed. There appears to be no obvious correlation between solvents in which **1.38** forms and does not form a gels: gels are formed in acetone, but not the slightly larger butan-2-one; if gelation were purely dependent on the size of the solvent, then ethyl acetate should not be gelled, but it is. The solvents' polarities also show no correlation as the dielectric constants of acetone and butan-2-one are quite similar.

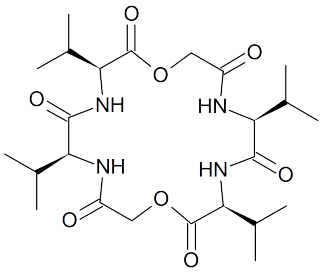

1.38

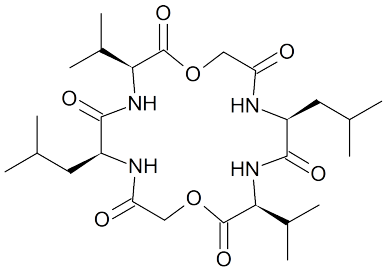

1.39

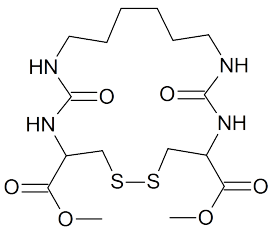

1.40

A larger compound, **1.38** has also been synthesised[54] and found to be a good gelator of water, if first dissolved in a drop of DMSO. The structurally very similar **1.39** shows no gelation ability in any solvent. Large cyclodipeptides such as **1.40** have been synthesised and characterised using X-ray crystallography. In the solid state, the eighteen member rings are stacked to form tubes that are open-ended and hollow extending to infinity and held together by four hydrogen-bonds between pairs of molecules. The tubes are then held together by hydrophobic interactions.[55]

1.2.4 Ureas

The molecules that will be investigated in this project all contain two urea groups. More specific gelators which are appended with pyridyl groups will be discussed in chapter 5 but this section will introduce ureas, bis-ureas and aryl ureas. Like amino acids, ureas aggregate by hydrogen-bonding, but are also capable of binding anions in addition to gelling.[56]

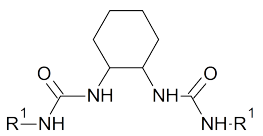

1.41 (*S,S*) $R^1 = -(CH_2)_{11}CH_3$

1.42 (*R,R*) $R^1 = -(CH_2)_{11}CH_3$

1.43 (*R,R*) $R^1 = -CH(CH_2CH_3)(CH_2)_3CH_3$

1.44 (*R,R*) $R^1 =$ 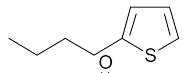

1.45 (*R,R*) $R^1 =$ 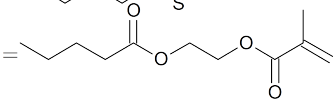

1.46 (*R,S*) $R^1 = -(CH_2)_{11}CH_3$

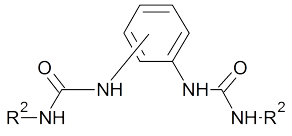

1.47 *ortho* $R^2 = -(CH_2)_{11}CH_3$

1.48 *ortho* $R^2 =$ 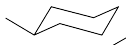

1.49 *ortho* $R^2 =$ 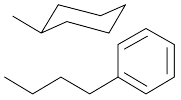

1.50 *ortho* $R^2 =$ 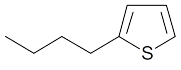

1.51 *meta* $R^2 = -(CH_2)_{11}CH_3$

1.52 *para* $R^2 = -(CH_2)_{11}CH_3$

The gelling ability of a set of bis-ureas containing either a cyclohexane or phenylene spacer unit has been investigated.[57–60] All are sparingly soluble in polar and non-polar organic solvents but dissolve upon heating and as they cool, and all except **1.46**, **1.51** and **1.52**, show gelling behaviour. All compounds except **1.41** and **1.42** are unable to gel methanol, ethanol, isopropanol and DMSO; *i.e.* solvents which strongly compete for hydrogen-bonding. There is no significant relationship between the gelling ability of a bis-urea and the type of attached R groups, but when the ureas are *syn*, *i.e.* one axial and one equatorial, as opposed to both equatorial, viscous solutions are obtained instead of gels suggesting there is an anisotropic requirement for gelation, with the groups pointing in opposite directions but parallel to each other. Similar behaviour is found with the aromatic bis-ureas where the gelation ability is only affected by the relative positions of the urea groups on the ring. Except for **1.42** in *n*-hexadecane, both **1.42** and **1.51** do not show any gelling ability in those solvents that are gelled by compounds **1.47**, **1.48**, **1.49** and **1.50** (albeit with higher minimum gelation concentrations), such as toluene, 1,2-dichloromethane, and *p*-xylene. Those gels that were formed with compounds **1.47**, **1.48**, **1.49** and **1.50** showed a marked difference in stability with the cyclohexyl compounds, often precipitating or crystallising between a few days and some weeks.

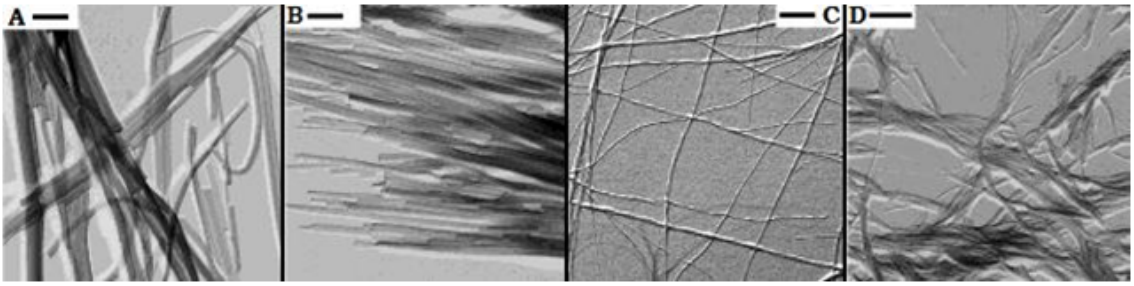

Figure 1.2: Electron micrographs of **1.41** in (A) *p*-xylene, (B) toluene, (C) cyclohexanone and (D) compound **1.42** in ethanol. In each case, the scale bar is 500 nm long.[57]

Electron microscopy, infra-red spectroscopy and molecular modelling can shed some light on how these molecules aggregate in the gel. Figure 1.2 shows electron micrographs of **1.41** and **1.42** in four different solvents. In each case, fibres have formed which are no more than 50 nm wide. Comparing the infra-red spectra of the solution and gel states shows that below the minimum gelation concentration, the N–H amide I and amide II stretches decrease from 3360 to 3327, 1651 to 1632, and 1654 to 1589 cm^{-1} respectively. A weakening of these bonds indicates that the ureas are hydrogen-bonding in some manner.

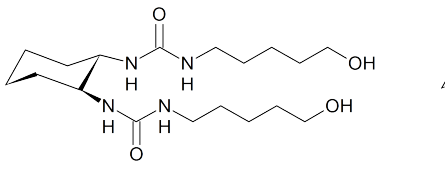

1.53

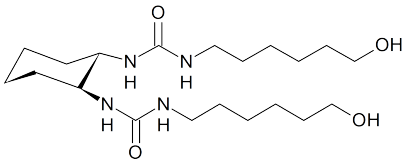

1.54

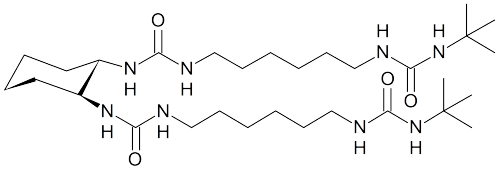

1.55

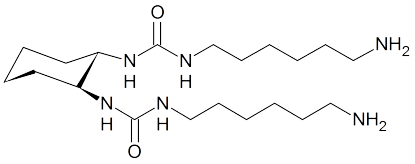

1.56

Compounds **1.53**–**1.56** have been found to gel selected solvents.[61] Compound **1.53** gels 1-octanol, 1,2-dichloroethane and *n*-butyl acetate. The *S,S* form of **1.54** gels *n*-butyl acetate in comparison to a racemic mixture of the *S,S* and *R,R* forms which does not. Both the *S,S* and the racemate for gels in tetraline, and 1,2-dichloroethane. The *S,S* form of **1.55** is able to gel the widest range of solvents

such as *p*-xylene, tetraline and *n*-butyl acetate and partial gels are formed in *i*-propanol, 1-octanol and cyclohexanone.

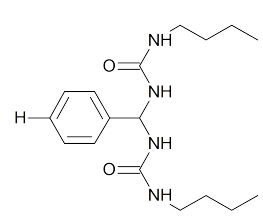

1.57

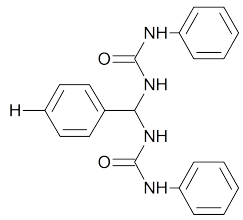

1.58

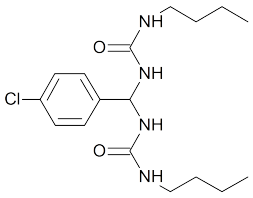

1.59

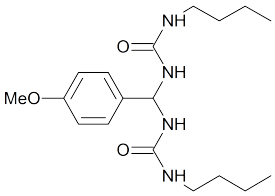

1.60

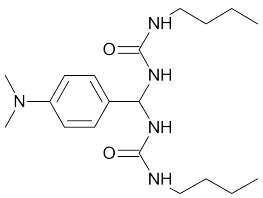

1.61

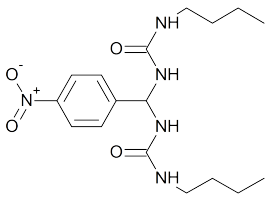

1.62

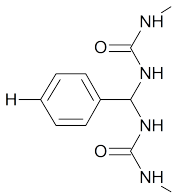

1.63

A series of geminal bis-ureas (**1.57**–**1.61**) have been synthesised and tested for their gelling ability.[62] Compound **1.58** tends to crystallise out of solution rather than form a gel possibly due to the inflexibility of the phenyl substituent compared to the butyl group. All of these geminal bis-ureas are soluble in protic solvents, however ^{1}H NMR spectroscopy shows that in this type of solvent, a decomposition takes place to give an acetal and monoalkylurea which are both soluble in protic solvents. Compound **1.57** was found to gel the most out of those solvents tested, including hexadecane, toluene, 1,2-dichloroethane and dibutyl ether. The stability of the gels was dependent on the solvent they were formed in. Hexadecane gels of **1.57** and **1.61** are very turbid but are destroyed by shaking; gels formed from **1.60** and **1.57** in *p*-xylene and toluene are transparent and stable. A tetraline gel with **1.60** displays thixotropic behaviour: when shaken, the gel breaks up and flows but after standing for a few minutes, the gel properties return completely. Using ^{1}H NMR spectroscopy and comparisons of the infra-red spectrum of the neat gelator to that of its gel, it is likely that these gels are held together by hydrogen-bonding between urea moieties.

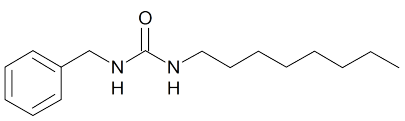

1.64

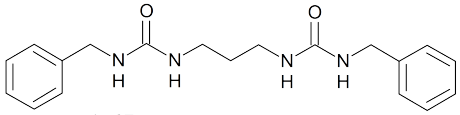

1.65

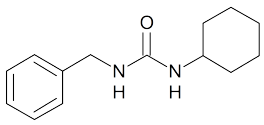

1.66

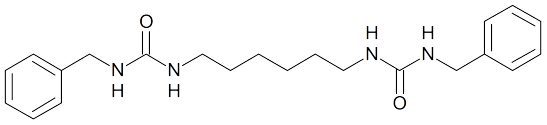

1.67

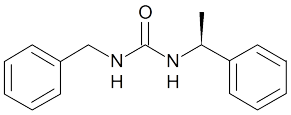

1.68

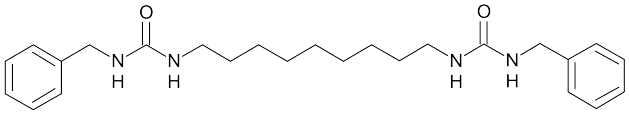

1.69

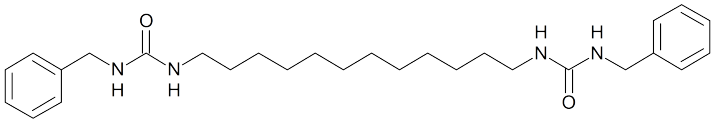

1.70

A series of compounds (**1.64**–**1.70**) incorporating an aryl-urea group have been synthesised and their gelling ability tested.[63] The phenyl group of compounds was included to encourage one dimensional aggregation by π-π stacking and the urea motif for aggregation by hydrogen-bonding. Compounds **1.64**, **1.66**, and **1.68** are moderately soluble in solvents such as ethyl acetate and dichloromethane, and highly soluble in DMSO, dimethyl formamide and aliphatic alcohols. Gels were only formed using these three compounds in one case: **1.64** was able to gel hexadecane. Compounds **1.65**, **1.67**, **1.69**, and **1.70** on the other hand are much less soluble at room temperature than **1.64**, **1.66**, and **1.68**, but gradually dissolve upon heating. Electron microscopy has shown that gels formed by **1.69** in tetraline are comprised of large planar sheets, up to several tens of micrometers long. In this case, molecules in the gel fibres may be arranged with the alkyl chains forming the core of the lamella and the aryl groups are exposed to the solvent, with a hydrogen-bonded urea core.[63]

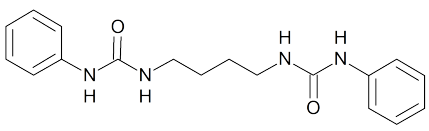

1.71

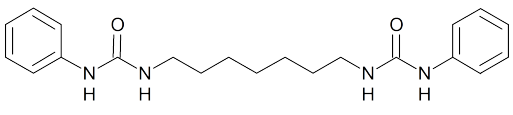

1.72

Compounds **1.71** and **1.72** have been synthesised, but not extensively tested for gelling ability.[64] Both **1.71** and **1.72** were characterized by X-ray crystallography using crystals obtained from slow diffusion of water into a solution of either in DMSO and both stack together in the crystal structure using bifurcated hydrogen-bonding between adjacent ureas.

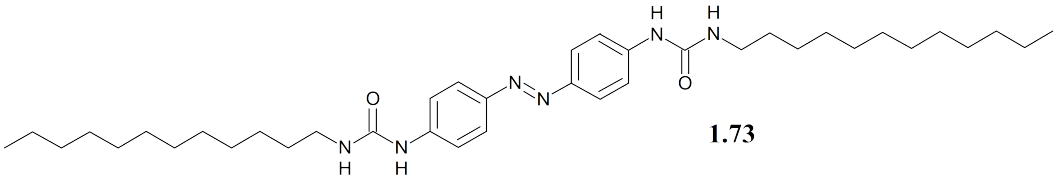

1.73

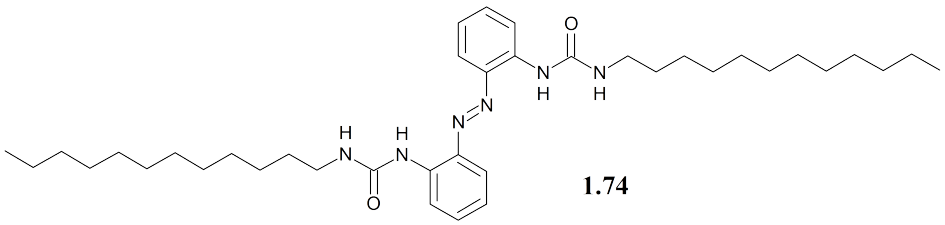

1.74

Two bis-ureas (**1.73** and **1.74**) incorporating an azobenzene spacer unit have been synthesised.[65] Both have azobenzene and urea groups to encourage one dimensional aggregation, but they each display different properties: both **1.73** and **1.74** are insoluble in most organic solvents at room temperature, but gradually dissolve when heated. Upon cooling, **1.73** precipitates from the majority of solvents tried; only in aromatic solvents such as toluene and *p*-xylene are gels formed. In these cases, light microscopy reveals that the gels consisted of elongated fibres with diameters up to 5 μm. Compound **1.74** behaves differently by dissolving at much lower temperatures and in all cases, except in cyclohexanone and 1,2-dichloroethane and polar solvents such as DMSO and water, gels were formed.

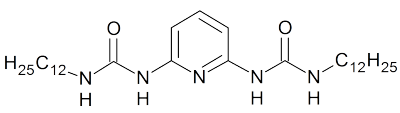

1.75

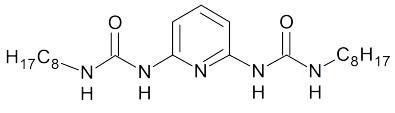

1.76

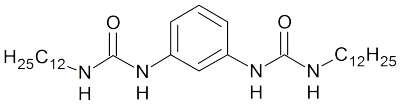

1.77

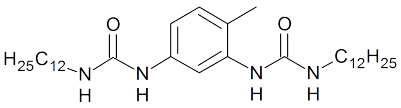

1.78

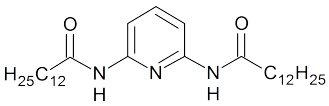

1.79

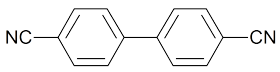

1.80

A series of bis-ureas with either a pyridyl or phenylene spacer have been synthesised and tested for their gelling ability.[66,67] Compound **1.75** is able to gel aromatic solvents such as pyridine and benzene, as well as halogenated solvents such as chloroform and tetrachloromethane. Analogous compounds **1.77** and **1.78** however, are only able to form stable gels in the nematic liquid crystal **1.80** at room temperature, showing that the pyridyl nitrogen is essential for wider range of gelling ability. No gelation is observed for the amide **1.79**. When the alkyl chains in **1.75** are shortened to produce **1.76**, gelling ability is lost and the compound crystallises in a layered zigzag structure in which the 1D structure is built using intermolecular hydrogen-bonding between one urea group of each molecule to form a ladder structure. The remaining urea forms an intramolecular hydrogen-bond with the pyridyl nitrogen which allows the formation of new hydrogen-bonds between two ladders as shown in Figure 1.3

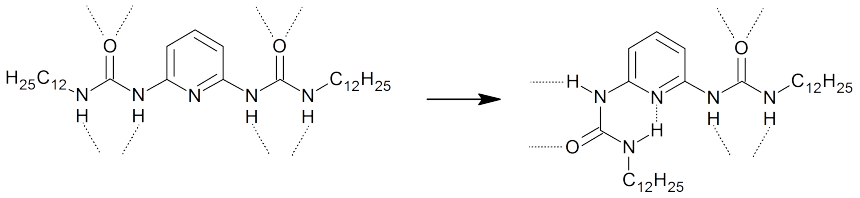

Figure 1.3: Inter- and intramolecular hydrogen-bonding modes of **1.75**.

1.2.5 Metallogelators

Some gelators are known to form gels in the presence of a metal salt, or the strength of their pre-formed organogels may be enhanced or perturbed upon the addition of the salt.[6,17,68–75] This section will introduce several examples of where gels in which metals are present.

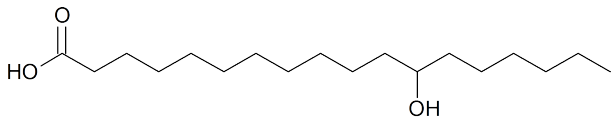

1.81

Out of various fatty acid gelators,[76–78] 12-hydroxyoctadecanoic acid (**1.81**) and its metal salts are particularly versatile gelators and are used in the lubrication industry, acting like a "sponge" in that they keep the oil component in lubricating greases close to the friction regions of various mechanical systems. Gels are formed in nearly all types of solvent including alkanes, carbon tetrachloride, aromatic solvents such as toluene and more polar liquids such as nitrobenzene. Each gel is formed with a varying degree of opacity which is thought to be caused by varying degrees of crystallinity. Structural analysis techniques such as neutron and X-ray scattering as well as electron microscopy have shown that 12-hydroxydecanoic acid and related soaps self-assemble into chains using dipolar interactions between the head groups that are complemented by hydrogen-bonding between the hydroxyl group at C_{12} on adjacent hydrophobic tails. Continued aggregation of the chains forms the fibres that are several micrometers in length and various multiples of the bimolecular length of 12-hydroxyoctadecanoic wide.[32,79–81]

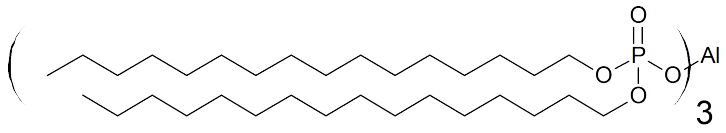

1.82

Compound **1.82**, the aluminium salt of a dihexadecyl phosphate, has also been used as a lubricant.[82,83] Chains of molecules are formed in a similar manner to 12-hydroxyoctadecanoic acid: the aluminium ions, bridged by hydroxyl groups, form

the backbone of the gel fibres with the alkyl chain almost perpendicular to it. Rheological measurements have shown that traces of water increase the viscosity by possibly promoting the transition from micelles to fibres through inter-linking by hydrogen-bonds and this is supported by the observation that the chains breakup upon addition of alkyl amines which bond preferentially to the aluminium ions.[78]

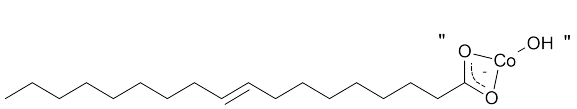

1.83

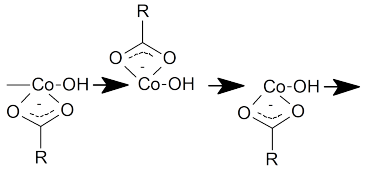

1.84

Compound **1.83** forms gels in benzene and heptane at concentrations between 0.1 and 3 wt % in a similar manner to **1.81** and **1.82**. On addition of acetylacetone or pyridine, there is a decrease in viscosity as both these species coordinate strongly to cobalt, breaking up the chains by competitively disrupting the hydroxide bridges (**1.84**).[84]

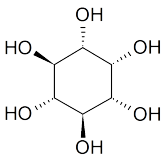

1.85

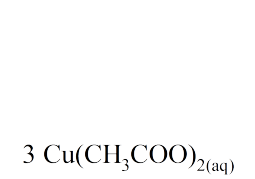

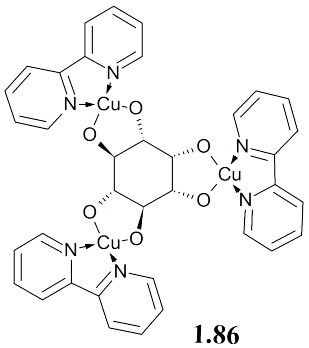

1.86

Myo-inositol (**1.85**) is a hexahydroxy compound which acts as a chelating bidendate ligand of Fe(III) and Cu(II). When *myo*-inositol (H_6ins) is reacted with copper(II) acetate at pH 9.8, a trinuclear complex $[Cu_3(ins)(H_2O)_6]$ is formed. When instead the compound is reacted with three equivalents of $[Cu(bipy)_3]^{2+}$ a further trinuclear complex **1.86** is formed which was characterised by TGA, MS and FT-IR spectroscopy. The reaction is performed between 60 and 70 °C and upon cooling, a transparent green gel results but not when either one or two equivalents of $[Cu(bipy)_3]^{2+}$ are used. When dried to form the xerogel, the gel may be reformed,

but only by water at a pH of 12.4. Along with ultraviolet-visible spectroscopy, it is suggested that the requirement for a high pH indicates that hydroxyl ions must be forming intermolecular bridges between each of the stacked complexes. The ions axially coordinate to the Cu(II) centre and hydrogen-bond to the inositol.[85]

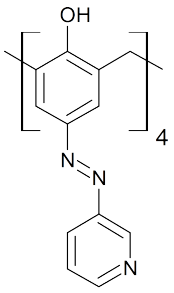

1.87

Selected calixarenes have been shown to act as gelators,[86–88] but 3-pyridine-azocalix[4]arene, **1.87**, is a metallogelator. When dissolved in DMSO, the compound forms a gel upon the addition of $[Pd(en)(H_2O)_2](NO_3)_2$ when the ratio of Pd(II) to ligand is approximately 2:1. At the lower concentration of 0.5 wt %, the metallogel formed is thermoreversible whereas at 2 wt % it cannot be re-dissolved upon heating or ultrasonicating. The palladium complex in this case acts as a crosslinker between molecules of calixarene and the same effect has been observed with $Pd(COD)Cl_2$.[70,89]

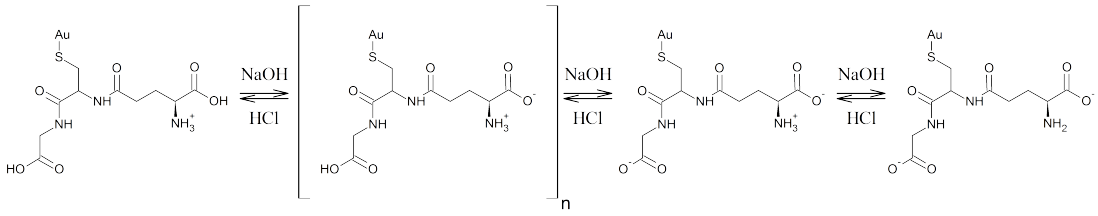

1.88 **1.89** **1.90** **1.91**

When glutathione is reacted with Au(III) chloride in water to give the coordination polymer **1.89**, a transparent gel is formed. When the gel was freeze-dried, its IR spectrum showed the absence of an S-H stretching band at 2525 cm^{-1} for free glutathione and elemental analysis was consistent with a GS–Au formula of 1:1. The hydrogel is pH responsive and although the exact aggregation mode is not clear, various charged species for each state have been proposed (**1.89**–**1.91**). Between pH 1.8 and 2.4 the system exists as a gel (**1.89**) and between 2.4 and 5.3

as a suspension (**1.90**). At other pH values (**1.88** and **1.91**) the gelator is dissolved and by adjusting the pH, with either sodium hydroxide or hydrochloric acid, the system can be switched between these states.[90]

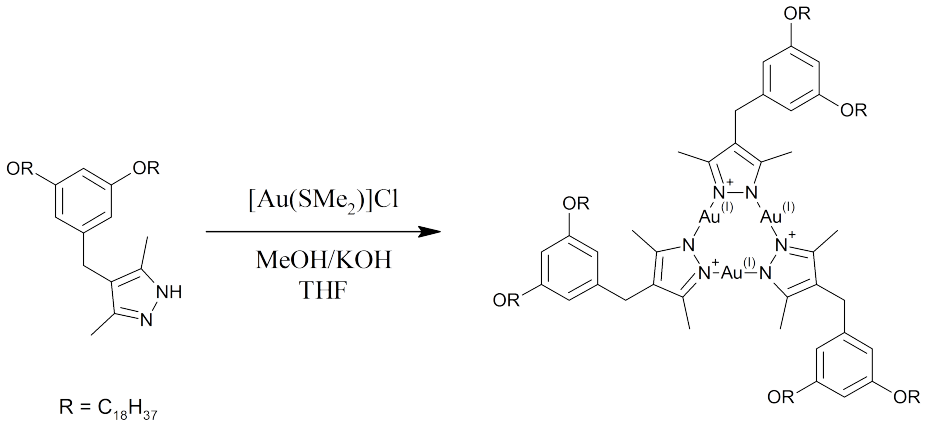

1.92

Scheme 1.1: The synthesis of gold(I) pyrazolate **1.92**.

The synthesis of a trinuclear gold(I) pyrazolate **1.92** is shown in Scheme 1.1. When dissolved in hot hexane and allowed to cool, an opaque gel forms which displays red luminescence under excitation at 254 nm by an ultraviolet lamp. When the gel is heated to a solution, a clear solution is formed and the red luminescence is lost. On addition of 1 equivalent of AgOTf to the hot hexane solution, a green-luminescent clear yellow solution resulted which does not gel upon cooling. When 0.01 equivalents are used instead, upon cooling, a blue luminescent gel results from which, the original red luminescent gel is formed when cetyltrimethylammonium chloride is added to remove the Ag^+ ions.[17,91]

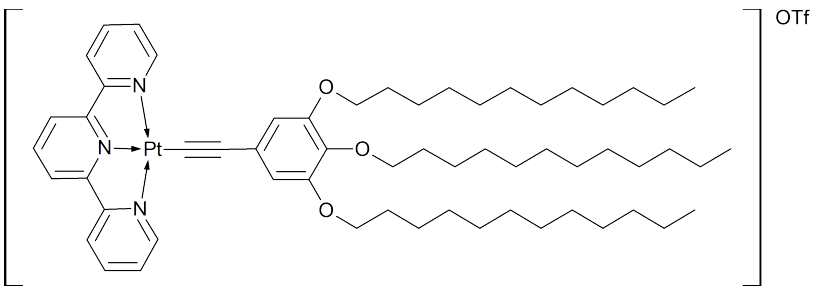

1.93

Several platinum complexes have been shown to act as gelators.[92] The platinum

terpyridyl complex **1.93** forms gels in DMSO as does the free alkyne ligand. While the complex gel is purple and stable for more than one week, the free ligand gel is unstable and collapses overnight which may indicate that Pt···Pt and π-π interactions stabilise the gel. Further evidence for this type of aggregation is found in the UV-visible spectra of gel as it is heated beyond its T_{gel}, at 55 °C. The metal-metal-to-ligand charge transfer transition at 580 nm gradually decreased in absorbance as the gel was heated from 10 to 41 °C and beyond 55 °C disappeared completely. When the counteranion was changed to hexafluorophosphate, the resultant gel is red in colour as opposed to purple, and shows the same activity in its UV-visible spectrum when heated beyond its T_{gel}.[93]

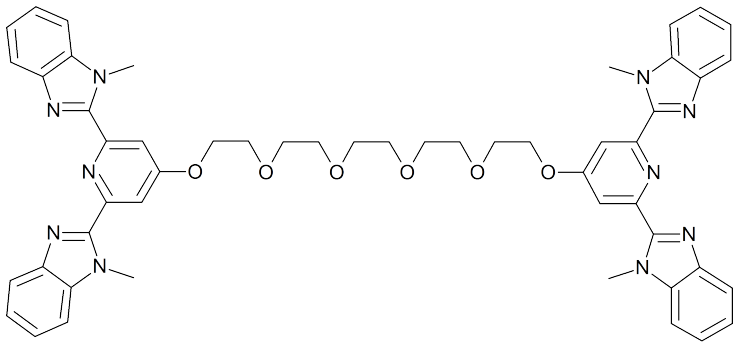

1.94

Compound **1.94** dissolves in a mixture of chloroform and acetonitrile. On the addition of a lanthanide nitrate followed by a transition metal perchlorate the solution forms a gel which displays thixotropic behaviour. Four combinations of transition metal and lanthanide were found to form gels: cobalt and lanthanum, cobalt and europium, zinc and lanthanum, and zinc and europium. After removal of the solvent, they could all be re-swollen with pure acetonitrile, to 0.13 wt %. All of these gels display thermoreversibility but beyond the transition temperature, the mixtures orange colour, which is characteristic of the cobalt-ligand binding, remains, so therefore it is proposed that the more labile lanthanide-ligand bonds are broken. Further evidence of this bonding is provided from an examination of the photoluminescent spectra of the gel formed using zinc and europium: when cold, there are four lanthanide-centred emissions (581, 594, 616 and 652 nm) and one transi-

tion metal-centred emission (397 nm) but when the gel is heated above its sol-gel transition temperature, there is a reduction in the intensity of the lanthanide emission, but not the transition element emission.[15] The lanthanides are known to bind strongly with carboxylic acid, and thus upon the addition of formic acid to the zinc and europium gel, it breaks down and the Eu(III) emission is quenched. Both of these observations are consistent with the formic acid displacing the linkers around the lanthanide.[94–96]

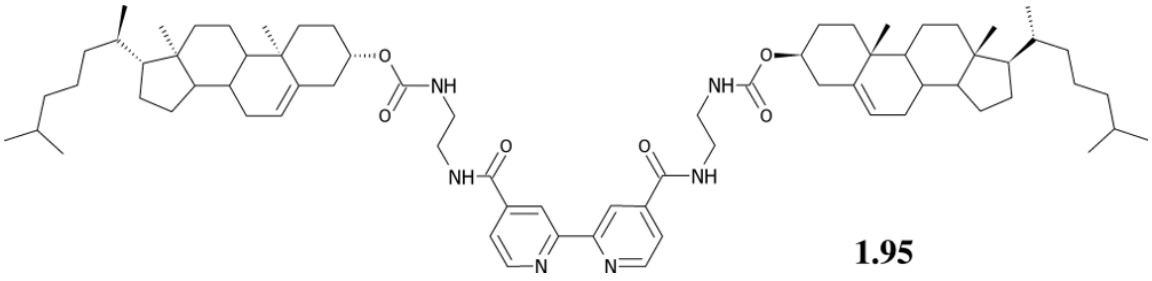

1.95

Another gel has been developed that shows thermo-chromic behaviour, changing its colour as it is heated past its sol-gel transition temperature.[16] Two molecules of **1.95** are bound to copper(I) to give a complex that gels benzonitrile, 1-butyronitrile, and a 1:1 mixture of THF and acetonitrile. The gel formed in 1-butyronitrile is reported to have a green-blue colour below its sol-gel transition temperature and red-brown above it. As the colour change is reversible over many cycles, it cannot be the result of the oxidation of copper(I) to copper(II). It is suggested that the colour change is the result of distortion of the complex in the fibres. The gel also shows chemoresponsiveness: the sol-gel transition can be induced by the addition of ascorbic acid reducing agent or nitrosyl tetrafluoroborate oxidising agent followed by heating, demonstrating that the oxidation state of the metal is crucial in the determining whether a gel will form.

1.3 Analysis Techniques

Various techniques are available to characterise gels, the aim of which is to understand their molecular level organisation and ultimately to be able to use such information to rationally design new gelators. The most commonly reported char-

acterisation method is the gel to solution transition temperature which can be measured in various ways. These include, the "dropping ball" experiment where a steel bearing is placed on top of a gel which is heated. The T_{gel} is recorded as that temperature upon which the ball breaks through the gel as the tertiary structure loses its weight bearing capacity.[97]

1.3.1 Rheometry

Rheology, the study of flow, can offer some insight into the gel's tertiary structure. For rheological measurements, a sample of the gel is spread into a thin layer between two components, one stationary, one moveable. There are a variety of component shapes: parallel plates, cone-and-plate and concentric cylinders. A sinusoidal oscillation is applied to the sample and by measuring the applied stress and the resulting strain, both the storage modulus G' and the loss modulus G'' can be obtained giving a measure of the gels strength. The sample may also be heated to determine a T_{gel}.[32,98]

1.3.2 Spectroscopy

Changes in the primary structure of the gel can be analyzed using nuclear magnetic resonance, ultra-violet and infra-red spectroscopies. Solution-state NMR spectroscopy can be used to identify the formation of hydrogen-bonds during gelation *via* changes in the chemical shifts; relaxation time measurements can be used to determine those parts of the molecule whose translational and conformational movement slow during gelation. Comparison of the solution NMR spectroscopic data with solid-state magic angle NMR spectroscopy measurements has been used to identify chemical shift changes from the solution to the gel state.[33]

IR spectroscopy can be used to identify the presence of hydrogen-bonding, such those between urea groups by a decrease in the stretching frequencies of N–H and C=O bonds; unfortunately the N–H peak is sometimes obscured by water in the sample.[33]

1.3.3 Microscopy and Diffraction

The nanostructure of the gels may be probed using a range of techniques including scanning and transmission electron microscopy, and small angle X-ray and neutron scattering. To view a gel under an electron microscope, it must first be completely dried for use in the high-vacuum conditions, and to enhance the quality of the image, the electron density of the assembly must be stained with chemicals such as osmium tetraoxide and phosphotungstate; both of these methods have the potential to distort the morphology of the gel. A possible solution is provided by either viewing the gel under a partial pressure of water in freezing the gel very quickly and imaging sections no more than 300 nm thick in a technique termed "cryoTEM". Plunging a sample into a bath of liquid ethane at -170 °C makes it possible obtain a cooling rate of 10,000 °C per second, which freezes the solvent and maintains the network of the gel.[99,100] Small angle X-ray and neutron scattering may be used to deduce the ordering of the molecules in the fibres: by using extensive mathematical treatment and fitting the gathered data to a chosen model such as rod-like micelles, the type of packing can be determined.[32]

1.4 Applications

A wide variety of applications for gels have been described in the literature[101] and include molecular recognition,[34] templates for nanostructures,[7,27,34] art conservation, drug delivery,[102] liquid-crystal displays,[7] gel electrolytes,[7] catalysis[103] and light harvesting.[7] Selected applications will be briefly discusssed here.

1.4.1 Nano-structured Materials

The self-assembly of gelators into ribbons, tubes, helices etc. can be exploited to form nanoscale structures including nano-porous silica. In a typical procedure, an organogel is formed in the presence of tetraethyl orthosilicate (TEOS) and a catalyst to hydrolyse the TEOS. The TEOS is hydrolysed and the condensation off the silicate around the gel fibres gives a silica gel which, after drying and removal

of the organic gelator with a suitable solvent, yields the porous silica.[7]

1.4.2 Drug Delivery

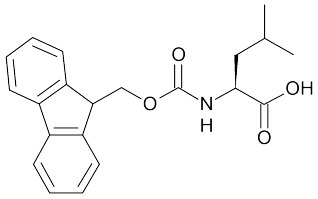

1.96

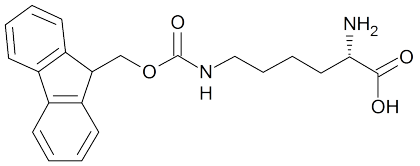

1.97

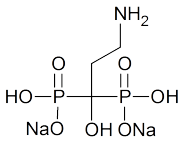

1.98

Recently, a hydrogel was developed as a potential treatment for uranium wounds. The hydrogel is a combination of three compounds, **1.96**, **1.97** and **1.98**.[104] Compound **1.98**, the pamidronate, is essential for gelling to occur as it can form hydrogen-bonds between **1.96** and **1.97** at pHs 9 to 10.4. Also, it is able to chelate uranyl nitrate. Being a gel, it would be easier to administer than a liquid-based treatment. The hydrogel was tested on rats with simulated uranium wounds and it proved a success, reducing the inflammation and chelating with UO_2^{2+} to prevent its uptake by the body. Compared to the control group, rats that were given the treatment experienced no weight loss nor did any expire.

1.4.3 Art Conservation

Cleaning old works of art that have slowly gathered dirt and grime on their surfaces without damaging the original painting is a challenge for conservators. The optimal surface cleaner would a) not remove the paint, b) not damage the surface chemically, c) not damage the surface when applied or removed and d) not leave residues on the surface after removal. The organic solvents that are currently used unfortunately penetrate into the original layers of the paint *via* capillary action leading to swelling and leeching of the varnishes and binders from the surface. However, it has been suggested[105] that this problem could be solved by employing a solvent in its gelled state; when immobilized within the gel network, the capillary action of the solvent into the surface is much reduced. With this approach, a wider range of solvents

would be accessible to use as cleaning agents because when applied as a pure solvent, they may rapidly evaporate. Of course, there would be problems associated with using gels, as the surface may be scratched when they are wiped from the surface. Using rheo-reversible gels may be the answer to this problem. The solvent may be applied to the surface as a gel, induced to flow by a chemical change and then gently absorbed into a cloth or sponge.

1.4.4 Dye Removal

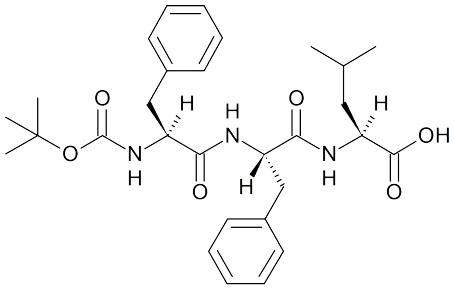

1.99

Peptide **1.99** is a hydrogelator, forming opaque gels in water with a minimum gel concentration of 1.68 % w/v between pHs 11.5 and 13.0. Dilute solutions of the dyes Rhodamine B, Reactive Blue 4 and Direct Red 80 were layered on top of hydrogels of **1.99** at 6.5 % w/v. If left for two days, there is complete adsorption of the dyes into the gels, which suggests they may be used for the removal of more toxic dyes in real conditions. The gels are also reusable: when the pH of the dyed hydrogels was adjusted to 7.55 by the addition of HCl, colourless compound **1.99** precipitates and may be isolated by simple filtering and repeated washing with deionised water.[106]

1.5 Aims of the Project

A set of bis-urea ligands functionalised with pyridyl functionalities will be synthesised. In order to better understand what structural features make gelators, the spacer group will be varied and each ligand subject to gelation tests in many solvents, mixed solvents systems, and with as many metal salts as possible working

towards the synthesis of metallogels and chemoresponsiveness or controlled gel flow behaviour.[13] Gels formed will be characterised using standard techniques.

Chapter 2

Intermolecular Bonding in Crystals of Selected Bis(pyridylurea)s

2.1 Introduction

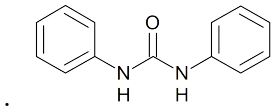

Figure 2.1: *N,N′*-diphenylurea.

An example of a diaryl urea molecule is shown in Figure 2.1. As with all ureas, the molecule contains both a hydrogen-bond acceptor, in the oxygen atom and two hydrogen-bond donors, the N–H bonds. Possessing both a donor and an acceptor, one would expect the hydrogen-bonding pattern in the solid state to be a chain comprised of bifurcated hydrogen-bonds between the carbonyl oxygen and N–H protons of adjacent molecules. This is the case with the simplest example, *N,N′*-diphenylurea, and its hydrogen-bonding pattern is shown in Figure 2.2, a so-called α-tape.[107]

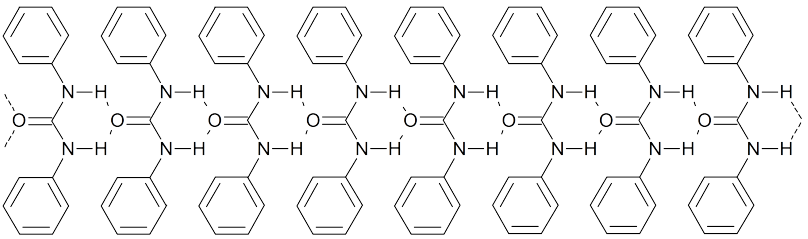

Figure 2.2: The bifurcated hydrogen-bonding of *N,N′*-diphenylurea.

In some cases, when *N,N′*-diphenylurea is substituted on the aryl ring, this α-tape is disrupted and the urea binds to a guest proton acceptor by a bifurcated hydrogen-bond (graph set notation $R_2^2(8)$.[108,109]) as shown in Figure 2.3; the urea oxygen remains unbound.

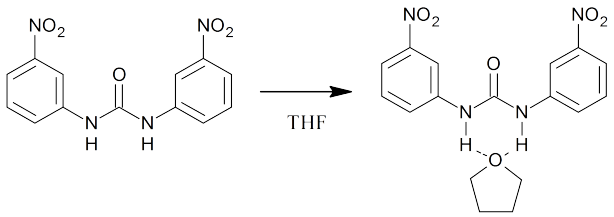

Figure 2.3: The complexation of THF with 1,3-bis(*m*-nitrophenyl)urea. .

Figure 2.4 and Figure 2.5 show those substituted *N,N′*-diphenylureas which cocrystallise with proton acceptors and those that do not, respectively. Comparing the structures of the two groups, it can be seen that the behaviour results from diaryl ureas substituted at the *meta* position with electron withdrawing groups such as $–NO_3$ or $–CF_3$; when the nitrates are *ortho* or *para* to the urea, complexation does not occur. Complexation does also not occur when the groups are electron donors, such as –OMe and $–CH_3$. One of these complexing ureas, 1,3-bis(*m*-nitrophenyl)urea, forms co-crystals with the solvent when crystallised from solvents which are only proton acceptors: acetone, THF and DMSO. It similarly forms 1:1 complexes when it is crystallised in the presence of a third proton acceptor such as triphenylphosphine oxide, *N,N′*-dimethyl-*p*-nitroaniline or diethylene glycol.

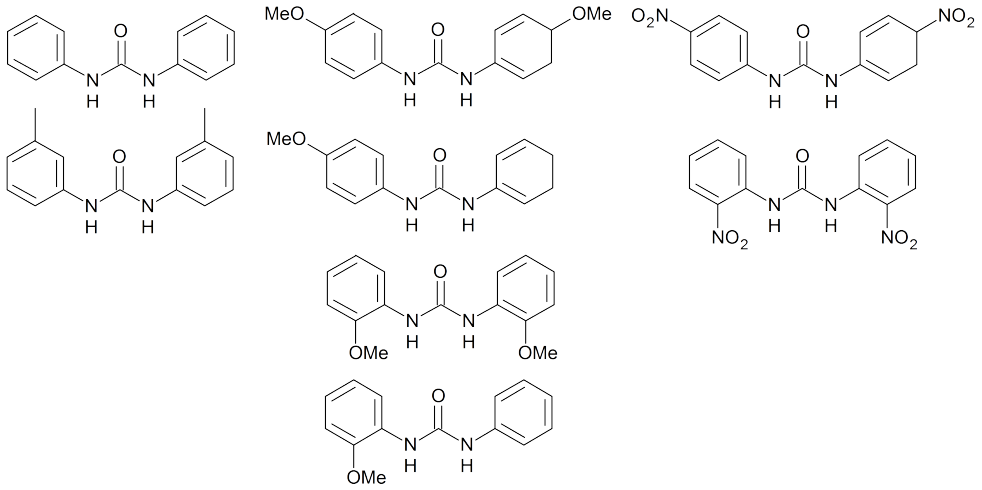

Figure 2.4: Diaryl ureas known not to form cocrystals with proton acceptors.

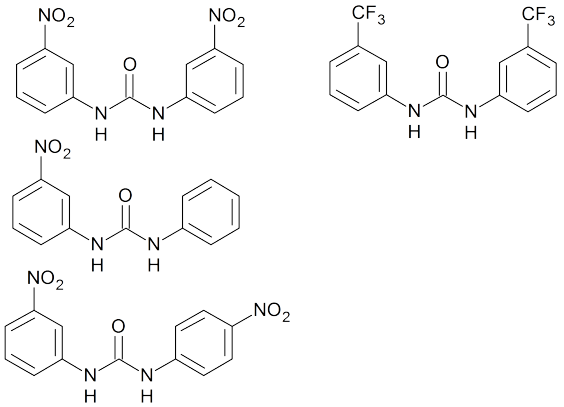

Figure 2.5: Diaryl ureas known to form cocrystals with proton acceptors.

A possible explanation for the complexation behaviour of 1,3-bis(*m*-nitrophenyl)urea is by the formation of a CH···O_{urea} interaction between the activated protons on the aryl ring and the carbonyl oxygen. This intramolecular hydrogen-bond reduces the effective ability of the carbonyl oxygen to donate an electron pair, measured as its β value.[110] This is also shown by the relative planarity of the complexing ureas compared to their non-complexing counterparts as the C–H proton lies as close as possible to the urea oxygen.[111–113]

Along with nitrate substituted aryl ureas, pyridyl ureas have also been shown not to give the classic urea tape.[114] When the nitrogen on the pyridyl ring is *ortho* to the urea, at the 2 position, both are co-planar. The classic tape is disrupted by the rotation on one side of the molecule around the bond between the urea nitrogen

and carbonyl group. This conformation is subsequently stabilised by the formation of an intramolecular NH···$N_{pyridyl}$ hydrogen-bond between the rotated pyridyl and opposite N–H. This conformation is shown in Figure 2.6.

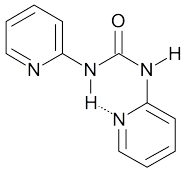

Figure 2.6: The intramolecular NH···$N_{pyridyl}$ bond of *N,N′*-bis(2-pyridyl)urea.

When the nitrogen is *meta* to the urea, the activated aryl protons again form an intramolecular CH···O_{urea} hydrogen-bond, with the pyridyl ring co-planar to the urea to maximise the interaction. The urea tape is disrupted by the formation of intermolecular NH···$N_{pyridyl}$ hydrogen-bonds from the urea NHs to different pyridyl nitrogen proton acceptors, shown in Figure 2.7.[114]

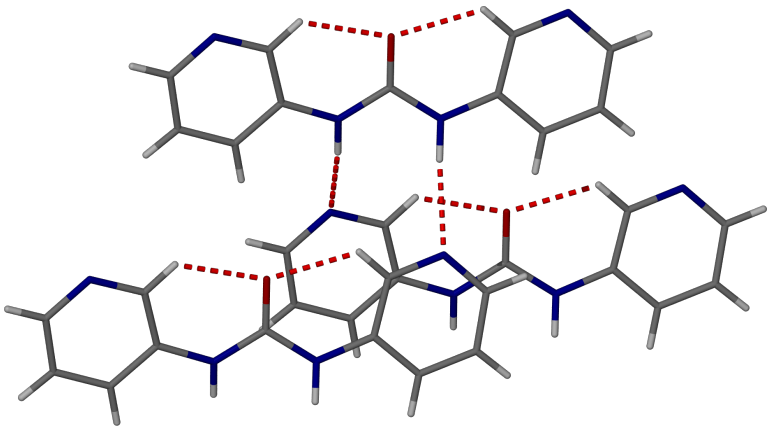

Figure 2.7: Intra- and intermolecular hydrogen-bonds of *N,N′*-bis(3-pyridyl)urea.

One may therefore conclude the following about the relationship between substitution on the aryl ring and subsequent formation or non-formation of a urea tape. When electron-withdrawing groups are placed *meta* to the urea, but are not hydrogen-bond acceptors, a classic urea tape is formed. When the group is electron donating, again, a urea tape forms. However, when the group is both electron withdrawing and a hydrogen-bond acceptor, as in nitrate and pyridyl, the CH···O_{urea} interaction dominates and the urea tape does not form.

2.1.1 Urea synthesis

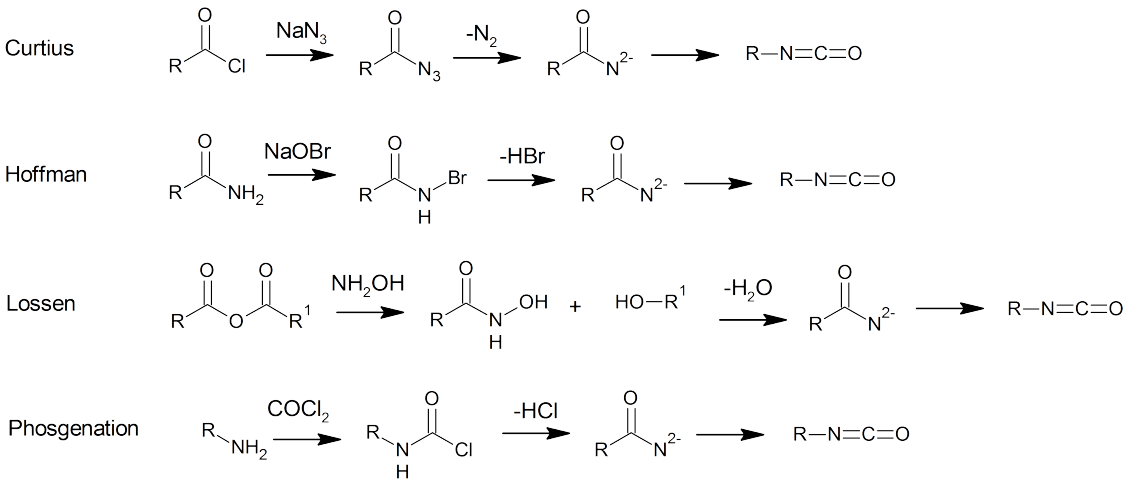

Scheme 2.1: Four traditional methods of isocyanate production.

A urea is formed when an amine reacts with an isocyanate.[115,116] An isocyanate is in turn synthesised using one of more than twenty-five methods,[117] four of which are shown in Scheme 2.1.[118] Three of these reactions, the Curtius, Hoffman and Lossen rearrangements are used in the laboratory and the fourth, phosgenation, is the most widely employed on an industrial scale.[119] The first three methods have their disadvantages: sodium azide used in the Curtius reaction is hazardous, and the Hoffmann and Lossen rearrangements are only suitable for the preparation of aliphatic isocyanates; aromatic isocyanates react with the aqueous solvent used to give substituted ureas. A non-aqueous alternative of *t*-butyl hypochlorite can be used, but is too costly for technical applications.[120]

Diphenyl diphosphoryl azide has been shown to be a more convenient reagent for the synthesis of isocyanates by way of a modified Curtius reaction.[121] Under mild conditions, aromatic, aliphatic and heterocyclic carboxylic acids were converted to urethanes, as shown in Scheme 2.2, *via* an azide intermediate. When the synthesis is performed in an alcohol, the resulting isocyanate formed from the decomposition of the azide reacts with the solvent to give a urethane shown in Scheme 2.2. A proposed mechanism for the formation of an isocyanate is shown in Scheme 2.3.

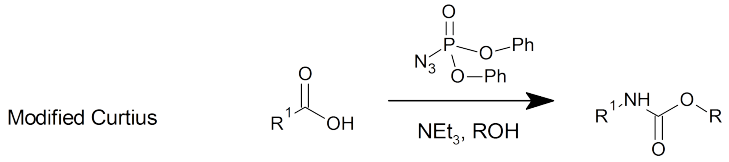

Scheme 2.2: The synthesis of a urethane by a modified Curtius reaction.

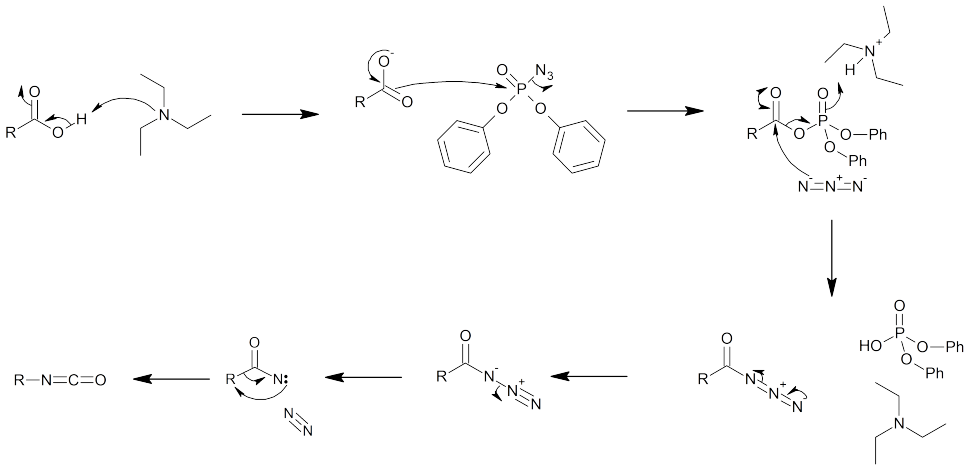

Scheme 2.3: A proposed mechanism of isocyanate formation by a modified Curtius reaction.

2.2 Aims

Ureas and pyridylureas are used in applications such as anion binders,[122–132] molecular capsules[133–137] or gels.[62,63,138,139] Greater understanding of the factors influencing the formation of either NH···$N_{pyridyl}$ bonds or bifurcated NH···O_{urea} in pyridylureas is essential for good ligand design. In this chapter, a homologous series of bipyridylureas and related aryl analogues will be examined. Compared to *N,N′*-bis(3-pyridyl)urea, this series of compounds have a pyridyl group on one side of the urea and an alkyl group the other and based on reported observations on the singly substituted *N*-phenyl-*N′*-(3-pyridyl)urea and 1-(*m*-nitrophenyl)-3-phenylurea, these compounds may still display NH···$N_{pyridyl}$ hydrogen-bonding. The alkyl chain length and type will be varied to determine if there is any influence on behaviour.[140]

2.3 Synthesis

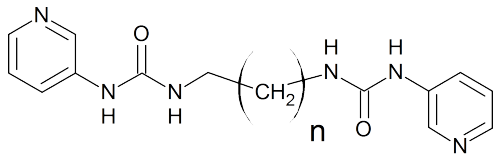

2.n

To synthesise compounds **2.1**–**2.9**, the classical reaction between diisocyanates and 3-aminopyridine was used first. In a typical experiment, a diisocyanate was dissolved in dichloromethane and upon addition of a slight excess of 3-aminopyridine, the product immediately precipitated. Using this method, compounds **2.3**, **2.5** and **2.7** could be synthesised but the starting materials for the remaining compounds were not commercially available.

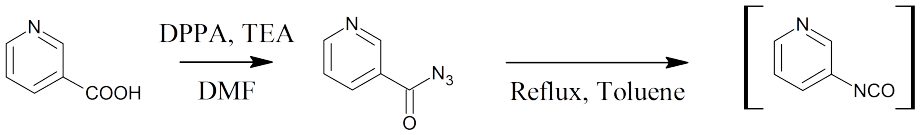

Scheme 2.4: The synthesis of 3-isocyanatopyridine.

To complete the series, α,ω-diamino alkanes were reacted with 3-isocyanatopyridine prepared *in situ* (Scheme 2.4). Diphenyldiphosphoryl azide and triethylamine are reacted with nicotinic acid in DMF over ninety minutes at room temperature. Subsequent extraction of the azide into diethyl ether gave the product as clear colourless crystals upon evaporation of the solvent.

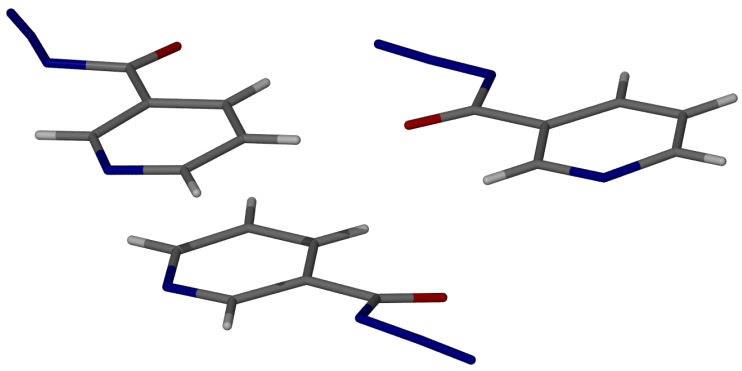

Figure 2.8: The asymmetric unit of nicotinoyl azide where $Z' = 3$.

Crystals of nicotinoyl azide where subsequently dissolved in toluene and refluxed to form the isocyanate by a Curtius rearrangement. The reaction was monitored by the evolution of nitrogen gas, and when this ceased, the necessary α,ω-diamino alkane was added to precipitate the product as a colourless solid. To synthesise the aryl ureas, the same procedures were followed but acetonitrile was used instead due to the insolubility of the aryl amines in toluene.

2.4 Results and Discussion

Crystallisations of compounds in the series **2.1**–**2.9** were attempted in mixtures of THF and water (3:2). In all cases, crystals were grown, but only those of the smaller ligands (**2.1**–**2.3**) were suitable for X-ray crystallography and they were characterised.

2.4.1 *N,N″*-ethylene-1,2-diylbis(*N′*-pyridin-3-ylurea)

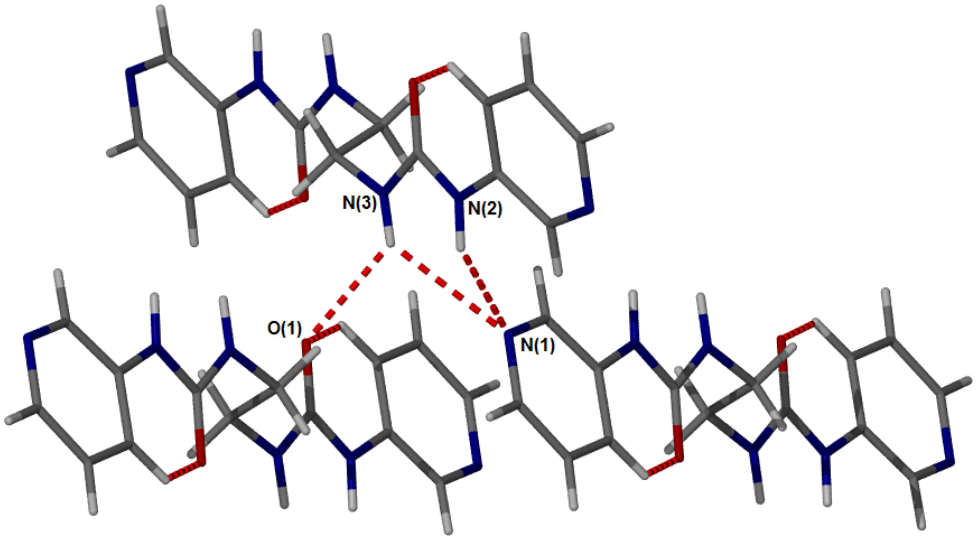

Figure 2.9: The X-ray crystal structure of compound **2.1**. Hydrogen-bond distances N(2)···N(1) 2.990, N(3)···N(1) 3.303, N(3)···O(1) 2.950 Å.

The X-ray crystal structure of *N,N″*-ethylene-1,2-diylbis(*N′*-pyridin-3-ylurea, compound **2.1**, is shown in Figure 2.9. The structure is comprised entirely of both NH···$N_{pyridyl}$ and NH···O_{urea} hydrogen-bonds and the molecules are kinked in the

middle as the ethylene bridge adopts a gauche conformation (Figure 2.10). The NH closest to the aryl group forms a NH···$N_{pyridyl}$ hydrogen-bond with the pyridyl nitrogen of an adjacent molecule but the NH donor closest to the ethylene spacer forms a bifurcated interaction to both the pyridyl nitrogen and a urea oxygen.[141] Each urea oxygen forms an intramolecular hydrogen-bond to the aryl CH *para* to the pyridyl nitrogen

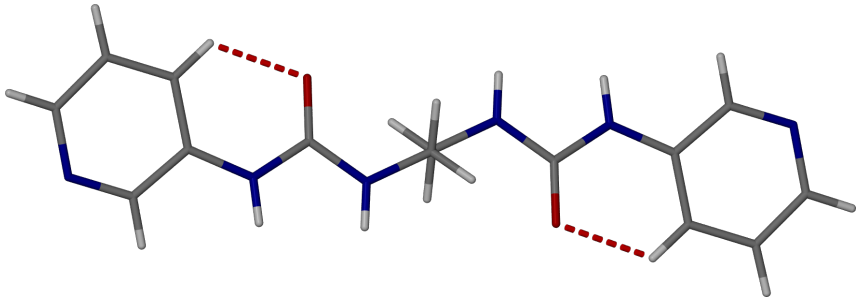

Figure 2.10: The intramolecular CH···O_{urea} bonds formed and the gauche conformation adopted by the ethylene bridge in compound **2.1** in the solid-state.

2.4.2 *N,N″*-propylene-1,3-diylbis(*N′*-pyridin-3-ylurea)

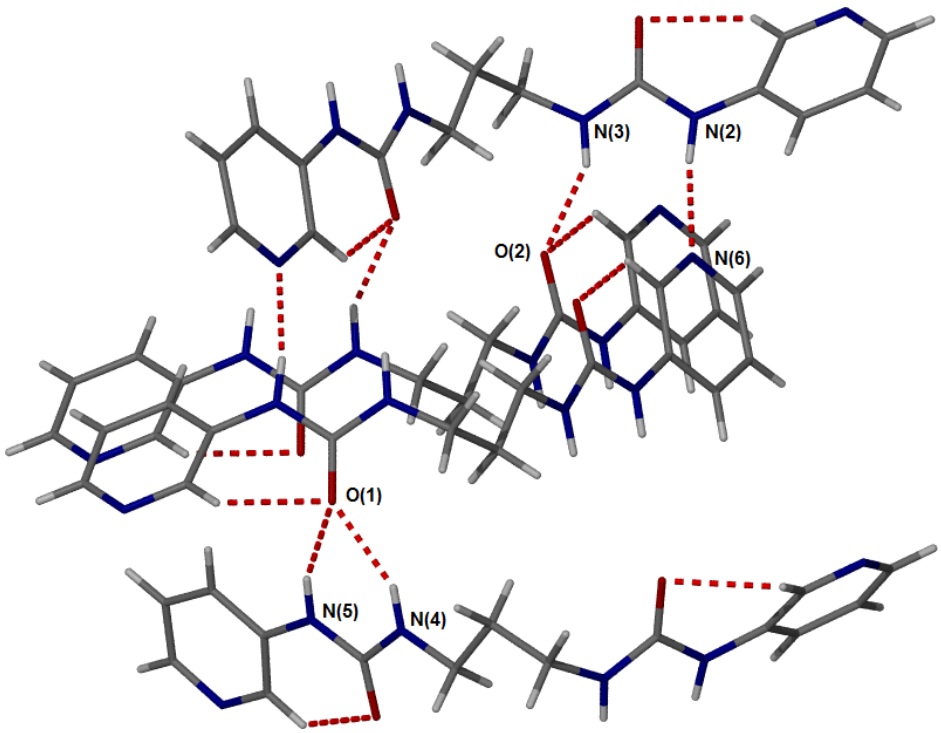

Figure 2.11: The X-ray crystal structure of compound **2.2**. Hydrogen-bond distances N(2)···N(6) 2.892, N(3)···O(2) 2.799, N(4)···O(1) 2.900, N(5)···O(1) 2.917 Å.

The crystal structure of *N,N″*-propyl-1,2-diylbis(*N′*-pyridin-3-ylurea), compound **2.2**, is shown in Figure 2.11. The structure is a mixture of both NH···$N_{pyridyl}$ and NH···O_{urea} hydrogen-bonds as its ethylene counterpart and the molecules adopt a bent conformation overall (shown in Figure 2.12), with one gauche and one anti N–C–C–C torsion angle in the propylene bridge. Whereas in compound **2.1** the asymmetric unit is half of a molecule, in this case it is the complete molecule and there are two unique urea moieties. With both ureas their carbonyl oxgyens are bonded intramolecularly to an adjacent acidic proton on the aryl ring. One urea, next to the anti substituent chain, forms a bifurcated hydrogen-bond (Figure 2.13) akin to a α-tape whilst the other adopts a different binding mode in which the NH adjacent to the aryl group interacts with an orthogonal pyridyl nitrogen and the other forms a non-bifurcated hydrogen-bond with a urea carbonyl from a third molecule. This, and the tape motif alternate along the stack of urea groups and therefore there is a continuous hydrogen-bonded urea chain orthogonal to the classical infinite α-tape as shown in Figure 2.15. By adopting this crystal structure arrangement, the methylene groups of the propylene bridge appear to maximize van der Waals stacking.[140]

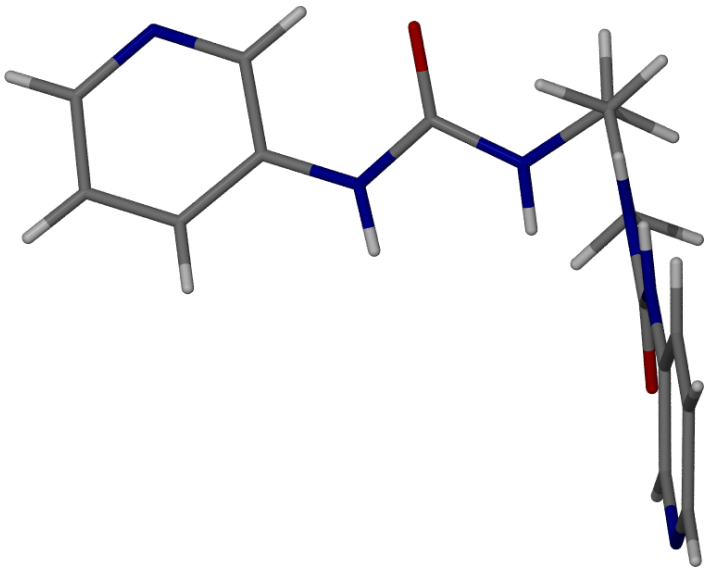

Figure 2.12: The ‘bent’ conformation of compound **2.2**.

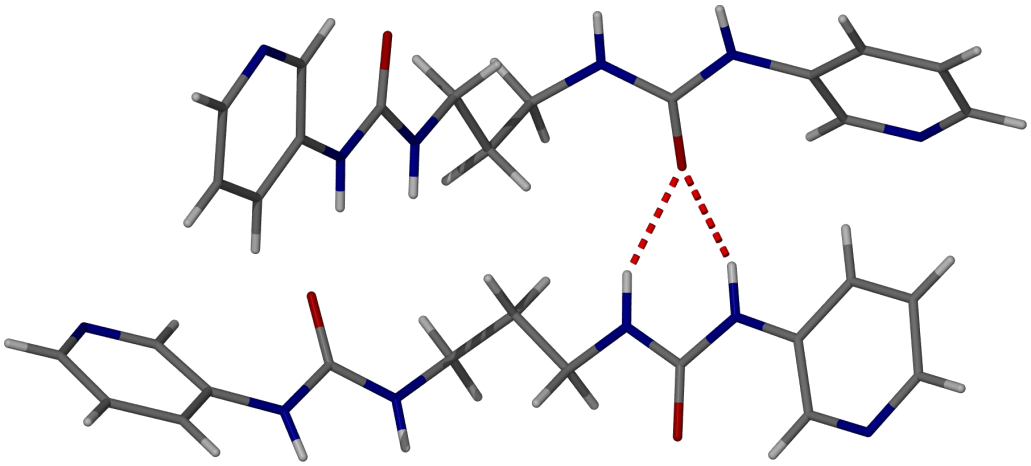

Figure 2.13: The bifurcated hydrogen-bonding mode adopted by one urea moiety of compound **2.2**.

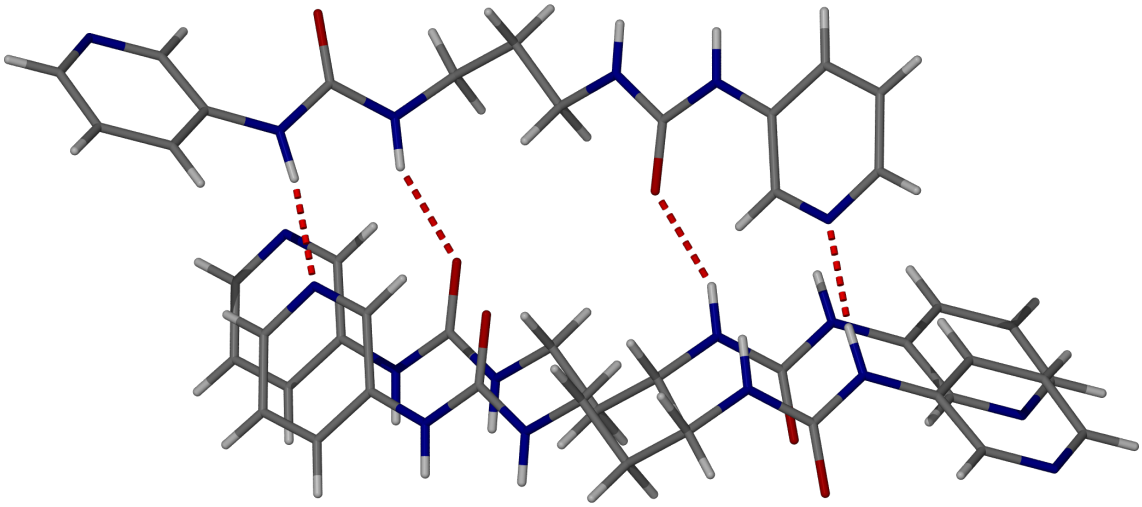

Figure 2.14: The alternate urea hydrogen-bonding mode of compound **2.2** comprising both a NH···O_{urea} and NH···$N_{pyridyl}$ interaction. **2.2**.

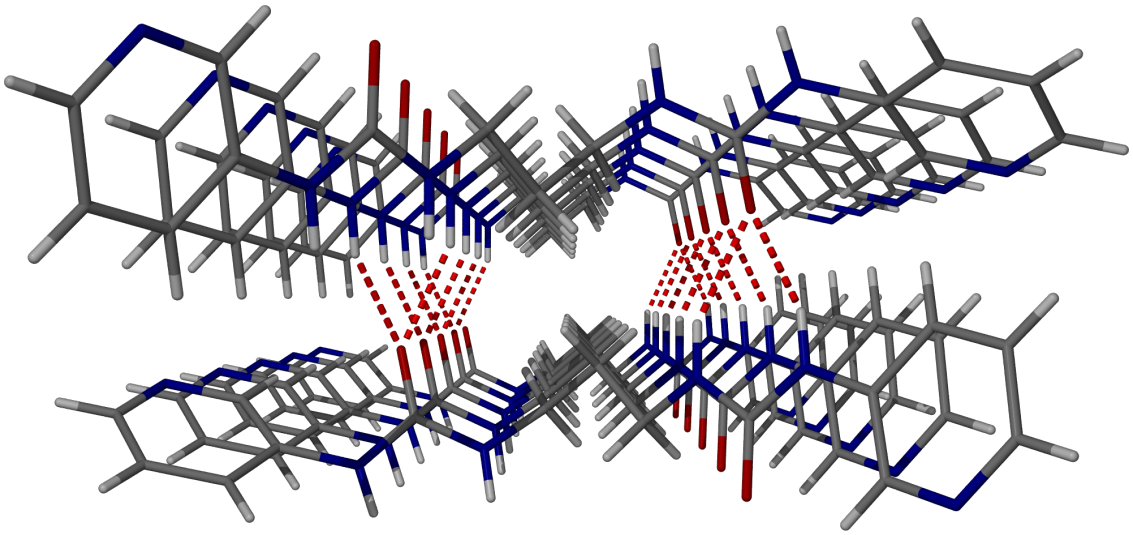

Figure 2.15: The 'orthogonal α-tape' of compound **2.2**.

2.4.3 *N,N″*-butylene-1,4-diylbis(*N′*-pyridin-3-ylurea)

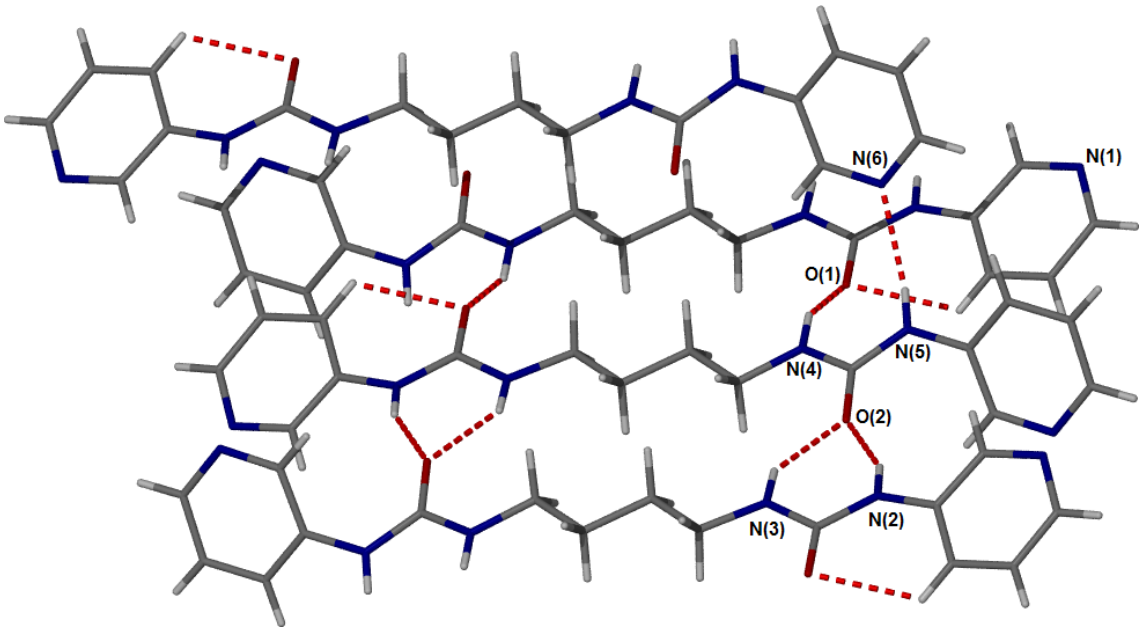

Figure 2.16: The X-ray crystal structure of compound **2.3**. Hydrogen-bond distances N(2)···O(2) 2.880, N(3)···O(2) 2.920, N(4)···O1 2.925, N(5)···N(6) 3.024 Å.

The X-ray crystal structure of *N,N″*-butylene-1,4-diylbis(*N′*-pyridin-3-ylurea), compound **2.3**, is shown in Figure 2.16. In comparison to compound **2.2**, the N–C–C–C and C–C–C–C torsion angles of the butylene bridge are all *anti*, leading to a more co-linear arrangement of the molecules which allows efficient stacking of the methy-

lene groups. The bonding is again a mixture of hydrogen-bonding modes and the ureas alternate between a bifurcated hydrogen-bonding and a combination of a single urea-urea NH···O_{urea} bond and a NH···$N_{pyridyl}$ to an adjacent pyridyl. If efficient stacking of the spacer group is important in determining the crystal structure, then as the chain length increases, stacking should be favoured and alternative binding modes other than the α-tape should be disfavoured. In a similar manner, aromatic systems, such as phenylene or napthylene bridges which are capable of π-stacking should favour the formation of α-tapes of ureas.

2.4.4 *N,N″*-phenylene-1,4-diylbis(*N′*-pyridin-3-ylurea)

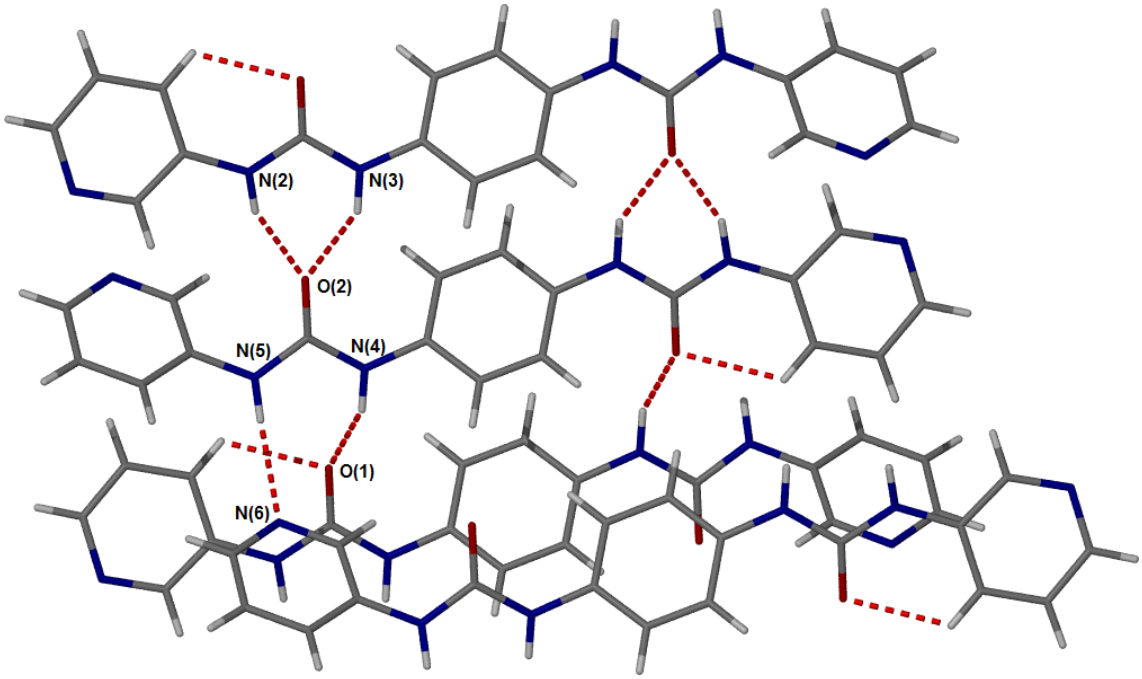

Figure 2.17: The X-ray crystal structure of compound **2.10**. Hydrogen-bond distances N(2)···O(2) 2.851, N(3)···O(2) 2.925, N(4)···O(1) 2.853, N(5)···N(6) 3.082, N(5)···O(1) 3.219 Å.

N,N″-1,4-phenylenebis(*N′*-pyridin-3-ylurea), compound **2.10**, was crystallised from 10 % aqueous THF solvent and the crystal structure (Figure 2.17) was determined. The structure is isomorphous with that of compound **2.3**, forming a double urea tape motif which is broken only by one of the four unique NH groups twisting to form a short interaction with a pyridyl nitrogen instead of the nearby urea carbonyl oxygen atom. The *p*-phenylene spacers π-stack in an analogous way to the *anti*

butylene chain in compound **2.3**.

2.4.5 *N,N″*-naphthalene-1,5-diylbis(*N′*-pyridin-3-ylurea)

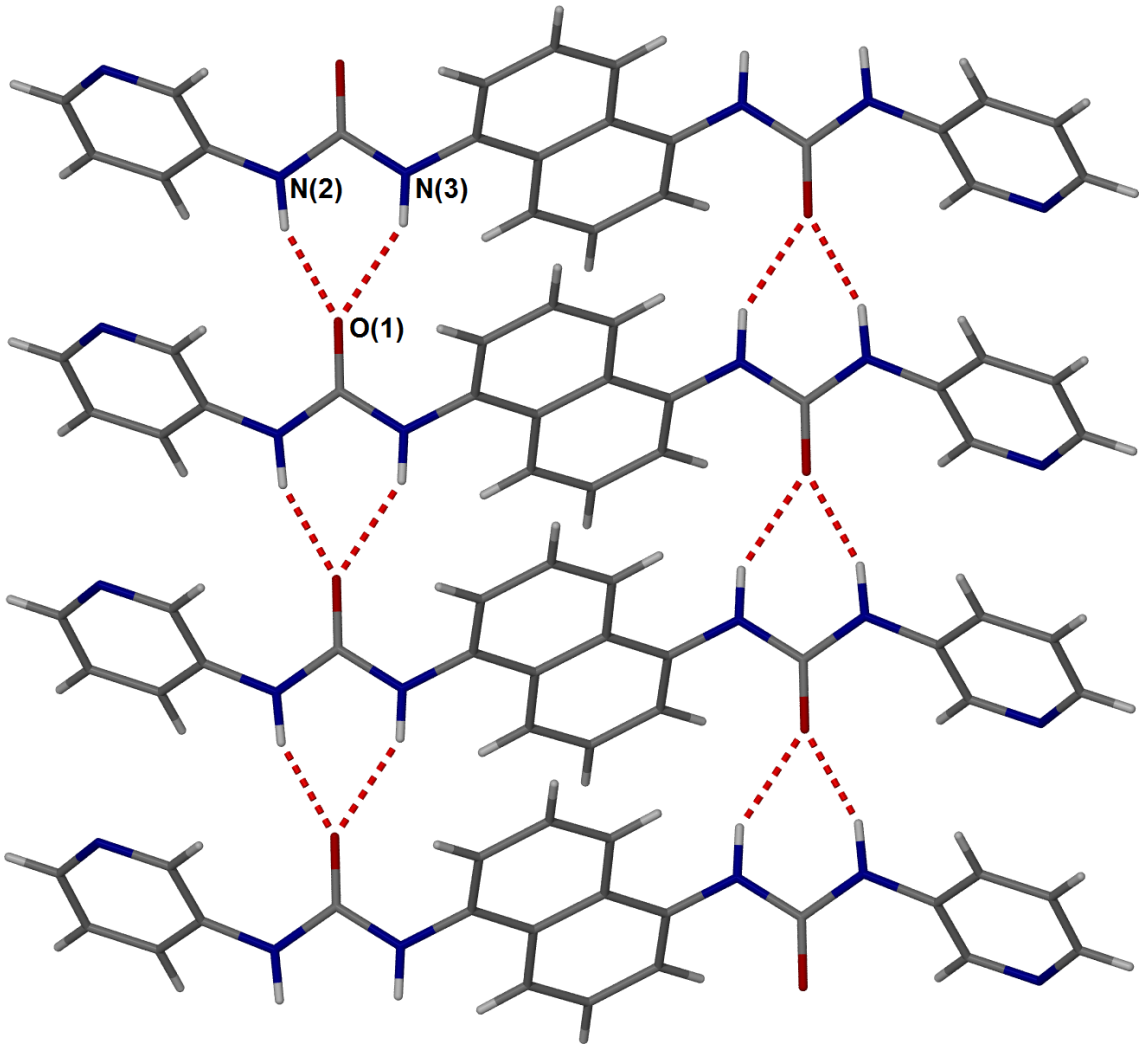

Figure 2.18: The X-ray crystal structure of compound **2.11**. Hydrogen-bond distances N(2)···(1) 2.788, N(3)···O(1) 2.891 Å.

In the synthesis of *N,N″*-naphthalene-1,5-diylbis(*N′*-pyridin-3-ylurea), compound **2.11**, crystals of the bis(urea) were grown by slow diffusion of water into a DMSO solution of the crude product. The crystal structure solution obtained using X-ray crystallography is shown in Figure 2.18 π-π stacking interactions between the naphthylene rings of adjacent molecules dominate and relinquish all interactions of the urea apart from the bifurcated hydrogen-bond to give an α-tape. To assist the

formation of the tape, both aryl rings are twisted out of the plane of the urea, as shown in Figure 2.19 making the carbonyl oxygen atom more accessible.

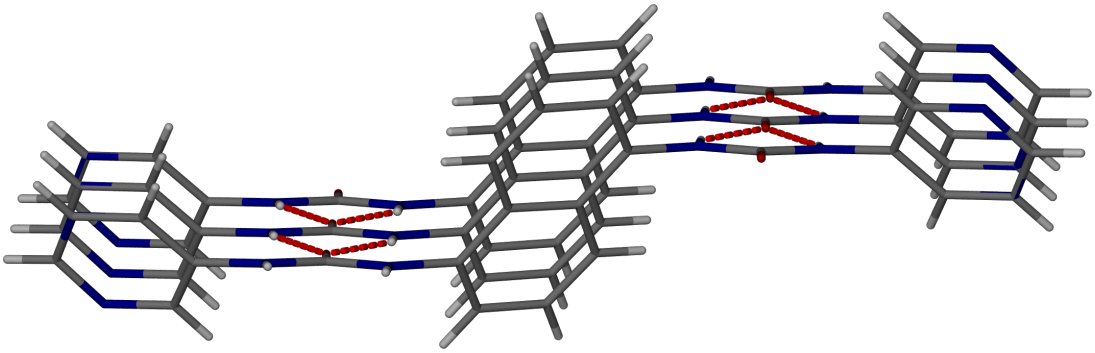

Figure 2.19: The twisting of the aryl rings out of the urea plane in compound **2.11**.

2.5 Conclusions

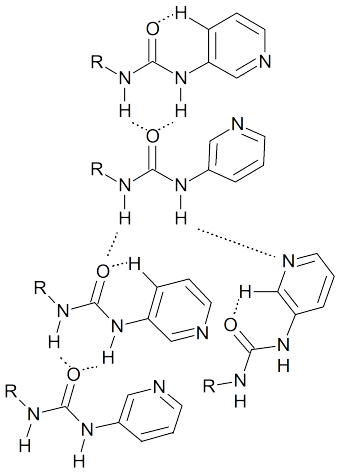

Figure 2.20: Intra- and intermolecular hydrogen bonding in crystals of **2.2**, **2.3** and **2.10**.

In this chapter, a series of bis(pyridylureas) were synthesised by the reaction of α,ω-diamino alkanes with 3-isocyanato-pyridine which was prepared *in situ* from nicotinoyl azide. Crystals of the resulting compounds were grown and the structures solved using X-ray crystallography.

For the compounds **2.2**, **2.3** and **2.10**, the intermolecular bonding, represented in Figure 2.19, is essentially a combination of both the α-tape formed by *N,N′*-diphenylurea and the complexing behaviour of 1,3-bis(*m*-nitrophenyl)urea. This is due to the fact that by only having one pyridyl ring adjacent to the urea group,

only one intramolecular CH···O_{urea} bond can form meaning that the oxygen is a still a sufficient proton acceptor but that the urea NHs have become acidic enough to preferentially form a bifurcated hydrogen-bond. In forming a bifurfacted hydrogen bond, the electron withdrawing effects of the pyridyl nitrogen are not felt by the urea NHs and thus they cannot compete with the CH···O bond in a third molecule. Consequently, a single NH···O_{urea} bond is formed and the remaining NH forms a NH···$N_{pyridyl}$ interaction with the free pyridyl ring of the second bisurea.

One may therefore ask why the bifurcated hydrogen-bonding motif is absent in compound **2.1** but dominates in compound **2.11**. This transition, from none, to half, to all, may only be explained by the structural demands of the spacer group. As these interactions become stronger, either by greater van der Waals attraction in a longer oligomethylene chain or the greater π-π stacking interactions of the naphthalene ring, adjacent urea groups become closer and bind preferentially to form the α-tape.

Chapter 3

Borromean Networks and other Coordination Polymers with *N,N″*-Ethylene-1,2-diylbis(*N′*-pyridin-3-ylurea)

3.1 Introduction

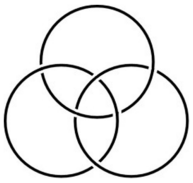

Figure 3.1: A Borromean link.

The Borromean link, shown in Figure 3.1 and Figure 3.2, is three rings which are locked together, but do not interpenetrate *i.e.* removal of one of the rings causes the other two to fall apart. Chemical Borromean ring systems have been reported which are either molecular or found within coordination polymers.[142]

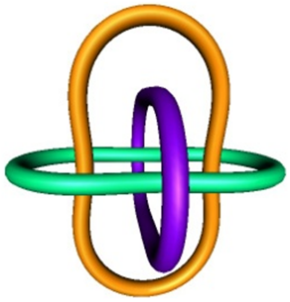

Figure 3.2: Three dimensional representation of the Borromean link.

3.1.1 Molecular Borromean

Molecular Borromean rings are formed during a metal-templated reaction between 2,6-diformylpyridine and a diamine to form the macrocycle shown in Scheme 3.1.[143–147]

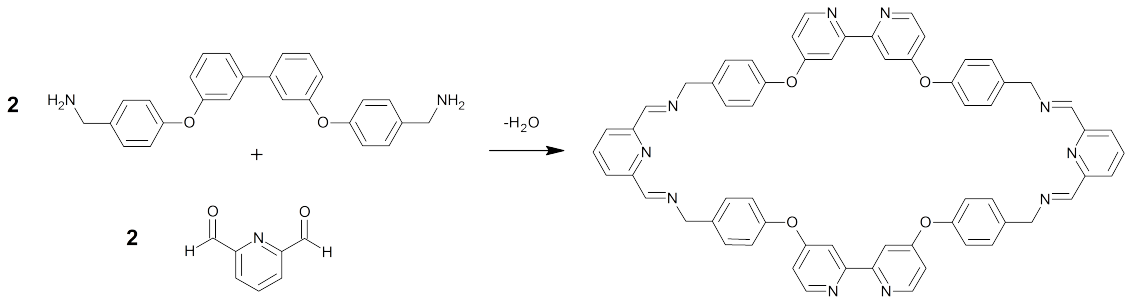

Scheme 3.1: Metal-templated reaction forming a macrocycle.

Without metal templation, a complex mixture of polymeric and macrocyclic products would be expected to form in this reaction, but when zinc(II) acetate is added, the macrocycle forms as a three membered interwoven Borromean with two hexadditional molecules. The final product is bound together by six zinc cations, each coordinated to two macrocycles. One side of each cation is coordinated to a macrocycle *via* its exocyclic bidentate bipyridine, and the other side is bound *via* the endocyclic tridentate diiminopyridine moiety.

3.1.2 Polymeric Borromeans

The Borromean rings are found in the crystal structures of certain coordination polymers but as part of a lattice made up of large undulating hexagonal rings. At each node there is usually a metal ion which is bridged by organic bidentate

ligands. Three lattices interlock but do not interpenetrate thus forming a Borromean weave, as shown in Figure 3.3. Examples of polymeric Borromeans will be discussed forthwith.

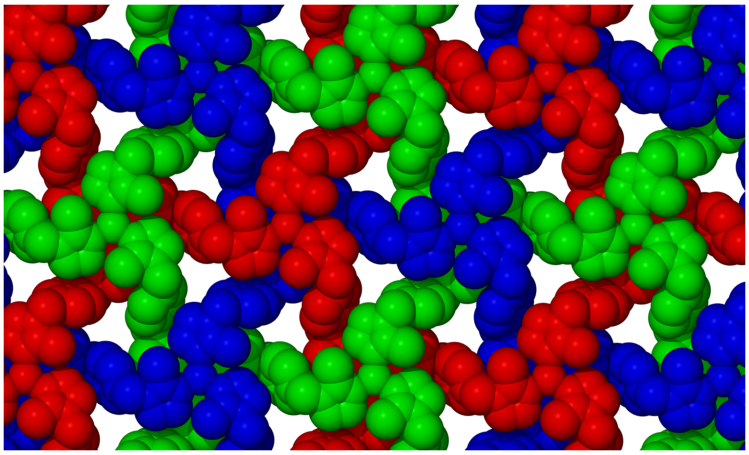

Figure 3.3: A space-filling representation of a Borromean weave.

When a mixture of $[Et_4N]_4[W_4Cu_4S_{12}O_4]$, 4,4′-bipyridine, 4-nitroaniline, CuI and DMF are heated in an evacuated, sealed tube for one day, crystals with the structural formula $[WOS_3Cu_3(4,4'\text{-bipy})_3][I]$ are produced.[148] The lattice is constructed from WOS_3Cu_3 nodes bridged by molecules of 4,4′-bipyridine, as shown in Figure 3.4. The Borromean structure is shown in Figure 3.5. The structure may be reinforced by edge-to-face C–H$\cdots\pi$ interactions between the pyridine rings of adjacent layers where the shortest C$\cdots\pi$ centroid distance is 3.97 Å. Layers are stacked perfectly on top of each other and interact through weak van der Waals interactions.

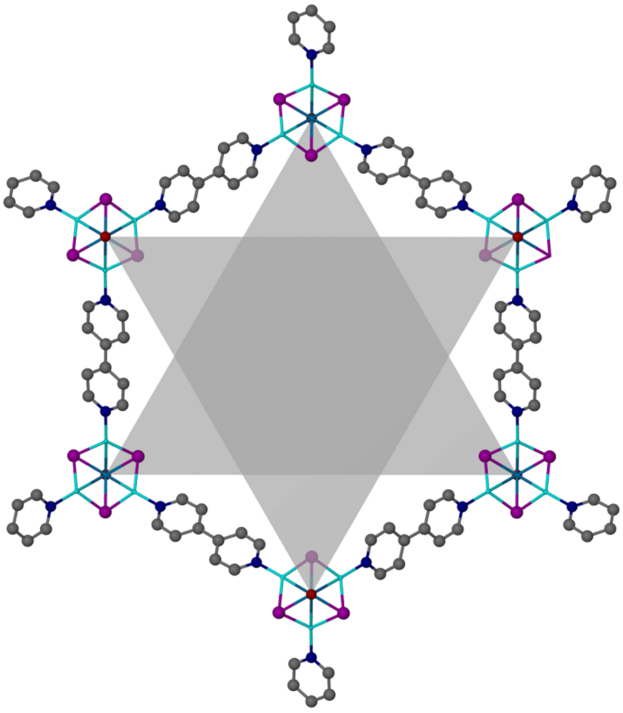

Figure 3.4: Lattice hexagons of 4,4′-bipyridine and WOS_3Cu_3.

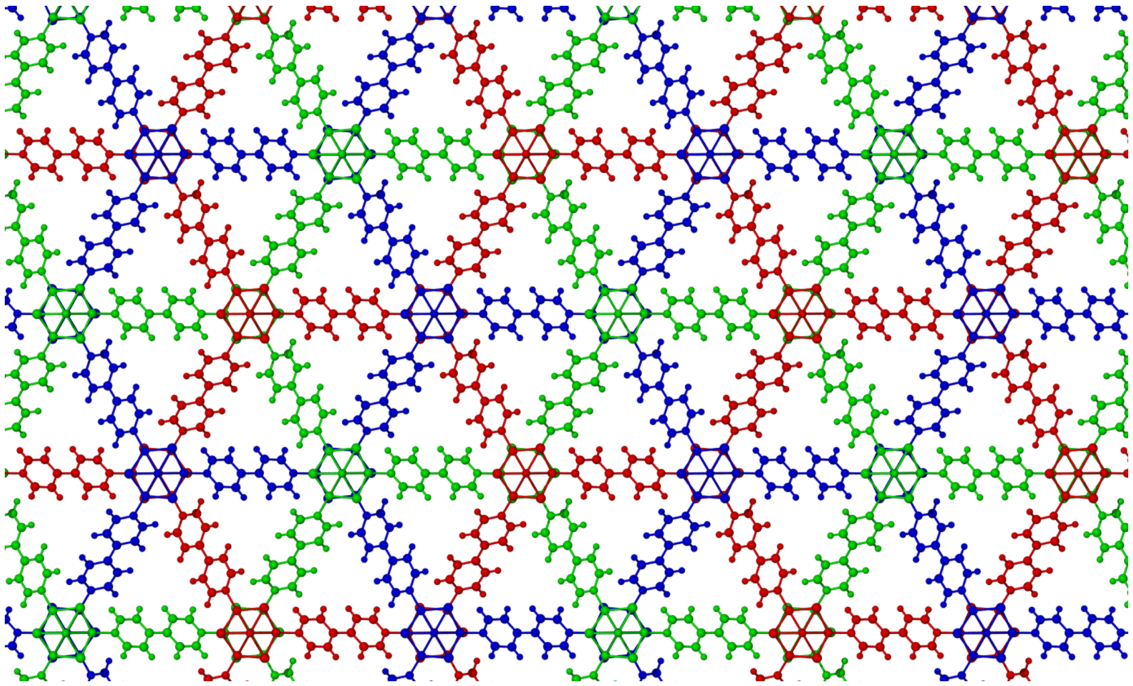

Figure 3.5: Ball and stick representation of the Borromean weave formed with WOS_3Cu_3 and 4,4′-bipyridine.

When the cryptand shown in Figure 3.6 is re-crystallised with potassium iodide and 1,1,2,2,3,3,4,4,5,5,6,6,7,7,8,8-hexadecafluoro-1,8-diiodooctane, a Borromean weave

is formed. The lattice is constructed from nodes of iodine anions which are bridged by the fluorinated octane molecules as shown in Figure 3.7.[149] Each iodine anion is coordinated to three perfluoroalkane molecules *via* their terminal iodine groups. The Borromean weave is shown in Figure 3.8.

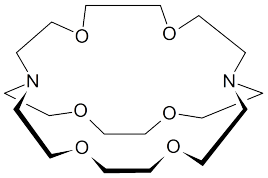

Figure 3.6: The cryptand involved in the formation of a Borromean weave.

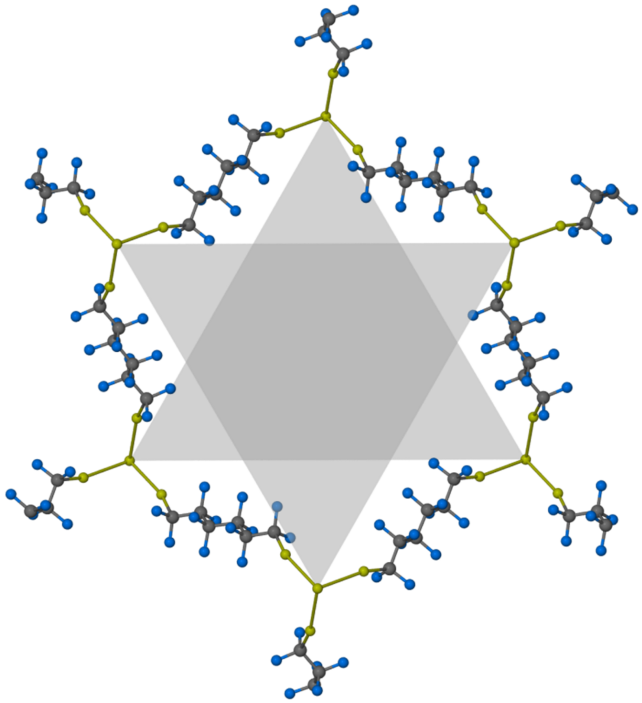

Figure 3.7: Hexagonal Rings from 1,1,2,2,3,3,4,4,5,5,6,6,7,7,8,8-hexadecafluoro-1,8-diiodooctane and Iodine.

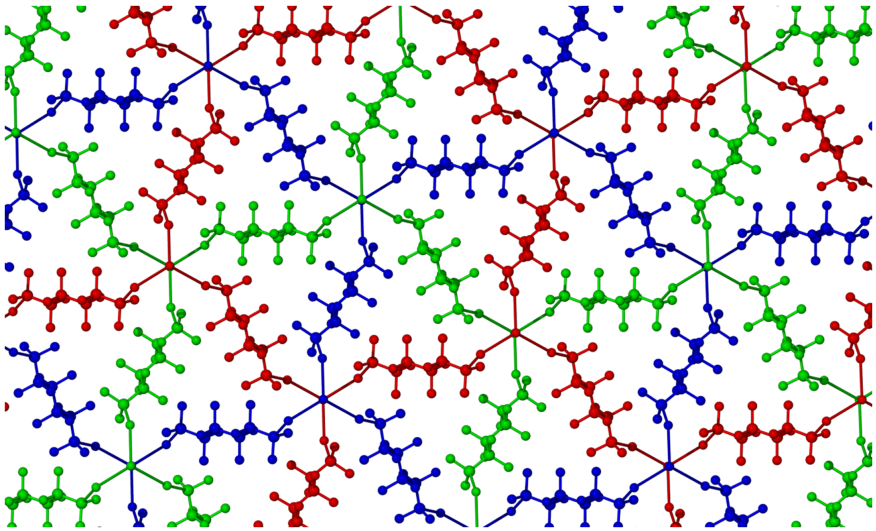

Figure 3.8: Colour coded diagram of the Borromean weave formed from diiodoperfluoroalkanes and iodine anions.

Perhaps structurally the closest to the bis(pyridylureas) mentioned in chapter 2, 1,4-(bis(2-methylimidazol-1-ylmethyl)benzene forms a Borromean coordination polymer with silver(I) tetrafluoroborate when they are re-crystallised from acetonitrile in a 4:1 molar ratio. The ligand adopts a boat conformation in the crystal structure and bridges two silver ions, which are in turn coordinated to two more ligands, leading eventually to a hexagonal ring structure. The Borromean structure is reinforced by *via* Ag···Ag interactions between pairs of lattices and in the remaining space are tetrafluoroborate anions.

3.2 Aims

The interpenetration inherent in Borromean-type structures may afford them increased mechanical strength since the three lattices may only be separated by breaking relatively strong chemical bonds. While this interpenetration is likely to reduced the available free space, it increases the surface area of the framework thereby promoting the adsorption of gases.[150] Within coordination polymer chemistry, there is interest in creating strong porous materials capable of adsorbing guest molecules[150–154] and the aim of this chapter is to follow-up the accidental discovery of **3.1** by synthesising analogous structures with different solvents and counteranions.

3.3 Results and Discussion

Bispyridylureas (**2.1**–**2.3**) were dissolved in mixtures of solvents and crystallisations were attempted in the presence of various metal salts. While the longer **2.2** and **2.3** failed to form complexes, the relatively inflexible **2.1** formed a variety of structures with a number of silver salts. The crystal structures were solved and will be presented herein, as either Borromean-type structures with silver(I) nitrate and non-Borromean-type structures with other silver salts.

3.3.1 Silver(I) nitrate Borromean with water

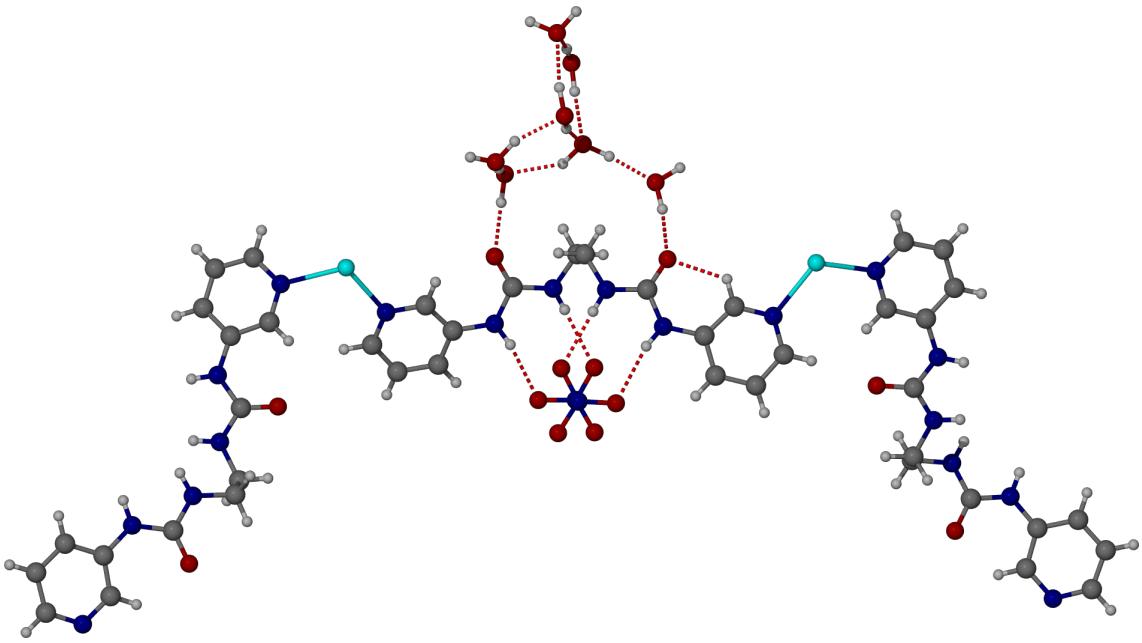

Figure 3.9: The asymmetric unit of $[Ag_2(\mathbf{2.1})_3](NO_3)_2{\cdot}7H_2O$, compound **3.1**.

Slow evaporation of an aqueous DMF solution of **2.1** and silver(I) nitrate led to the formation of crystals. Analysis by X-ray crystallography showed that the crystals are a Borromean-weave coordination polymer with the formula $[Ag_2(\mathbf{2.1}_3](NO_3)_2{\cdot}7H_2O$ and its asymmetric unit is shown in Figure 3.9. Both Ag(I) atoms in the asymmetric unit act as nodes in a lattice made up of large hexanuclear rings (Figure 3.10) formed from the doubly connected, dipyridyl ligands as shown in Figure 3.11.

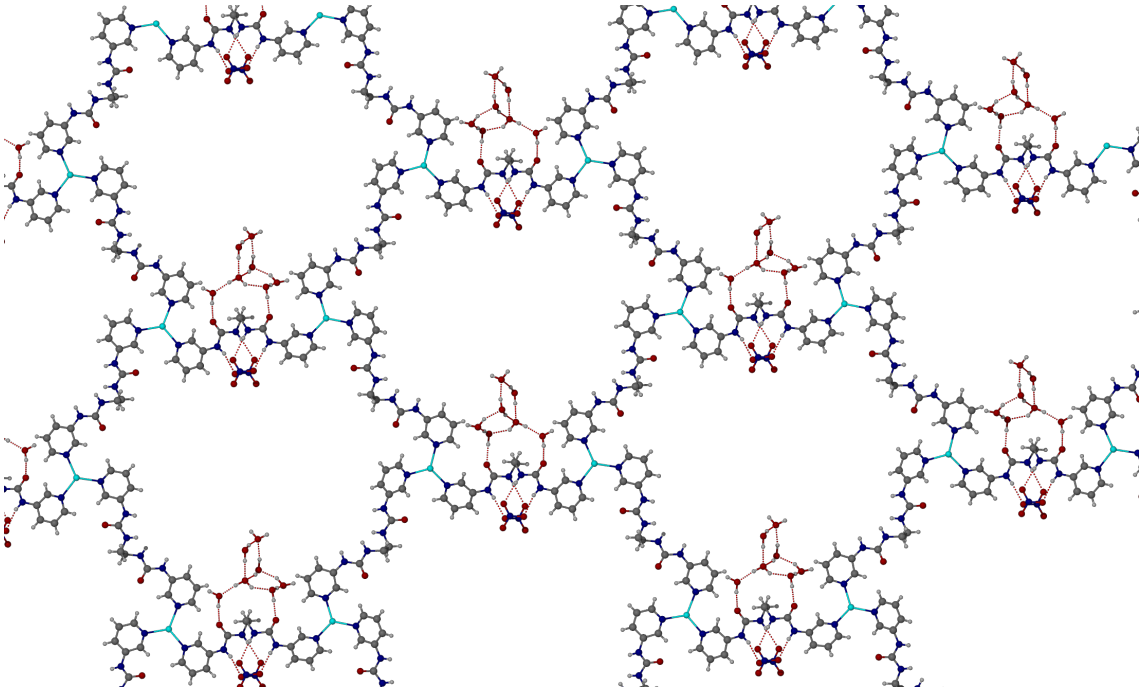

Figure 3.10: The hexanuclear rings of the Borromean weave.

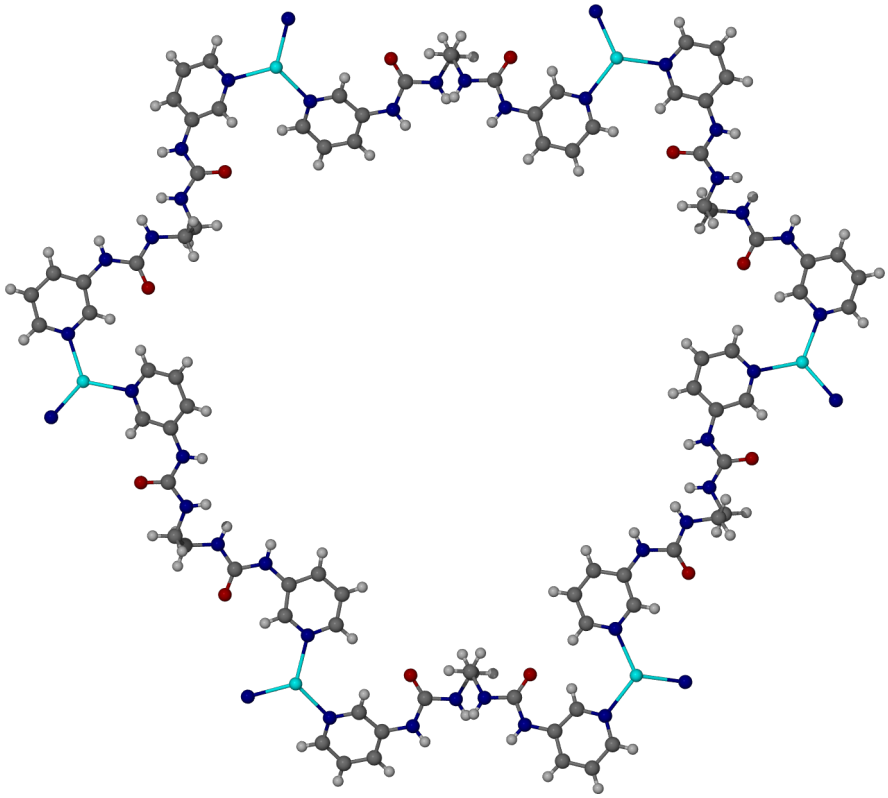

Figure 3.11: The macrocyclic ring in **3.1** (diameter approximately 31.5 Å) comprising six Ag(I) ions and six ligands. Three ligands have their NH groups pointing into the macrocycle and three point outside to give an approximately threefold symmetry.

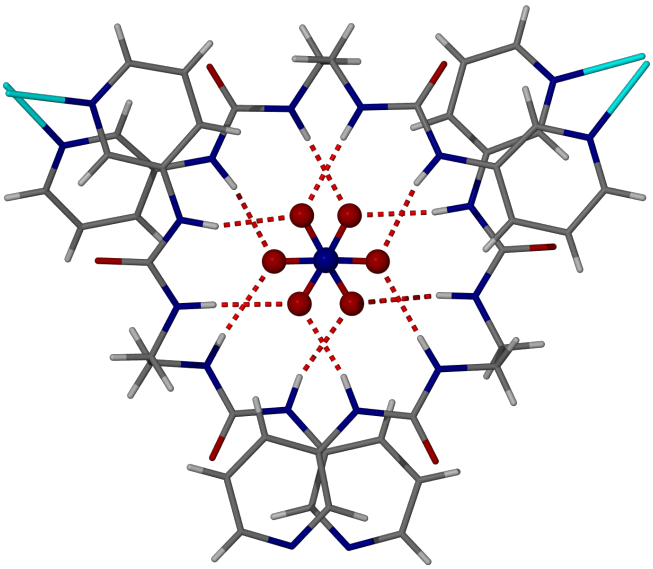

Figure 3.12: Two nitrate anions bonded to three separate ligands.

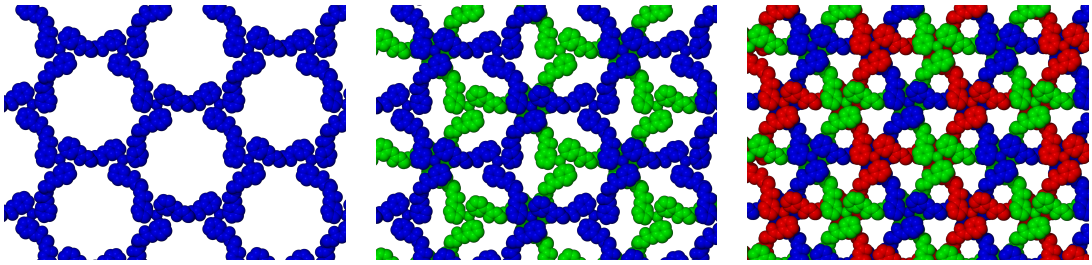

(a) The blue network made up of large hexanuclear rings

(b) The green network lies underneath the blue network

(c) All three networks lock to give a Borromean weave.

Figure 3.13: Interlocking of the Borromean Weave

Out of the six bis(pyridylurea) ligands that make up the macrocycle, three have their NH groups pointing inward, three point outwards, and all bind to the nitrate anions. Throughout the structure, the nitrate anions form infinite stacks, with each anion surrounded by a total of three urea groups from three different ligands, each belonging to a separate sheet, as shown in Figure 3.12. Each urea···nitrate interaction is an eight-membered hydrogen-bonded ring and as each anion is surrounded by six NH hydrogen-bond donors, the bonding is completely saturated. Compared to the free ligand, the hydrogen-bonding to the nitrate in the complex is weaker than that of the free ligand (which engages in strong NH···$N_{pyridyl}$ interactions) as $\tilde{\nu}$(NH) in the solid-state IR spectrum shifts from 3301 to 3337 cm^{-1}. The interlocking non-interpenetrating nature of the structure, what defines it as a Borromean, can

be seen in the series of space-filling models of Figure 3.13. At every crossing point, the blue network passes over the green network. Were it not for the red network in 3.13c, which passes over the blue network but underneath the green network, the two would be easily separable. The 3.21 Å spacing between the anions within the Borromean weave allows the stack to be supported by argentophilic interactions between three pairs of stacked Ag(I) cations (Ag···Ag 3.54 Å) that surround the anion cavity. Along with the nitrate anion cavity, there is an additional cavity that is occupied by a seven-membered water cluster, shown in Figure 3.14. The cluster is bound on one side *via* an apical water molecule to two pyridyl groups *via* a pair of CH···O hydrogen-bonds and on the other by an Ag···O interaction. The cluster also forms strong OH···O interactions with the urea carbonyl groups.

Thermogravimetric analysis of the compound showed that the water cluster is extremely tightly held by the network, with no weight loss occurring prior to decomposition at 172 °C.

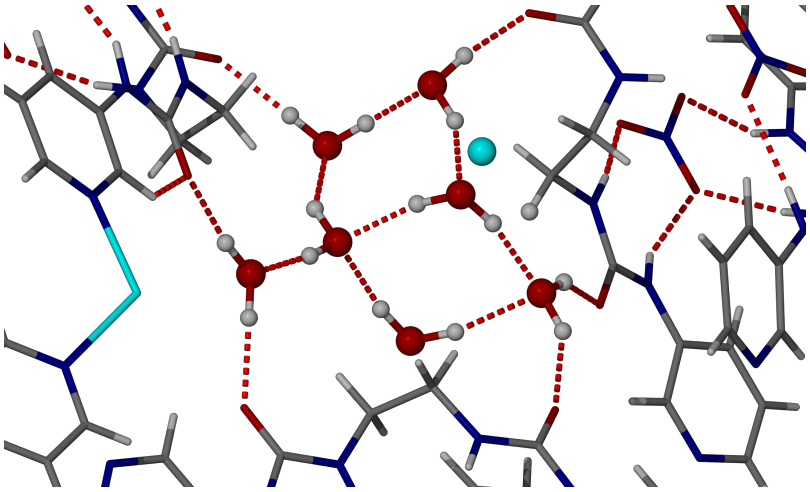

Figure 3.14: The seven-membered water cluster in $[Ag_2(\mathbf{2.1})_3](NO_3)_2{\cdot}7H_2O$.

3.3.2 Other silver(I) nitrate Borromeans

When the crystallisation of **2.1** in the presence of silver(I) nitrate was performed in a selection of other solvents, four different crystal structures were obtained; their molecular formula, including that of **3.1**, was determined by elemental analysis and/or X-ray crystallography and are shown in Table 3.1.

Table 3.1: Formulae of five Borromeans of **2.1** and silver(I) nitrate from a variety of solvent mixtures.

Borromean	Formula	Solvent System
3.1	$[Ag_2(\mathbf{2.1})_3](NO_3)_2{\cdot}7H_2O$	DMF and water (1:1, 6 mL)
3.2	$[Ag_2(\mathbf{2.1})_3](NO_3)_2{\cdot}5H_2O{\cdot}MeOH$	MeOH and water (1:1, 6 mL)
3.3	$3[Ag(\mathbf{2.1})_{1.5}]NO_3{\cdot}3MeCN{\cdot}2CHCl_3{\cdot}MeOH$	MeCN, $CHCl_3$ and MeOH (3:3:4, 15 mL)
3.4	$[Ag_2(\mathbf{2.1})_3](NO_3)_2{\cdot}5H_2O{\cdot}MeCN$	MeCN and water (1:1, 6 mL)
3.5	$[Ag_2(\mathbf{2.1})_3](NO_3)_2{\cdot}7H_2O{\cdot}2MeCN$	MeCN and $CHCl_3$ (1:1, 9 mL)

The four additional structures, **3.2**–**3.5** are essentially pseudopolymorphs of the previously described **3.1**. Each is a Borromean, sharing the same structure in which each weave (shown in Figure 3.15) is adjacent to its mirror image equivalent. Within a pair, the solvent clusters are always adjacent to an Ag_2 unit and the nitrates stacked and therefore, depending on how the paired weaves, or layers stack, each Borromean contains a minimum of a four-membered nitrate channel. As with **3.1**, the layers in **3.2** and **3.3** are stacked to form infinite nitrate channels and the solvent clusters always have an Ag_2 unit adjacent to them on both sides, as shown in Figure 3.16.

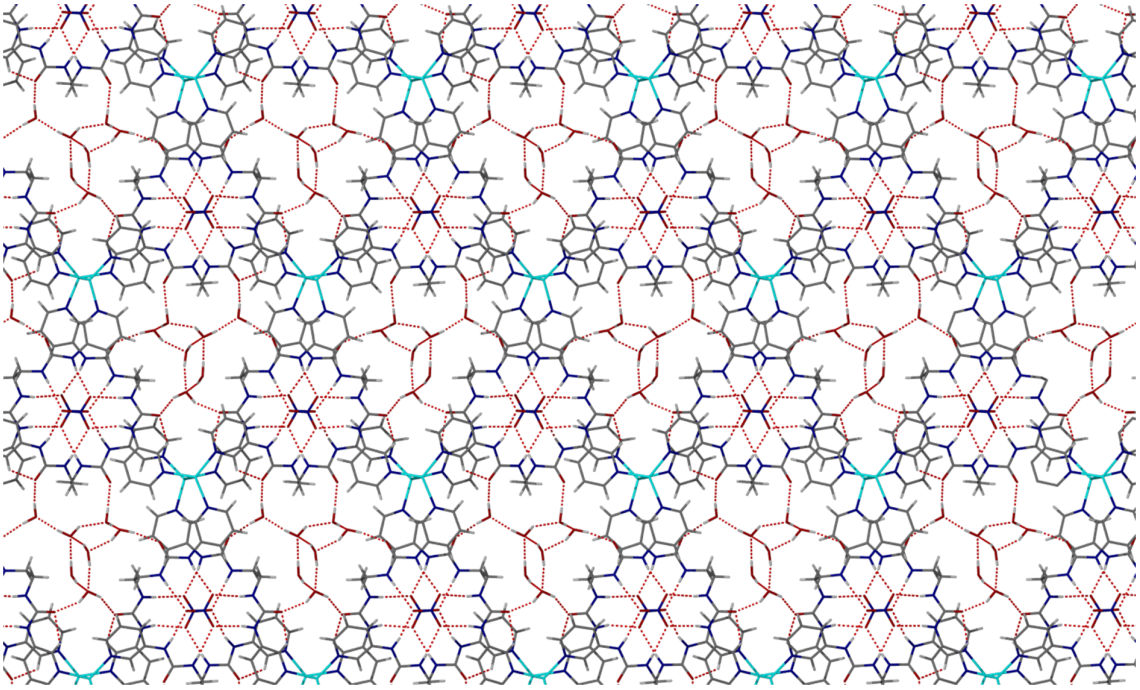

Figure 3.15: A single weave of **3.1**.

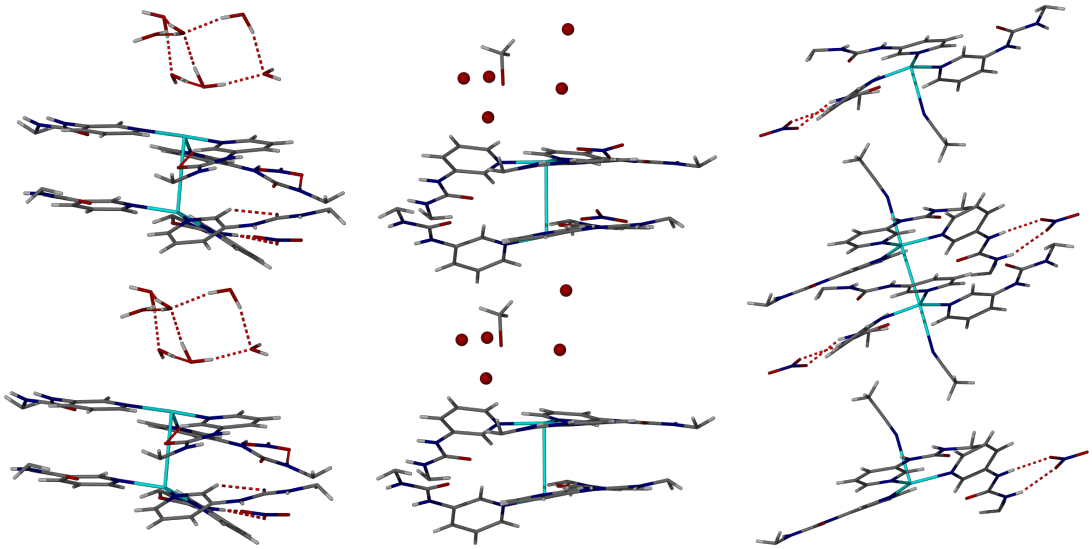

(a) **3.1** (b) **3.2** (c) **3.3**

Figure 3.16: The stacked solvent cluster–Ag_2 units of **3.1**, **3.2** and **3.3**

3.1 and **3.2** are related further as the solvent cluster of the former is equivalent to that of **3.2** except the central quadruply hydrogen-bonded water is replaced by a molecule of methanol. The solvent cluster of **3.3** is made up of two molecules of acetonitrile and two additional molecules which are, by elemental analysis, one

third of the time methanol and two thirds chloroform. In this case therefore, a single solvent cluster is able to co-ordinate to two Ag_2 units in adjacent weaves. Thus, channels of nitrate form and the Ag_2 units stack alternately with the solvent clusters.

With **3.4** and **3.5**, this alternate stacking of Ag_2 and solvent cluster is not present and a translation between the layers removes the nitrate channels. In **3.4**, the solvent cluster is comprised of five molecules of water and one of acetonitrile by X-ray crystallography. Layers are arranged so that the Ag_2–solvent clusters are stacked alternately with a four-membered nitrate channel, as shown in Figure 3.17 possibly driven by the lack of a second molecule of acetonitrile to allow adjacent layers to interact. This arrangement, as well as the out-of-plane twisting of the pyridyls at the Ag(I) centres, allows adjacent layers to stack *via* π-π stacking (Figure 3.18).

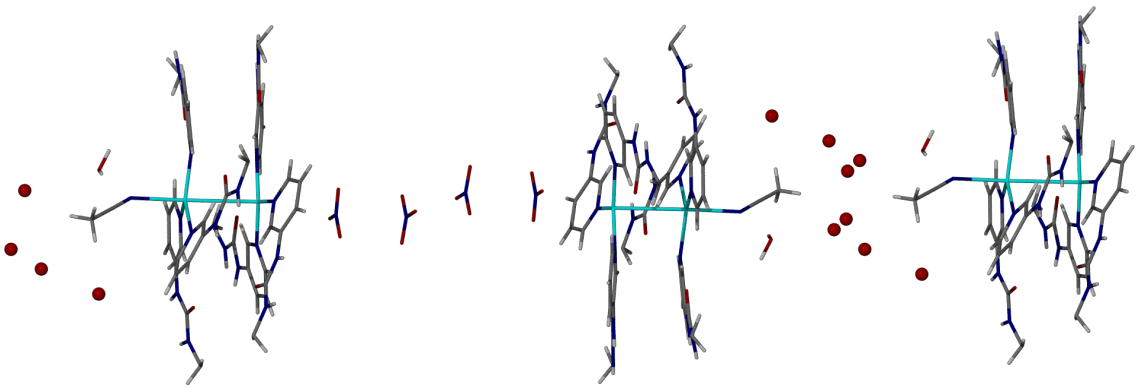

Figure 3.17: Stacking of the layers in **3.4**. The Ag_2–solvent clusters from one layer are alternately stacked with the four-membered nitrate channel of the adjacent layers.

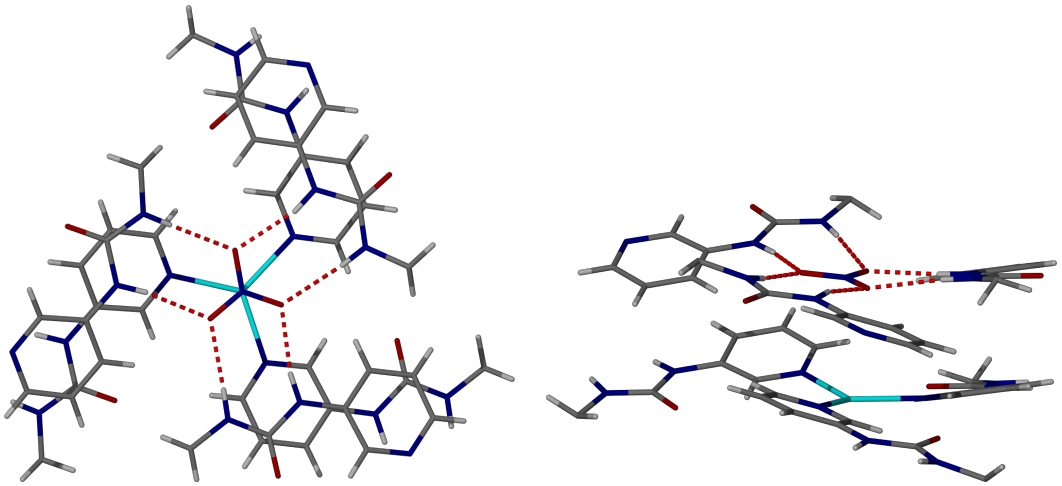

(a) (b)

Figure 3.18: The π-π stacking interaction between adjacent layers of **3.4**.

In **3.5**, the silver(I) pair lies between an ethylene bridge of one of the ligands in the adjacent layer and the solvent cluster from the adjacent weave which 'caps' the silver(I) pair was shown to be comprised of seven molecules of water and two of acetonitrile by elemental analysis. Although the exact positions of the cluster contents is unclear, there appears to be a water molecule in each layer that is 2.822 and 2.764 Å from the oxygens of two urea carbonyl groups. This water molecule in turn is 2.860 Å from another which lies between the layers, an occupant of both (Figure 3.19). With no stacking of either the pyridyl groups (Figure 3.18) or the Ag_2 and solvent clusters, the layers therefore may be interacting through these hydrogen-bonds (Figure 3.20).

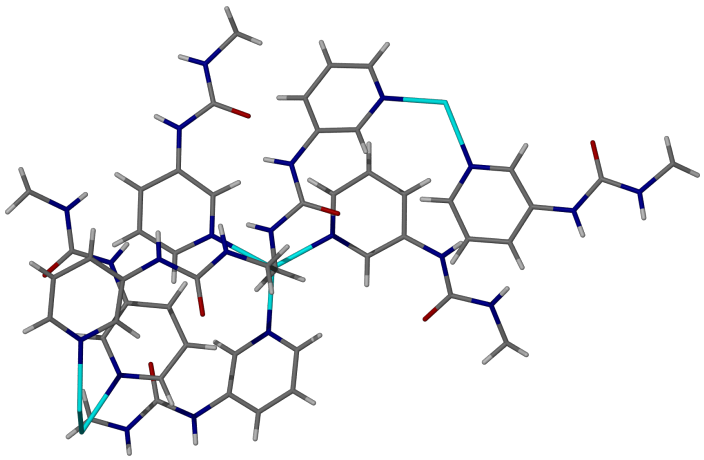

Figure 3.19: The non-π-π stacking of layers in **3.5**.

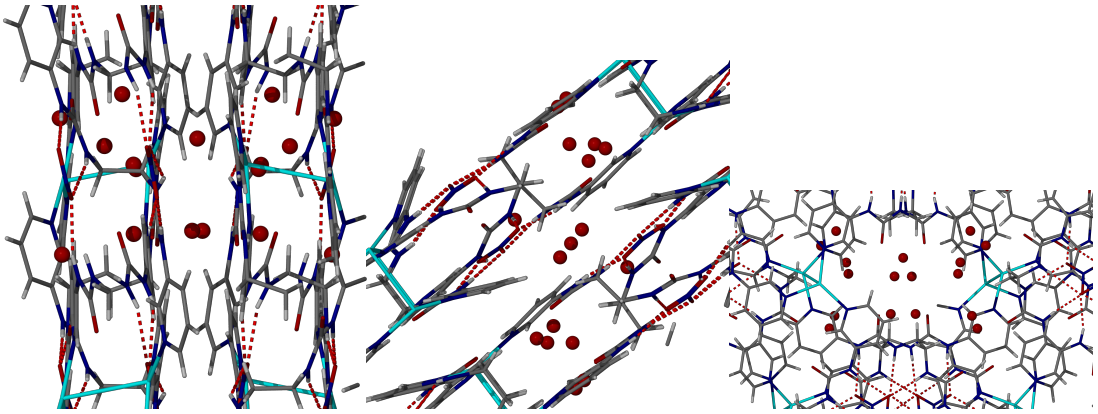

(a) a axis (b) b axis (c) c axis

Figure 3.20: Three views of the solvent clusters of two layers in **3.5** along its three axes.

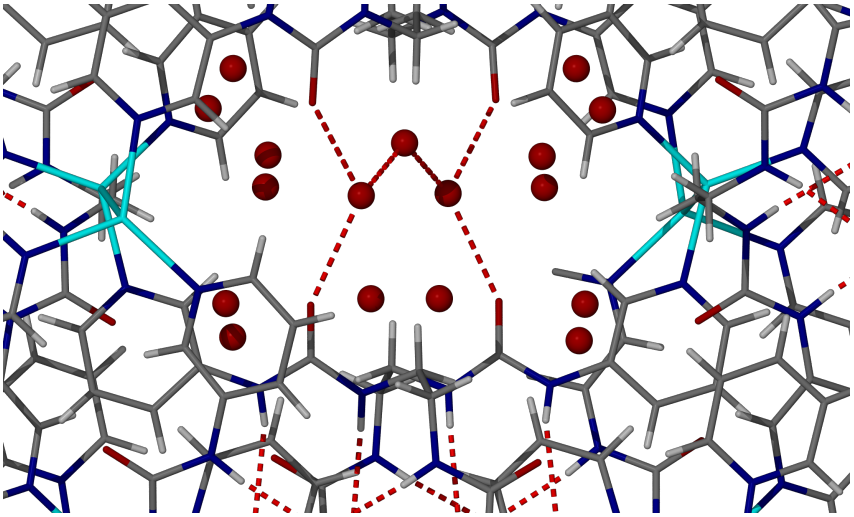

Figure 3.21: Tentative urea-water-water-water-urea hydrogen-bonding between the layers of **3.5**.

3.3.3 Coordination polymer with copper(II) nitrate

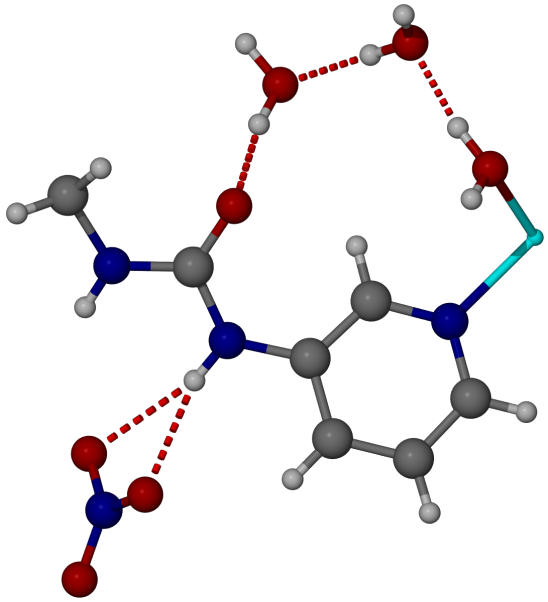

Figure 3.22: The asymmetric unit of a coordination polymer formed from **2.1** and copper(II) nitrate.

When **2.1** was re-crystallised in aqueous THF in the presence of copper(II) nitrate, crystals formed upon evaporation of the solvent. X-ray crystallographic analysis showed that the crystal structure is a 1:1 coordination polymer between the ligand and copper(II) nitrate. The asymmetric unit, contains half a molecule of *N,N″*-ethylene-1,2-diylbis(*N′*-pyridin-3-ylurea). The urea NH closest to the aryl ring binds to an adjacent nitrate anion by a $R_1^2(4)$ bifurcated hydrogen-bond, while the other remains unbound. The urea oxygen is hydrogen-bonded to a six-membered water cluster, one member of which coordinates to the copper(II) centre, *trans* to a water of an adjacent cluster. Along with the two molecules of water, the octahedral copper(II) centre, shown in Figure 3.23 also has two pyridyl nitrogens bound to it, and through this, the long chains are formed (Figure 3.24). There are two nitrate ions bound to the centre from chains which lie above and below.

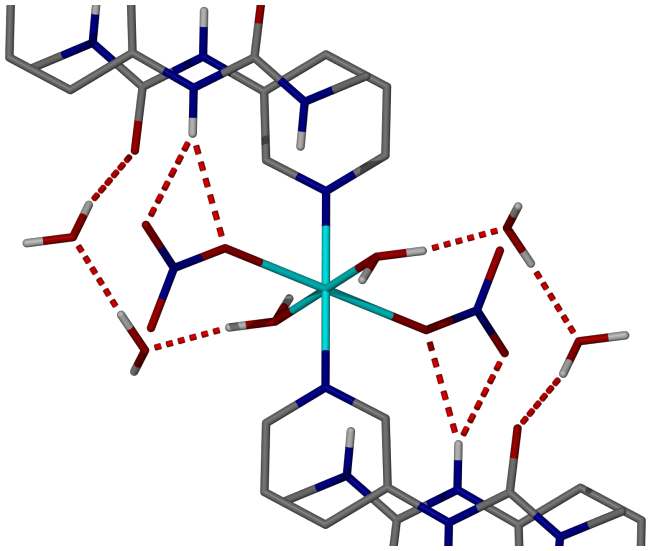

Figure 3.23: The octahedral copper(II) centre. Pyridyl and ethylene hydrogen atoms removed for clarity.

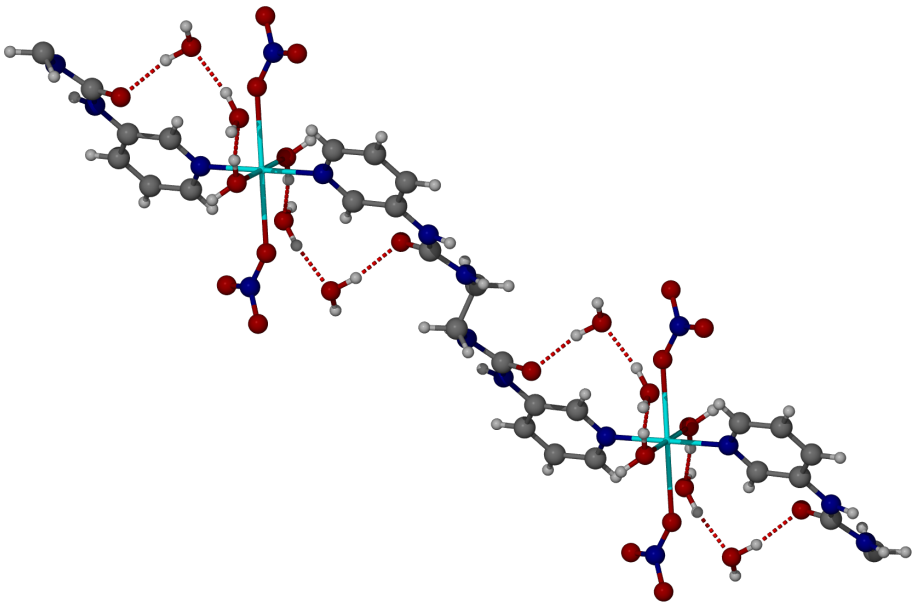

Figure 3.24: The coordination polymer formed from **2.1** and copper(II) nitrate.

3.3.4 Coordination polymer with silver(I) nitrate

When **2.1** was recrystallised in a mixture of acetonitrile, chloroform and methanol (3:3:4) in the presence of silver(I) nitrate, crystals formed within five minutes of standing. The structure was solved using X-ray crystallography and was shown to be a [2+2] metallomacrocycle as shown in Figure 3.25 similar to that reported

with *N,N″*-methylenebisphenyl-4,1-diylbis(*N′*-pyridin-3-ylurea).[155] Both pyridyl nitrogens coordinate to a silver(I) atom which are both in turn coordinated to a second molecule, thus forming the metallomacrocycle. The chain is subsequently formed by four $R_2^2(8)$ bifurcated hydrogen-bonds forming two ureanitrateurea interactions between the pairs of macrocycles. Molecules of chloroform and acetonitrile are coordinated to the nitrate and silver, respectively and the overall structure is packed through van der Waals interactions.

The solvent mixture used in this crystallisation is identical to that used to synthesise **3.3**, but at half the volume. Therefore as this structure is formed the fastest, it is likely to be the kinetic product of the crystallisation whereas **3.3** is the more stable thermodynamic product.

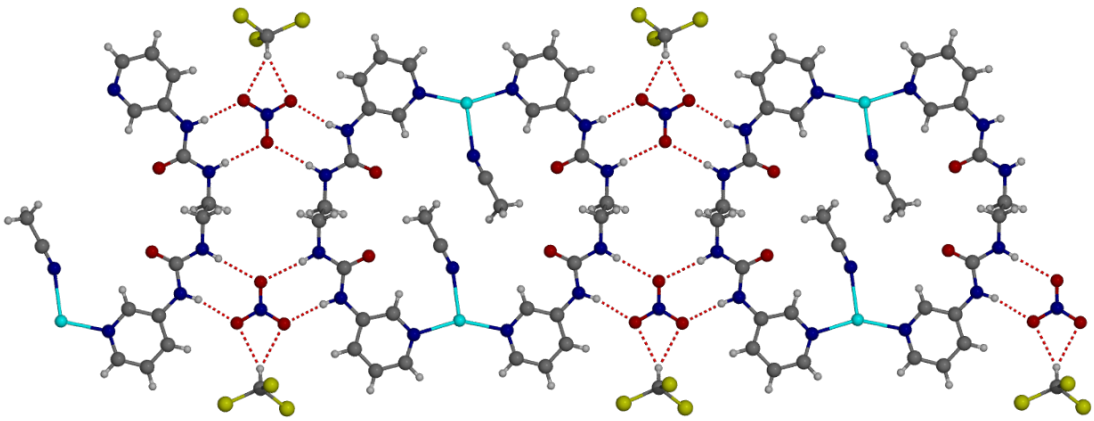

Figure 3.25: The metallomacrocycle formed from silver(I) nitrate and **2.1**.

3.3.5 Coordination polymer with silver(I) acetate

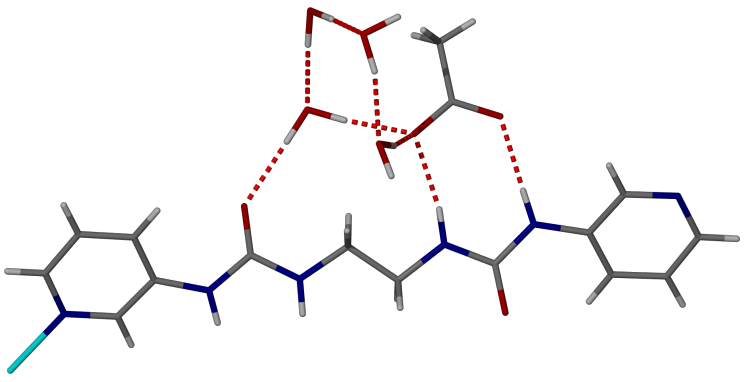

Figure 3.26: The asymmetric unit of a coordination polymer formed from **2.1** and silver(I) acetate.

When **2.1** was recrystallised in aqueous ethanol in the presence of silver(I) acetate, crystals formed upon slow evaporation of the solvent. The structure was solved using X-ray crystallography and was shown to be a 1:1 coordination polymer between the ligand and silver(I) acetate. The asymmetric unit, shown in Figure 3.26, contains a whole molecule of **2.1** as each urea takes part in a different binding mode. One urea is bonded to an acetate anion (containing a disordered methyl group) *via* a $R_8^8(8)$ bifurcated hydrogen-bond and the other is bound *via* a $R_2^1(6)$ hydrogen-bond to a urea oxygen on an adjacent chain. Thus adjacent chains are connected alternately *via* an acetate–water cluster and urea–urea bifurcated hydrogen-bonding, as shown in Figure 3.27. The sheets of double chains are stacked *via* the cluster with two hydrogen-bonds between an unbound hydrogen on the water attached to the acetate anion and a free lone pair on an adjacent water molecule, shown in Figure 3.28

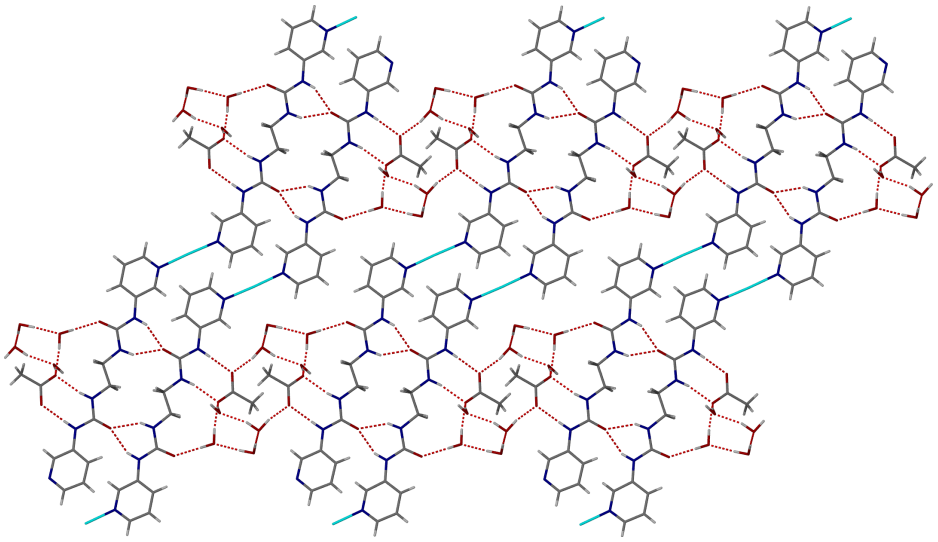

Figure 3.27: The acetate–water cluster and ureaurea alternation in crystals of **2.1** and silver(I) acetate.

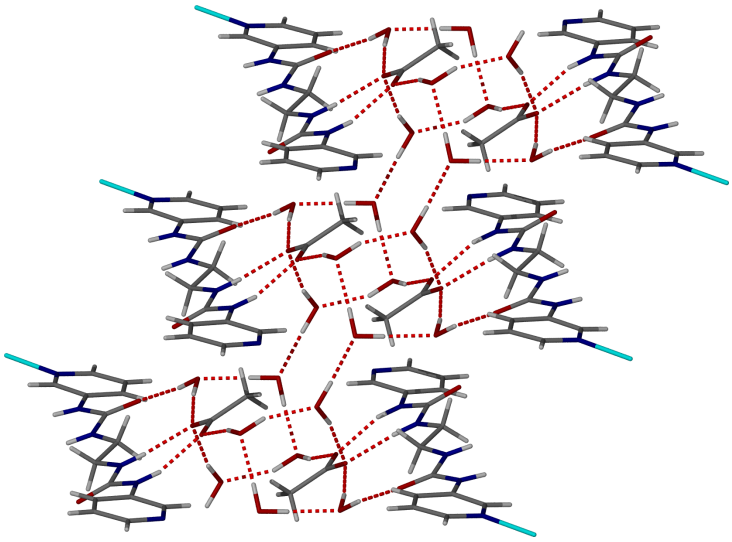

Figure 3.28: Stacking of the urea–acetate sheets through the water cluster.

3.3.6 Coordination polymer with silver(I) tetrafluoroborate

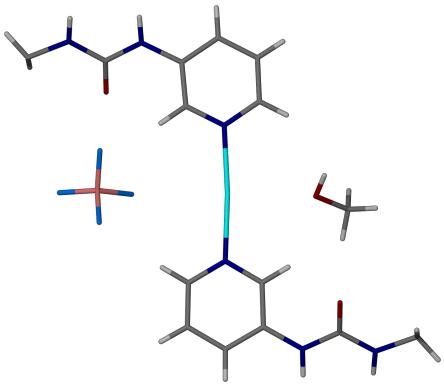

Figure 3.29: The asymmetric unit of the crystal formed with **2.1** and silver(I) tetrafluoroborate.

N,*N*″-ethylene-1,2-diylbis(*N*′-pyridin-3-ylurea) recrystallised in aqueous methanol in the presence of silver(I) tetrafluoroborate. Upon slow evaporation of the solvent, crystals formed which were analysed using X-ray crystallography and shown to have the asymmetric unit shown in Figure 3.29. The bis(urea) and silver(I) form long chains and are interconnected by bifurcated hydrogen bonding, as shown in Figure 3.30. The methanol and tetrafluroborate anions lie in between the stacked layers next to the silver(I) centres, shown in Figure 3.31.

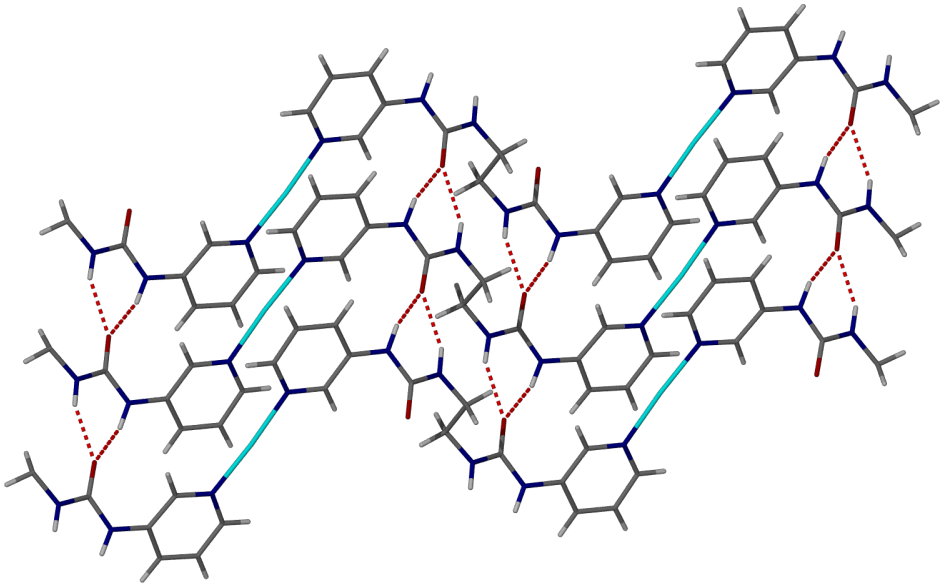

Figure 3.30: Bifurcated hydrogen-bonding between chains of **2.1** and silver(I) tetrafluorobroate.

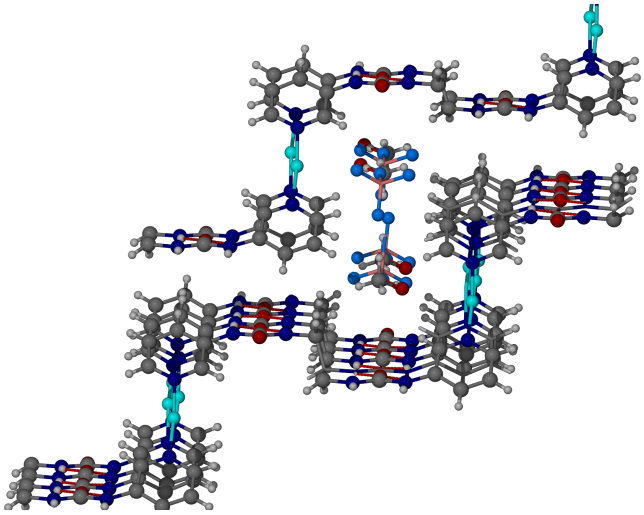

Figure 3.31: The methanol and tetrafluroborate anions lie in between the stacked layers next to the silver(I) centres.

3.3.7 Coordination polymer with silver(I) hexafluorophosphate

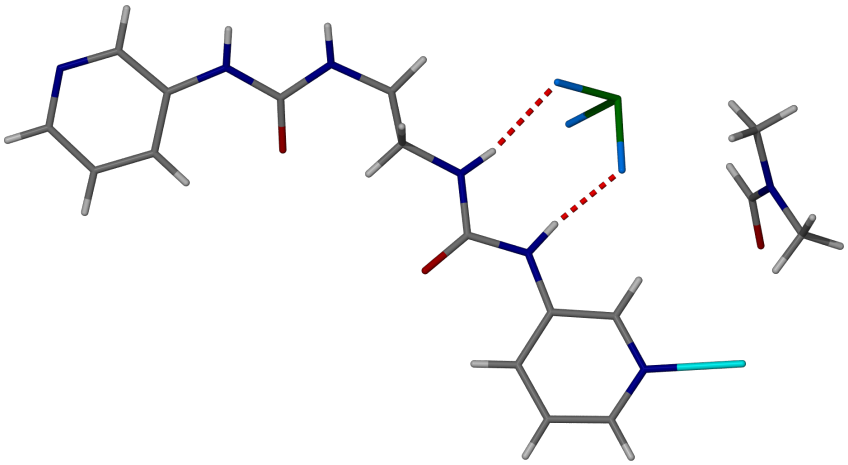

Figure 3.32: The asymmetric unit of the crystal formed with **2.1** and silver(I) hexafluorophosphate.

N,N″-ethylene-1,2-diylbis(*N′*-pyridin-3-ylurea) was recrystallised in a solution of silver(I) acetate in MeCN and DMF (1:1), Upon slow evaporation of the solvent, crystals formed which were analysed using X-ray crystallography, and its asymmetric unit is shown in Figure 3.32. Again, the structure is a 1:1 coordination polymer, and in this case, both ureas are bound to the hexafluorophosphate anion. with a $R_2^2(8)$ bifurcated hydrogen-bond. An additional three bis(urea) molecules bind to the anion as shown in Figure 3.33, the function of which is to allow stacking in the additional two dimensions by the formation of sheets, shown in Figure 3.34

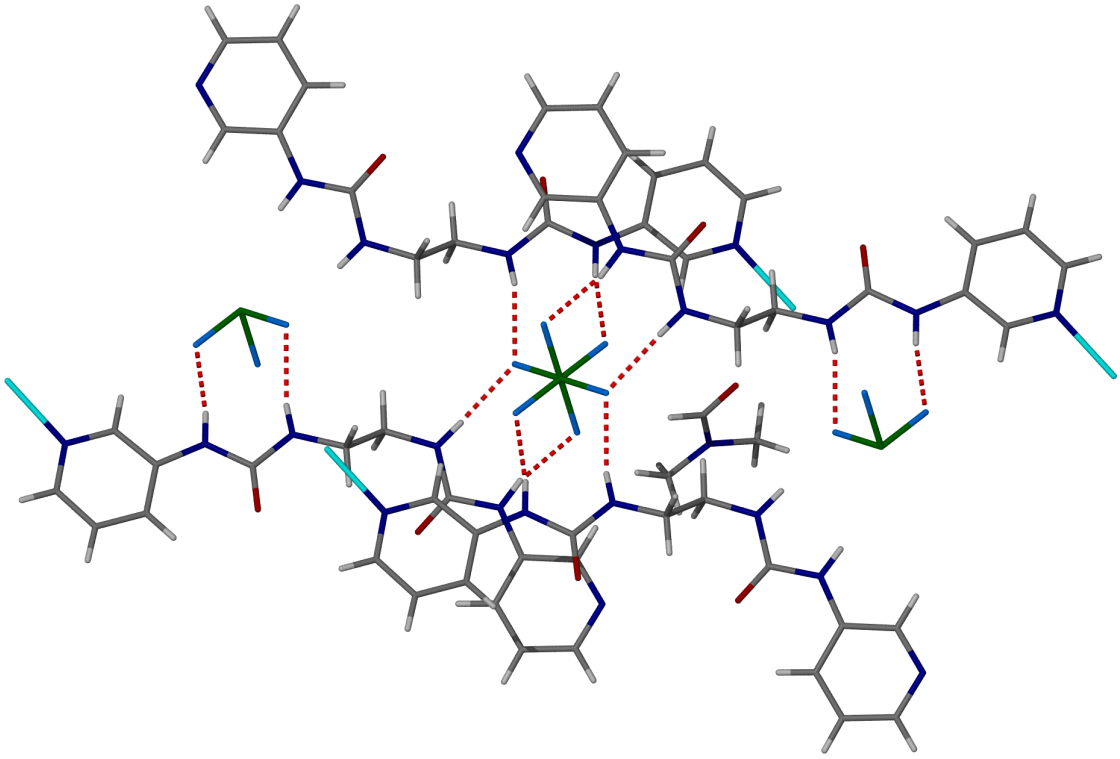

Figure 3.33: The hexafluorophospate 'capsule' formed with with **2.1** and silver(I) hexafluorophosphate.

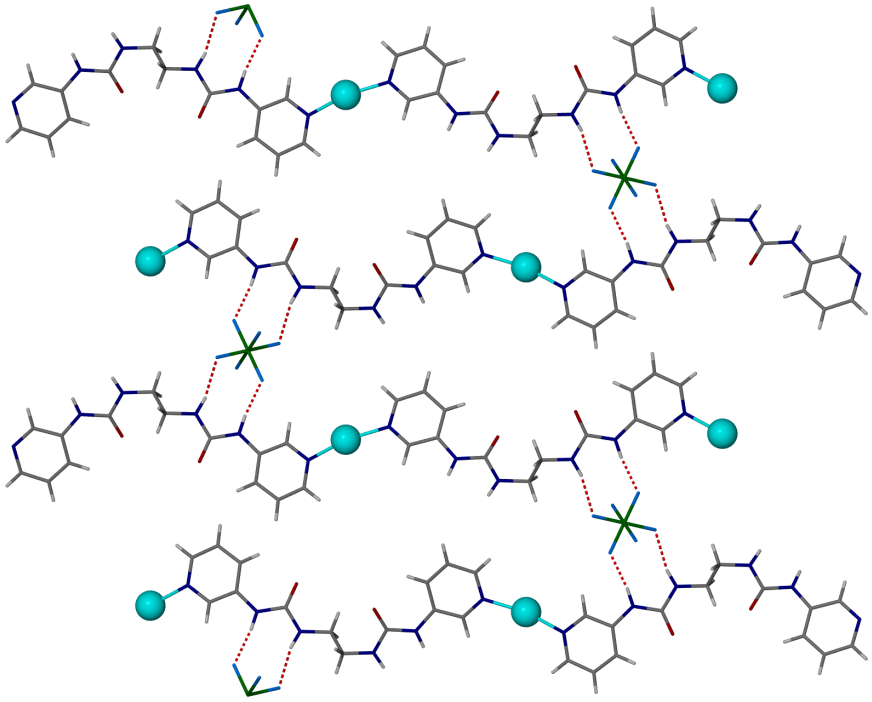

Figure 3.34: Sheets formed with **2.1** and silver(I) hexafluorophosphate.

3.4 Conclusion

In this chapter, *N,N″*-ethylene-1,2-diylbis(*N′*-pyridin-3-ylurea) was crystallised with silver(I) nitrate to form a series five pseudopolymorphs of a Borromean-type structure. While other Borromean structures have been reported based on π-stacking, halogen-bonding, argentophilic, and aurophilic interactions,[142,148,156–160] those synthesised in this chapter are the first to incorporate both a well-defined nitrate-binding motif[161] and a versatile cavity which is flexible enough to incorporate a variety of solvents. Considering how the layers stack together, the five structures fall into three types distinguished by how the components of the layers stack. In all five examples, the layers are always made up of two paired Borromean weaves, one of which is the mirror image of the other, in which the nitrates are stacked. Therefore, each Ag_2 node is always capped on one side, by a solvent pocket. In one type, adopted when the solvent pocket is comprised either of seven water molecules or two molecules of methanol and five of water or finally two molecules of acetonitrile and a 2:1 mixture of chloroform and methanol, the remaining side of the Ag_2 unit is capped by the solvent pocket of an adjacent weave. Thus in this Borromean, the nitrates of individual layers are adjacent to each other thereby forming infinite stacks.

In the second type, adopted when the solvent system is five molecules of water and one of acetonitrile, the remaining face of the Ag_2 node lies over a nitrate channel of an adjacent layer. This arrangement maximises the π-π stacking interaction between the pyridyl units bound to Ag(I) of one layer and three pyridyl units of three separate ligands bound to the nitrate that lies under the node.

In the third type, adopted when the solvent cavity was shown to be comprised of seven molecules of water and two of acetonitrile by elemental analysis, the remaining face of the Ag_2 node lies over an ethylene bridge of a ligand in the adjacent layer. This arrangement, aside from van der Waals interactions, may be stacked by the interaction of two solvent pockets of adjacent layers. Indeed, one water molecule is shared between two layers, hydrogen-bonded to two water molecules in the adjacent layers which are in turn hydrogen-bonded to a urea oxygen.

Additional structures were synthesised with copper(II) nitrate and silver(I) nitrate, acetate, tetrafluoroborate and hexafluorophosphate and crucially, none are of a Borromean-type structure and therefore it could be said that the specific metal salt directs the formation of the ring system. The additional structure formed with silver(I) nitrate, the metallomacrocycle, shows that the Borromean structure is one of at least two structures which are possible with this metal salt. Being formed the slowest, it represents the thermodynamic product of this reaction.

Chapter 4

A Quintuple Helix and other Coordination Polymers with *N,N″*-Pentylene-1,5-diylbis(*N′*-pyridin-3-ylurea)

4.1 Introduction

A helix is a three-dimensional curve which winds around a cylinder or cone, such that its angle to a plane perpendicular to the axis is constant. As the curve may either wind anti-clockwise or clockwise, helices possess chirality. In chemistry, coordination polymers are particularly suited to form helical structures due to their versatility and wide range of nodes, spacers and secondary functionality. The formation, or self-assembly of multiple helical structures can be characterised in three steps.[162] The first step is the formation of a single helix taking into account conformation effects, followed by the mutual intertwining of multiple helices, and thirdly, lateral association of the braids into a solid network. First level assembly of a single helix may be directed by molecular design, for example the incorporation of a twisted 1,1′-binaphthyl unit into a rigid bridging ligand to induce the coordination polymer to assemble into a helix.[163] Second-level assembly to give multiple helixes is also

subject to molecular design: incorporating a long spacer between the helical turns favours highly interbraided systems. Third level assembly may also be dependent on molecular design by the incorporation of a molecular functionality that directs lateral interactions and packing of the helices. Examples of single, double, triple and quadruple helices are relatively well known,[164] but there are few examples of quintuple helices.[163,165,166]

4.2 Aims

The design and control of supramolecular helicity is an area of interest within co-ordination polymer chemistry.[165,167–172] In this chapter, the design and control of a quintuple helix system shall be attempted using *N,N″*-pentylene-1,5-diylbis(*N′*-pyridin-3-ylurea) briefly mentioned in chapter 2. The pentamethylene spacer of ligand and indeed more generally those separated by long oligomethylene chains promotes the stacking of the molecules *via* van der Waals interactions. Whether this stacking gives rise to the desired helical structures should ultimately depend on the metal salts used in the crystallisation.

4.3 Results and Discussion

N,N″-pentylene-1,5-diylbis(*N′*-pyridin-3-ylurea) (**2.4**) was synthesised as described in chapter 2 and re-crystallised in the presence of various metal salts, from various solvent mixtures. Three solutions yielded crystals, and in each case, the ligand is planar and the oligomethylene chain adopts an all *anti* conformation which gives the molecule two faces: one is a hydrogen-bond donor face comprised of four NH groups and the other face is hydrogen-bond accepting from two urea carbonyl groups. In each case, at least one urea functionality is involved in $R_2^2(8)$ hydrogen-bonded ring to an anion and the other interacts with solvent molecules.

4.3.1 Planar Complex with Silver(I) Nitrate

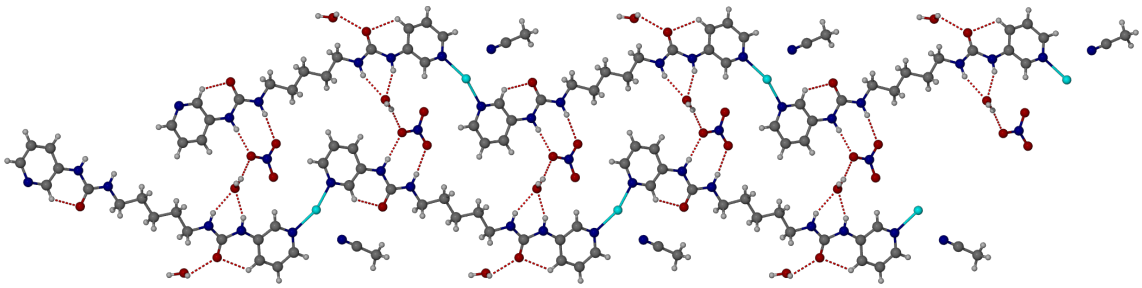

Figure 4.1: Coordination polymer chains formed from **2.4** and silver(I) nitrate.

When **2.4** was re-crystallised from a 1:1:1 mixture of methanol, chloroform, and acetonitrile in the presence of silver(I) nitrate, crystals formed upon slow evaporation. The crystals were characterised by X-ray crystallography and elemental analysis. X-ray crystallography showed that the bis(pyridylurea) forms a one dimensional coordination polymer with the silver(I) nitrate with the formula [Ag(**2.4**)]NO_3·MeCN·1.75H_2O. Acetonitrile and water are incorporated into the structure, with the latter acting as a bridge between adjacent chains with the nitrate anions (Figure 4.1). For each ligand, one urea group hydrogen-bonds to a nitrate anion with an $R_2^2(8)$ motif, and the other to a water molecule forming a $R_2^1(6)$ motif. The water molecule is in turn hydrogen-bonded to an adjacent nitrate anion and thus the NO_3–H_2O unit sits between two offset urea groups. Perpendicular to the nitrate plane, where it is not a good hydrogen-bond acceptor, the planar sheets are connected by the remaining water OH hydrogen atom *via* a hydrogen-bonds, as shown in Figure 4.2.[161,173,174]

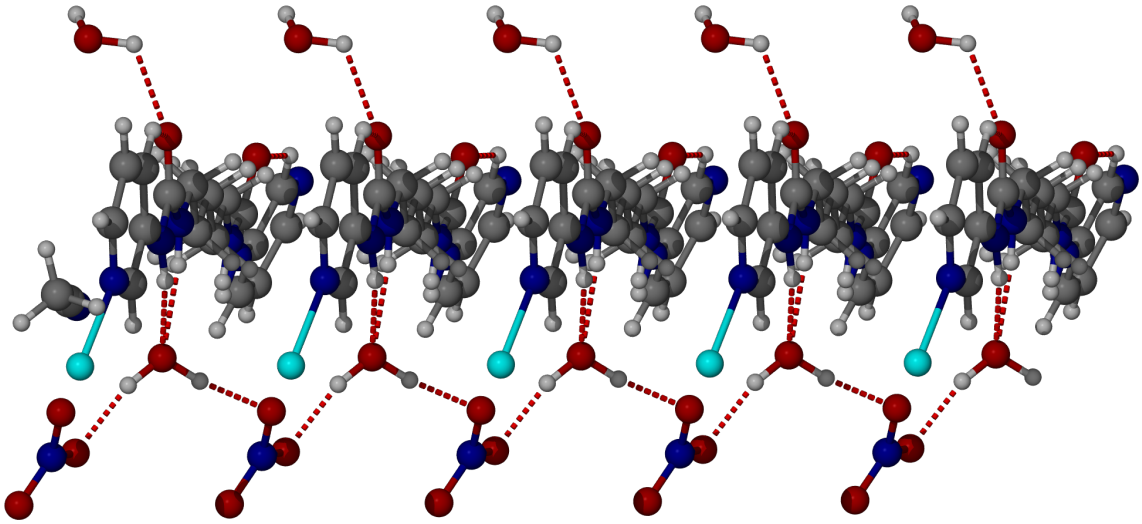

Figure 4.2: The bridging water molecules between stacked planar sheets.

4.3.2 Single Helix with Silver(I) Acetate

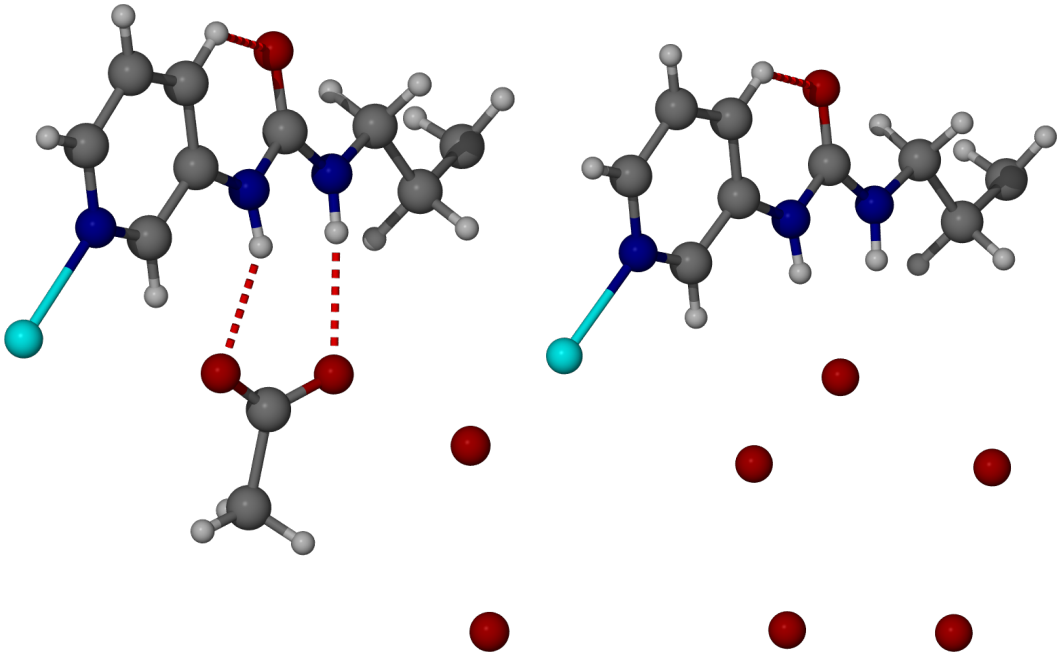

(a) The urea bonds to a five membered water cluster.

(b) The urea bonds to an acetate anion which in turn hydrogen-bonds two water molecules.

Figure 4.3: Two versions of the asymmetric unit, which occur in equal numbers in the crystal structure.

When *N,N″*-pentylene-1,5-diylbis(*N′*-pyridin-3-ylurea) was re-crystallised from aqueous THF in the presence of silver(I) acetate, crystals formed upon slow evaporation which were characterised by X-ray crystallography. The geometry of the

ligand and Ag^+ ions is essentially a single helix (shown in Figure 4.4), much like the structure with silver tetrafluoroborate, but less twisted around the metal and adjacent chains are not intertwined. The asymmetric unit is comprised of half of a ligand which is bound *via* the urea moiety, 50% of the time to a five membered water cluster and 50% of the time to an acetate molecule and two water molecules (Shown in Figure 4.3.). In both cases, the molecules bridge adjacent ligands and form channels through the crystal, shown in Figure 4.5.

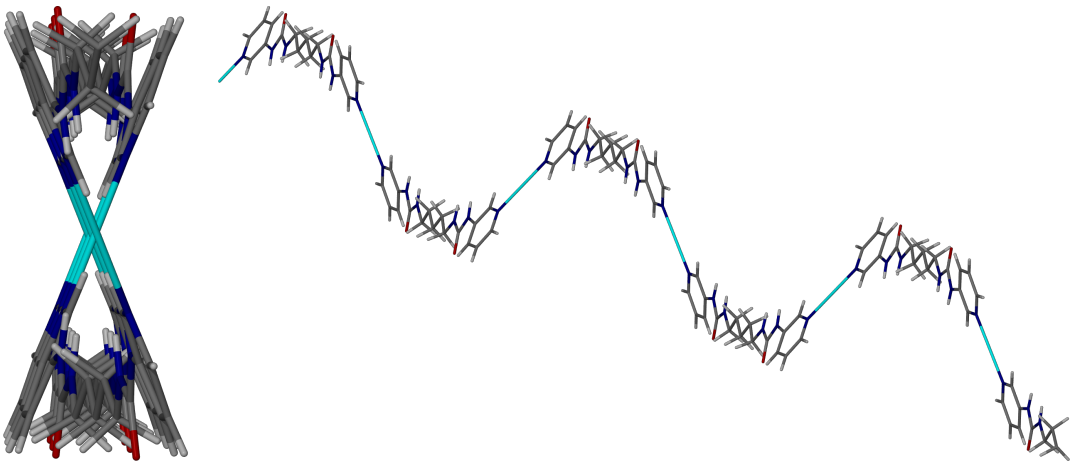

(a) (b)

Figure 4.4: The single helix of **2.4** and silver(I) acetate.

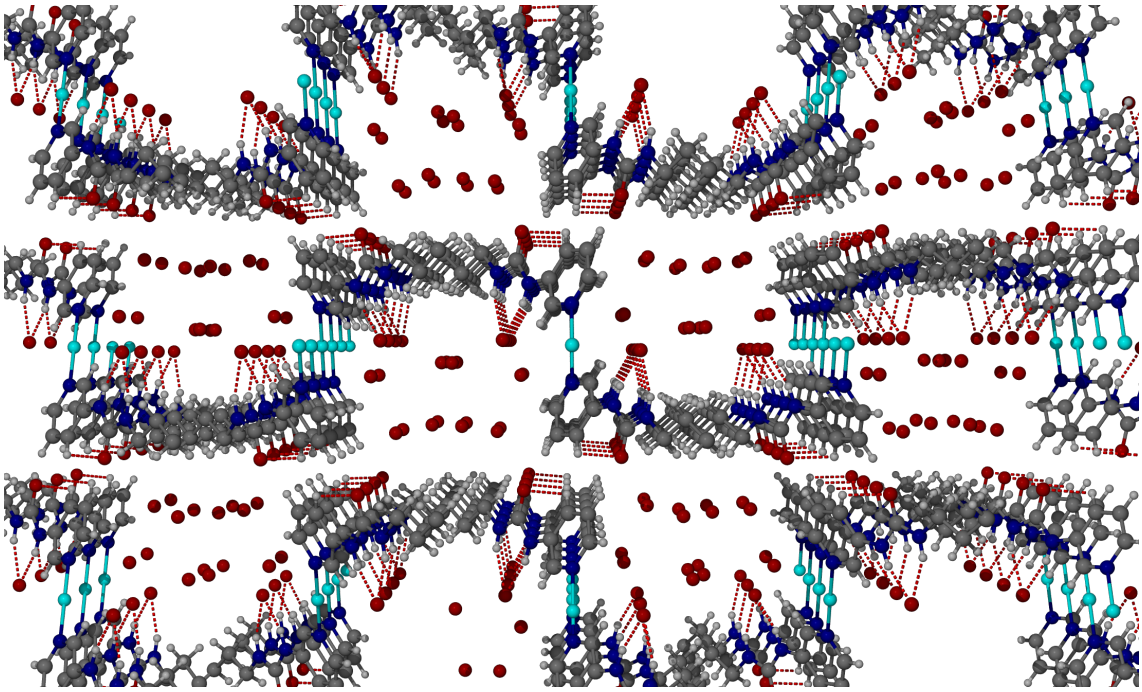

Figure 4.5: Water channels through the **2.4** and silver(I) acetate crystal.

4.3.3 Quintuple Helix with Silver(I) Tetrafluoroborate

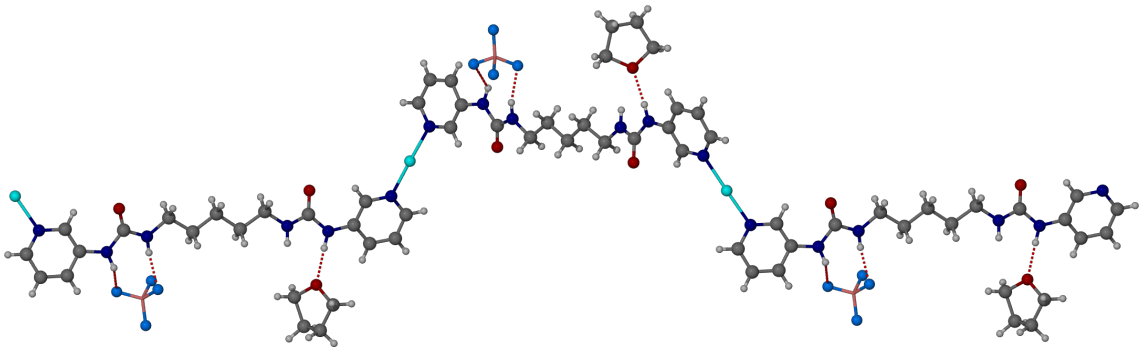

Figure 4.6: The coordination polymer formed from **2.4** and $AgBF_4$.

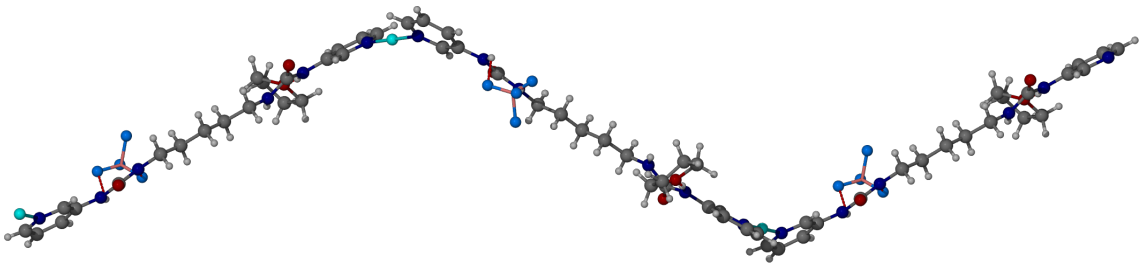

Figure 4.7: The coordination polymer formed from **2.4** adopts a zig-zag, helical structure.

When **2.4** was re-crystallised from aqueous THF in the presence of silver(I) tetrafluoroborate, crystals formed upon slow evaporation and these were characterised by X-ray crystallography.

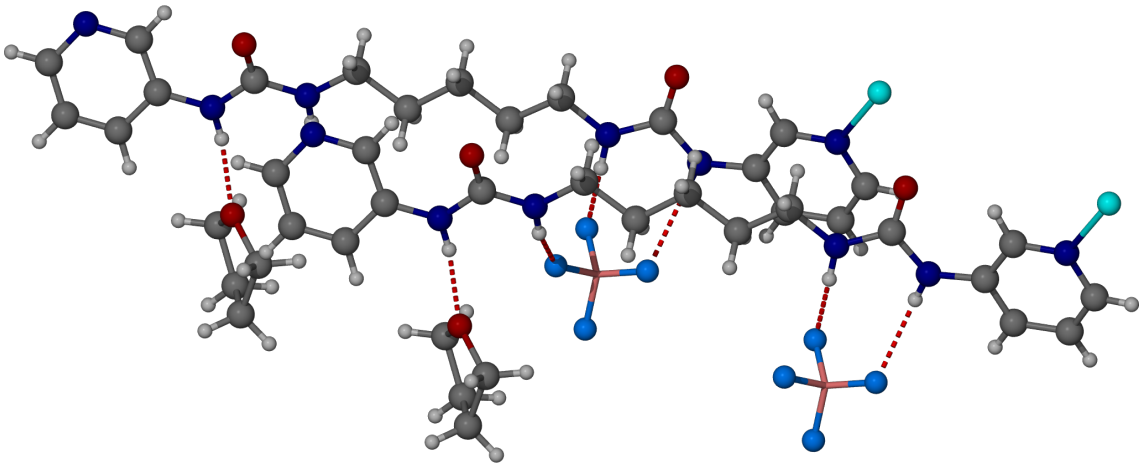

Figure 4.8: Two adjacent bis(pyridylurea) ligands connected *via* a NH···F interaction to a BF_4^- anion.

X-ray crystallography shows that the structure is a coordination polymer with Ag(I) ions bridging the bis(pyridylurea) ligands in the form of a single helix shown in Figure 4.6 and Figure 4.7. Of the two urea units, one is bound to a BF_4^- anion *via* an eight-membered hydrogen-bonded ring (graph set notation of $R_2^2(8)$) and with the other, one NH is bound 50% of the time to a molecule of THF, and 50% of the time to a water molecule. The remaining NH group bonds to an adjacent BF_4^- anion as shown in Figure 4.8. The water, THF and BF_4^- anions lie in layers in-between layers of coordination polymer. The ligands stack in a near-orthogonal arrangement which due to the pentamethylene chain, allows five helices to intertwine, as shown in Figure 4.9, and form a quintuple helical molecular braid, shown in Figure 4.10.

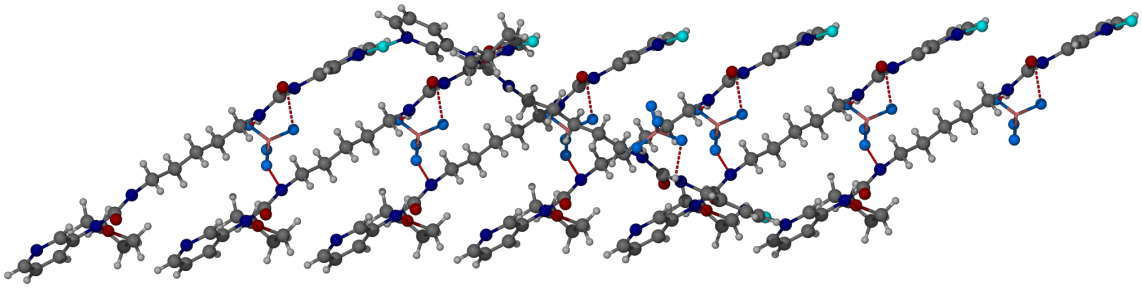

Figure 4.9: The penamethylene chain allows five helices to intertwine.

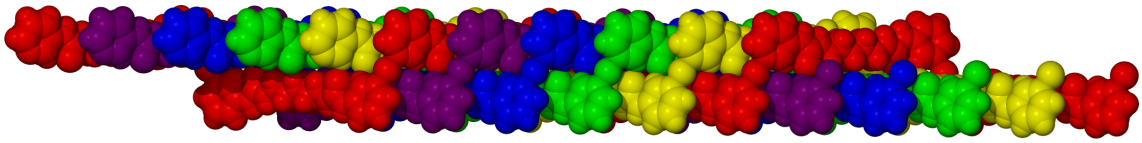

Figure 4.10: Space-filling representation of the quintuple helix formed.

4.4 Conclusion

In this chapter, three coordination polymers between *N,N″*-pentylene-1,5-diylbis(*N′*-pyridin-3-ylurea) and silver(I) nitrate, tetrafluoroborate and acetate have been synthesised. Each are similar in that they are a 1:1 coordination polymer between the silver(I) salt and the ligand, but the way they go on to stack is different. In the case of the nitrate, the structure is essentially planar, with ligands bound together through pyridyl–Ag and a nitrate–water pair. For both acetate and tetrafluoroborate, the ligands are connected again through the Ag(I), the opposing pyridyls are out-of-plane, leading to a wave-type structure. How these individual chains stack, and in the case of tetrafluoroborate, form a quintuple helix is ultimately driven by the interactions of anion and the solvent molecules present. It may be that the formation of a quintuple helix is, in part, directed by the intermolecular bonding mode of this anion between the urea groups of two adjacent chains.

Chapter 5

Gels from selected bis(pyridylurea)s

5.1 Introduction

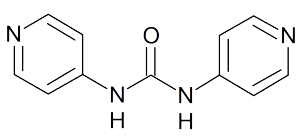

5.1

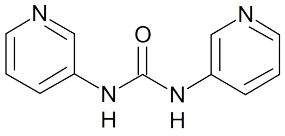

5.2

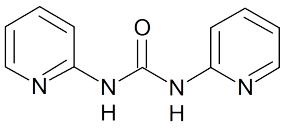

5.3

There are several examples of pyridyl-functionalised organogelators. Compounds **5.1**–**5.3**, are the three symmetrical isomers of *N,N′*-bis(pyridyl)urea. While compounds **5.2** and **5.3** are non-gelators, compound **5.1** forms opaque, thermoreversible gels in water with a minimum gelator concentration of 0.8 wt %. The IR spectrum of the gel shows that the C=O band which appears at 1740 cm^{-1} in neat samples of **5.1** is shifted 5 cm^{-1} lower in the gel. This shift indicates there is stronger hydrogen-bonding in the gel state. The gelling ability of compound **5.1** is pH sensitive. At the minimum gelator concentration, the pH of the solution is found to be 8.3; when this is lowered to 5.3 using 1% acetic acid, a gel fails to form. When the pH is raised back to between 9 and 10 with sodium hydrogen carbonate, gels are formed. These observations suggest that the pyridyl nitrogen may need to be

unprotonated for self-assembly and gel formation. This is further shown by the inability of the monohydrochloride salt of **5.1** to form gels.[175,176] When compound **5.1** is re-crystallised in the presence of zinc perchlorate, the urea moiety binds to the perchlorate anion and the zinc ions bridge the nitrogen atoms on adjacent pyridyl rings. The resulting structure is a diamondoid network as shown in Figure 5.1. On the other hand, when compound **5.2** is re-crystallised with zinc perchlorate, the low temperature structure is a square grid coordination polymer as also shown in Figure 5.1.[175] Compound **5.1** has also been reported to act as a chelating ligand in the complex *trans*-[Ni(ONO_2)$_2$(**5.1**)$_2$] where a pyridyl nitrogen atom coordinates to the nickel centre along with the urea oxygen atom.[177,178]

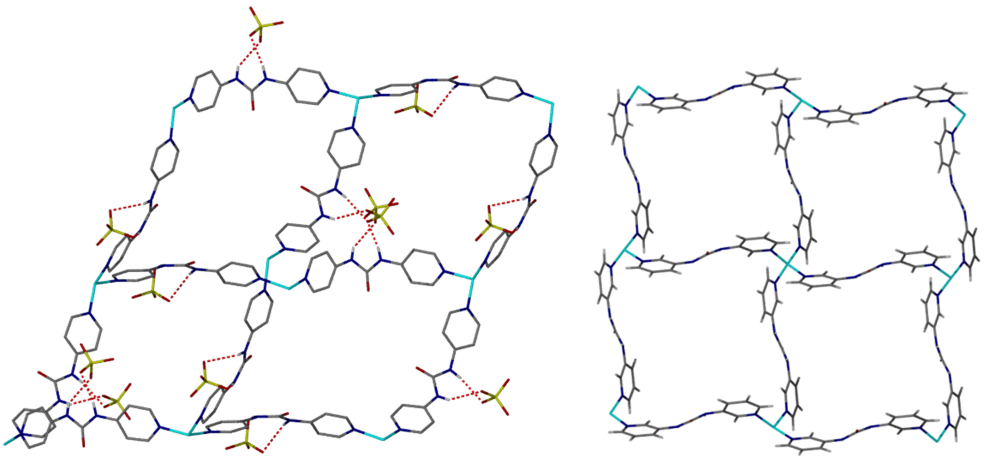

(a) *N,N′*-bis(4-pyridyl)urea forms a diamondoid network with zinc perchlorate

(b) *N,N′*-bis(3-pyridyl)urea forms a square grid with zinc perchlorate.

Figure 5.1: Two crystal structures formed from two bispyridylureas and zinc perchlorate.

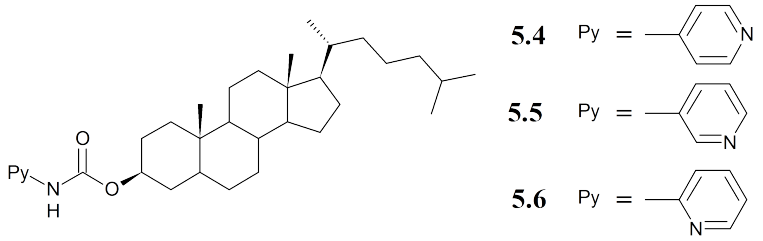

Compounds **5.4**–**5.6** are a set of cholesterols that are functionalised with the three pyridyl isomers. Compound **5.4** is able to gel a wide range of solvents, compound **5.6** forms partial gels and compound **5.5** is either soluble or precipitates.

Various metal ions were subsequently added to the solvents in the gelation tests and it was found that silver(I) triflate can induce gelation in **5.5** in benzene and diphenyl ether. For solutions of **5.5** at 10 g dm^{-3}, gels are formed when the AgOTf:**5.5** ratio is between 0.02 and 0.06. Below 0.02, the compound stays in solution and above 0.06, a precipitate forms. It is suggested that the Ag(I) interacts with the pyridyl nitrogen as ^{1}H NMR spectra of samples of **5.5** as a solution and a gel show that, in the latter, the 2H on the ring is shifted downfield. Compound **5.6** shows no responses to Ag(I) addition probably due to the poor coordination ability of the 2-pyridyl group, while the T_{gel} values for gels of **5.4** are lowered.[179]

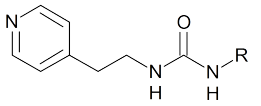

5.7 R = $-(CH_2)_5CH_3$

5.8 R = $-(CH_2)_7CH_3$

5.9 R = $-(CH_2)_{11}CH_3$

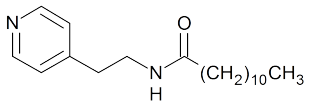

5.10

Compounds **5.7**–**5.9** are mono-urea derivatives that have been tested for their gelling ability. While they do not gel on their own, when silver(I) pentafluoropropionate is added to either a benzene, *p*-xylene or tetralin solution of **5.9**, an opaque, thermoreversible gel is formed. This effect is also observed with silver(I) perchlorate.

The mass spectrum of a sample of a *p*-xylene gel of **5.9** and silver pentafluoropropionate shows peaks at 773 and 775 corresponding to a 2:1 complex of **5.9** to silver. Additionally, the T_{gel} of the gels increases as the ratio of silver to **5.9** increases to a maximum between 0.5 and 0.6 equivalents, subsequently decreasing, indicative of a 2:1 complex. In addition to the pyridyl moiety being necessary, when the urea is replaced by an amide to give compound **5.10**, there is no gelation in either the presence or absence of silver(I). In the IR spectra of neat **5.9**, the urea absorption bands are also shifted, suggesting that in addition to silver(I) coordination, the gel formation is accompanied by the formation of hydrogen-bonds between urea groups.

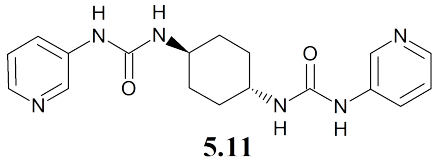

5.11

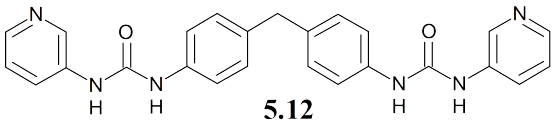

5.12

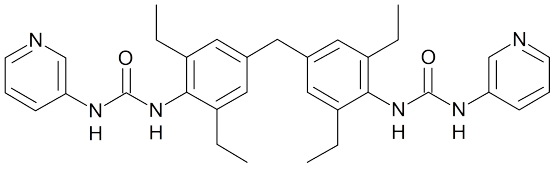

5.13

Compounds **5.11**–**5.13** have been synthesised and tested for their gel forming ability. Of the three, only compound **5.13** is reported to form a gel in a 1:1 mixture of chloroform and methanol. Compound **5.12** forms gels in the presence of silver(I) tetrafluoroborate and crystallises in the presence of silver(I) nitrate with the structure shown in Figure 5.2. The crystal structure may offer some suggestion as to why gelation is induced: the salt acts as a bridge between adjacent bis(pyridylurea)s. A similar effect is observed with **5.11** and copper(II) nitrate.[155]

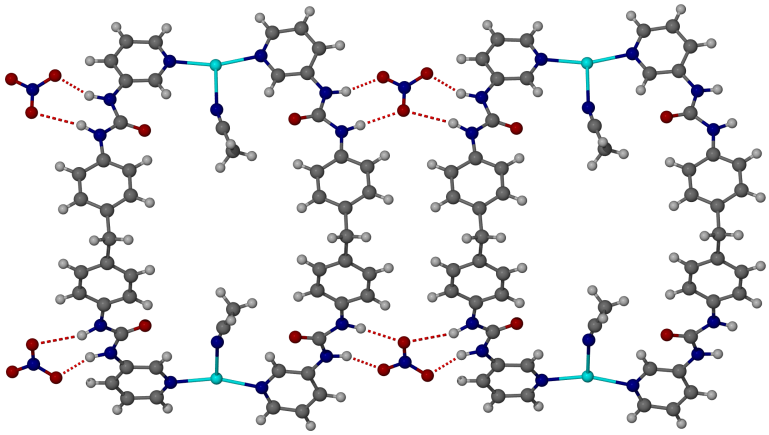

Figure 5.2: Crystal structure of the macrometallocycle formed between **5.12** and silver(I) nitrate.

5.2 Aims

As well as binding anions,[122–125,127,129–137,155,174] ureas and ureas appended with a pyridyl group are known to act as gelators and the examples in section 5.1 include those that gel upon the addition of a metal salt. These types of compounds, pyridylureas may be a route to new responsive gelators that either gel, or their gels are perturbed by, the addition of a metal salt.[6,13] In this chapter, the bis(pyridylurea) compounds discussed in chapter 2 and additional compounds incorporating various spacer groups will be synthesised and tested for their metallogelation ability with as wide a range of metal salts as possible, but especially copper and silver salts as these have already been used in forming metallogels.

5.3 Results and Discussion

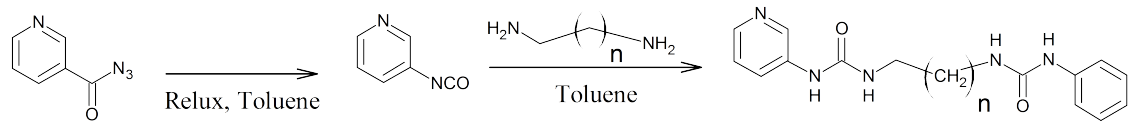

2.n

5.3.1 Metallogels from *N,N″*-ethylene-1,2-diylbis(*N′*-pyridin-3-ylurea) and derivatives

A series of bis(pyridylurea)s were synthesised using the same method discussed in chapter 2, whereby 3-isocyanatopyridine is prepared in situ and reacted with a diaminoalkane. Ligands **2.1**–**2.3** were shown in chapter 2 to have crystallised from solutions of aqueous THF. Therefore, we chose this solvent system in establishing the metallogelating ability of the ligands. In **2.2**–**2.6**, the ligands gel in the same conditions as **2.1**, but beyond this with ligands **2.7**–**2.9**, no gelation was observed.

Figure 5.3: A copper(II) chloride gel formed with **2.1**.

When one equivalent of copper(II) chloride is added to cold solutions of **2.1** in a water and THF mixture (3:2) (1 % w/v), an opaque green gel forms as shown in Figure 5.3. The gel is not thermoreversible and gradually loses solvent upon heating. At different ratios of copper(II) chloride to **2.1**, there is tentative evidence that a 1:1 equivalence is required for gel formation. Shown in Figure 5.4 are a selection of samples of which the sample containing a 1:1 ratio is a gel. If a 1:1 ratio is optimal, at half an equivalence of copper(II) chloride, a clear partial gel that is formed may be due to the low concentration of gel fibres. At two equivalents of copper(II) chloride, the partial gel that is formed is opaque likely as a result of precipitation of the gel fibres. Beyond two equivalents at four and eight, the samples are liquid-like.

The effect of changing the THF to water ratio was also investigated, and it was found that gels were formed **2.1** and copper(II) chloride between ratios of 2:8 and 1:1 (water:THF). Why gels form in this range is unknown, but clearly both solvents pay a part in the gel. The infra-red spectrum of compound **2.1** was recorded and compared to that of the copper(II) chloride xerogel. In the free ligand, peaks corresponding to a C=O stretch and N–H bend occur at 1640 and 1549 cm^{-1} respectively; in the xerogel, they are shifted to 1616 and 1554 cm^{-1}, behaviour consistent with a hydrogen-bonding urea.[180,181] Samples of a copper(II) chloride gel were dried under vacuum, coated with chromium and examined using scanning electron microscopy. Figure 5.6 is a micrograph of the xerogel and shows possible fibres less than 50 nm wide and up to 500 nm long. For comparison, a dried sample of a copper(II) bromide viscous liquid formed with **2.1** is shown in Figure 5.7. The apparent larger and

shorter fibres present in the bromide viscous liquid, may correspond to its liquid-like nature in the bulk.

Figure 5.4: Copper(II) chloride gels formed with **2.1** in varying ratios. Left to right: copper(II) chloride:Ligand: 0.5:1, 1:1, 2:1, 4:1 and 8:1.

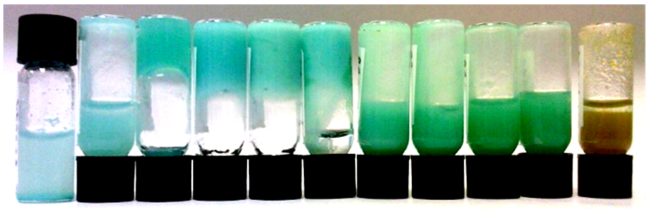

Figure 5.5: Metallogels and precipitates formed from 2.1 and $CuCl_2 \cdot 2H_2O$. Left to right: 10:0, 9:1, 8:2, 7:3, 6:4, 5:5, 4:6, 3:7, 2:8, 1:9 and 0:10 (water:THF) (R).

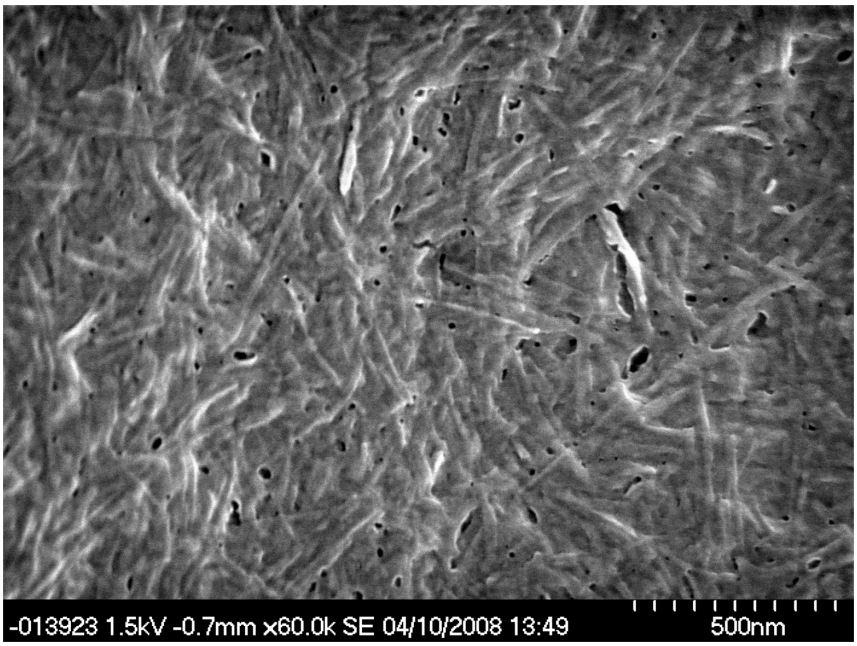

Figure 5.6: SEM micrograph of a xerogel prepared from **2.1** and copper(II) chloride.

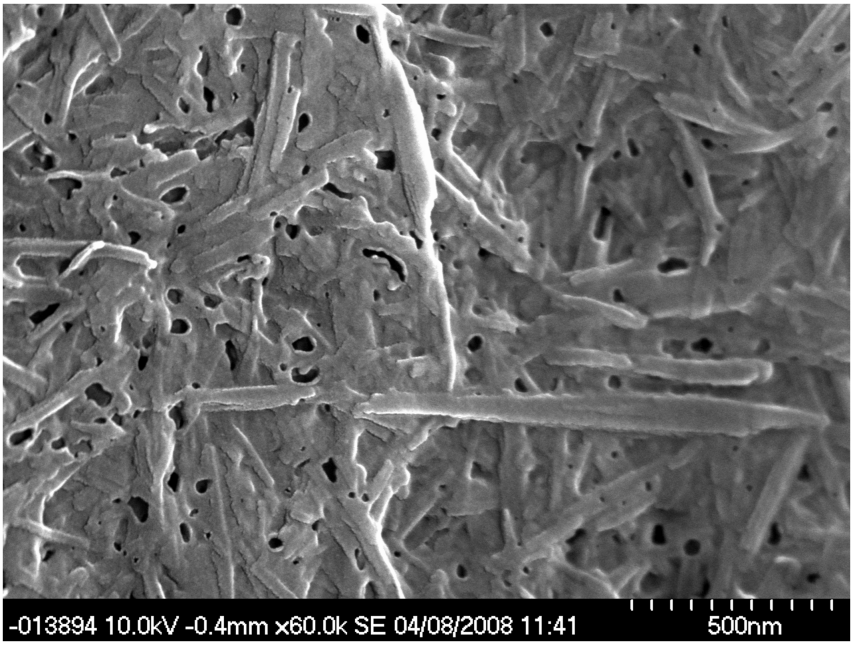

Figure 5.7: SEM micrograph of a dried sample of a partial gel prepared using **2.1** and copper(II) bromide.

Figure 5.8: Compound **2.1** in water and THF (3:2) is added to silver(I) nitrate.

When a solution of **2.1** in water and THF (3:2) is added to silver(I) nitrate and sonicated, the metal salt dissolves to a clear solution, and on further sonication, a colourless gel is formed, shown in Figure 5.8. Without the extended sonication, a white solid precipitates. The infra-red spectra of a xerogel of compound **2.1** with silver(I) nitrate was recorded and compared to that from the free ligand. In the free ligand, peaks corresponding to the C=O stretch and N–H bend occur at 1640 and 1549 cm^{-1} respectively and in the dried gel, they are shifted to 1614 $cm^{-}1$ and the NH at 1557 cm^{-1} consistent again with a hydrogen-bonded urea. We attempted to determine the T_{gel} value, but as with the copper(II) gels, the gels were not

thermoreversible but instead lost solvent upon heating. The tertiary structure of the gels was examined using SEM. Compared to those of copper(II) chloride and bromide, the xerogel structure formed with silver(I) nitrate (shown in Figure 5.9) is more distinct than with copper(II) chloride, and the viscous solution from copper(II) bromide. As can be seen in the micrographs in Figure 5.9, there is a stark difference in the macrostructure of the materials. The fibres in the silver(I) nitrate gel are approximately 50 nm wide and over 10 μm long but while the copper analogues are less distinct, the same fibrous structure can be observed.

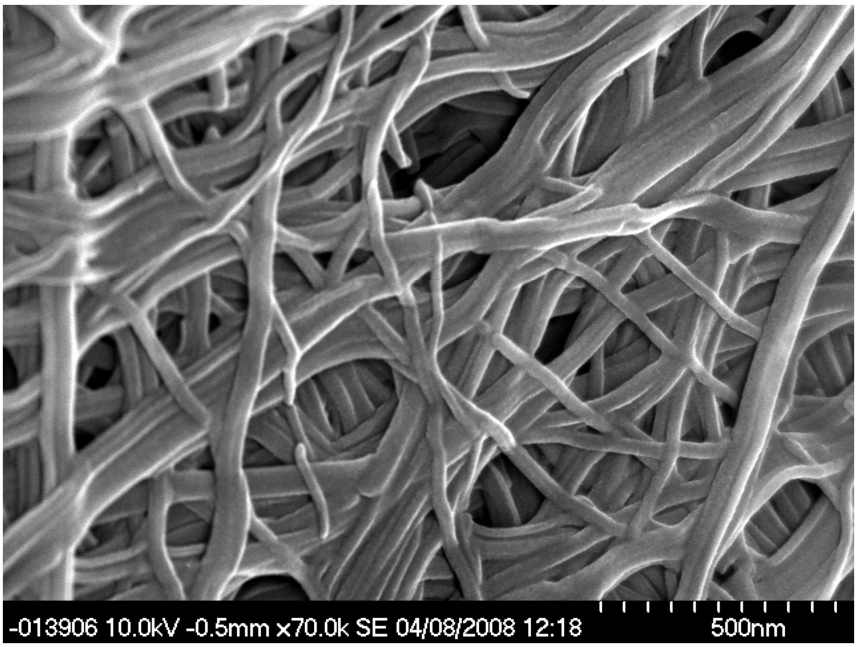

Figure 5.9: SEM micrograph of a partial gel prepared using **2.1** and silver(I) nitrate.

The exact structure of the fibres formed in the gel between **2.1** and silver(I) nitrate is unclear though it is useful to consider the structure obtained when the crystallisation is performed in chloroform, methanol and acetonitrile as mentioned previously in chapter 3. In that case, two structures are obtained from the crystallisation depending on the starting concentration: one, a [2+2] metallomacrocycle is formed when the concentration is high, and the second, a Borromean formed when the concentration is relatively low. In this case, a gel is formed with sonication within which, in one instance, crystals of a Borromean with the structure described in section 3.3.1 were formed upon standing. It may be that similar structures are

responsible for the behaviour of both systems and therefore the fastest-formed product in THF and water is a structure similar to that formed the fastest in chloroform, methanol and acetonitrile: *i.e.* a macrocycle; further evidence is required.

5.3.2 Metallogels from *N,N″*-pyridine-2,6-diylbis(*N′*-pyridin-3-ylurea

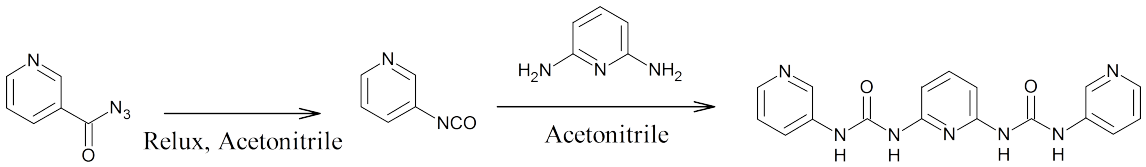

5.14

Compound **5.14**, *N,N″*-pyridine-2,6-diylbis(*N′*-pyridin-3-ylurea), was synthesised using the same method as **2.1** but with 2,6-diaminopyridine as a spacer. The compound was tested for gelation ability across a range of ratios of water and THF. In a water and THF mixture (3:2) a gel formed at a concentration of 1 % w/v in the presence of an equivalence of silver(I) nitrate shown in Figure 5.10. By IR spectroscopy, the N–H bend (Amide II) and C=O peak which occur at 1547 and 1698 cm^{-1} in the free ligand are shifted to 1558 and 1613 cm^{-1} respectively in the xerogel indicating that the urea groups are hydrogen-bonded.

Figure 5.10: Metallogel formed from **5.14** and silver(I) nitrate.

5.3.3 Metallogels from *N,N″*-cyclohexylene-1,2-diylbis(*N′*-pyridin-3-ylurea)

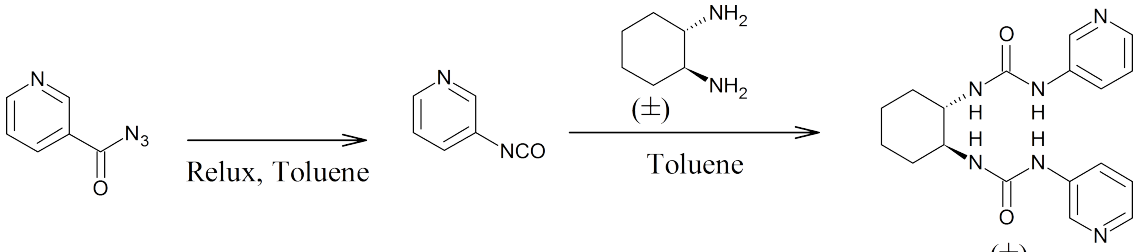

5.15

Compound **5.15** was synthesised using the same method as **2.1** but with a racemic mixture of *trans*-1,2-diaminocyclohexane as the spacer. Compound **5.15** was dissolved in a water and THF mixture (3:2) in the presence of one equivalent of silver(I) tetrafluoroborate and upon slow evaporation, the solution gelled. SEM was performed on the gel after it had been dried, and a typical micrograph is shown in Figure 5.15. The fibres are over 500 nm long and approximately 50 nm wide. When the metal salt was replaced with silver(I) nitrate in a 1:1 mixture of THF & water, the solution gelled but upon standing transformed into crystals whose structure was determined by X-ray crystallography and shown to be a 1:1 coordination polymer of the ligand and silver(I) nitrate. The asymmetric unit, shown in Figure 5.11 contains a molecule of **5.15** which is one half of a macrocycle in which two are connected through two silver atoms (Figure 5.12). The macrocycles in the crystal are subsequently connected to each other through a bifurcated hydrogen-bonding interaction between opposing faces of the urea groups of both sides, as shown in Figure 5.13. The remaining faces are hydrogen-bonded to a three-membered water cluster that connects adjacent chains of macrocycles. The urea oxygen forms a single hydrogen bond to a water molecule which is itself hydrogen-bonded to a central water molecule which is shared between the chains. A single N–H of the urea groups from both chains hydrogen-bonds to the central water molecule as shown in Figure 5.14.

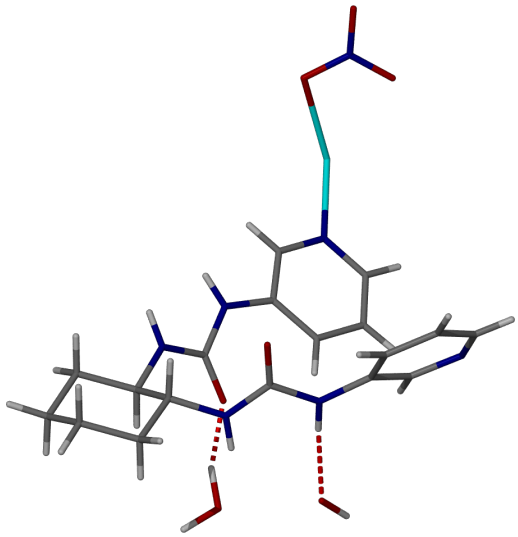

Figure 5.11: The asymmetric unit of a coordination polymer formed between compound **5.15** and silver(I) nitrate from a 1:1 mixture of THF and water.

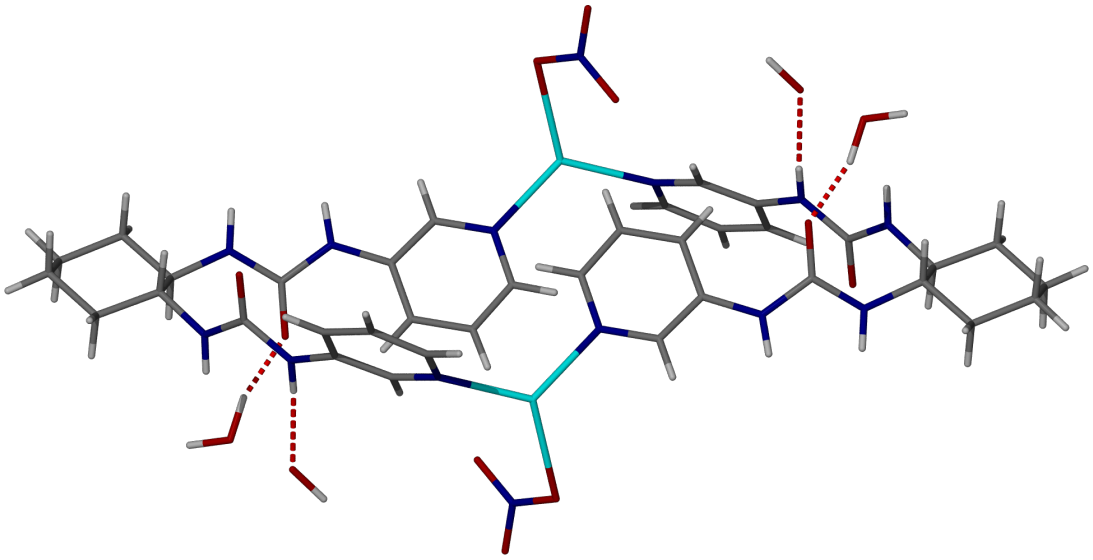

Figure 5.12: The macrocycle formed between **5.15** and silver(I) nitrate.

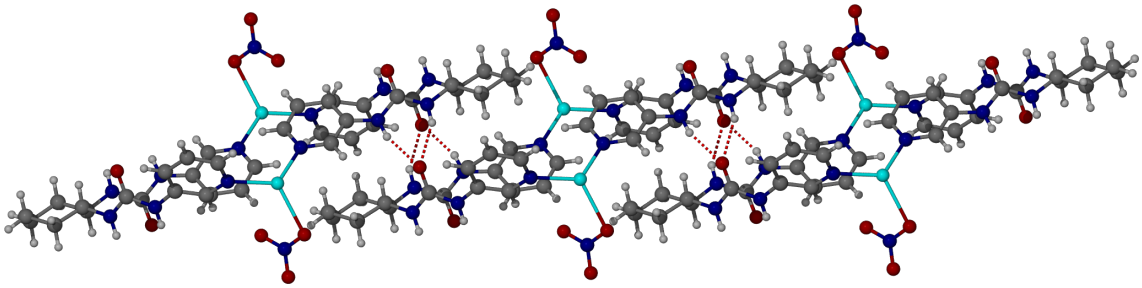

Figure 5.13: Crystal structure obtained from the slow crystallisation of a gel of **5.15** showing chains formed *via* Ag^{+} bridging atoms. Water molecules omitted for clarity.

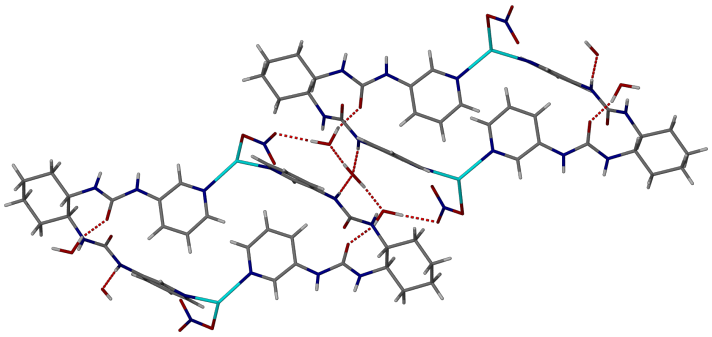

Figure 5.14: Adjacent chains of macrocycles formed from **5.15** and silver(I) nitrate are connected *via* a three-membered water cluster.

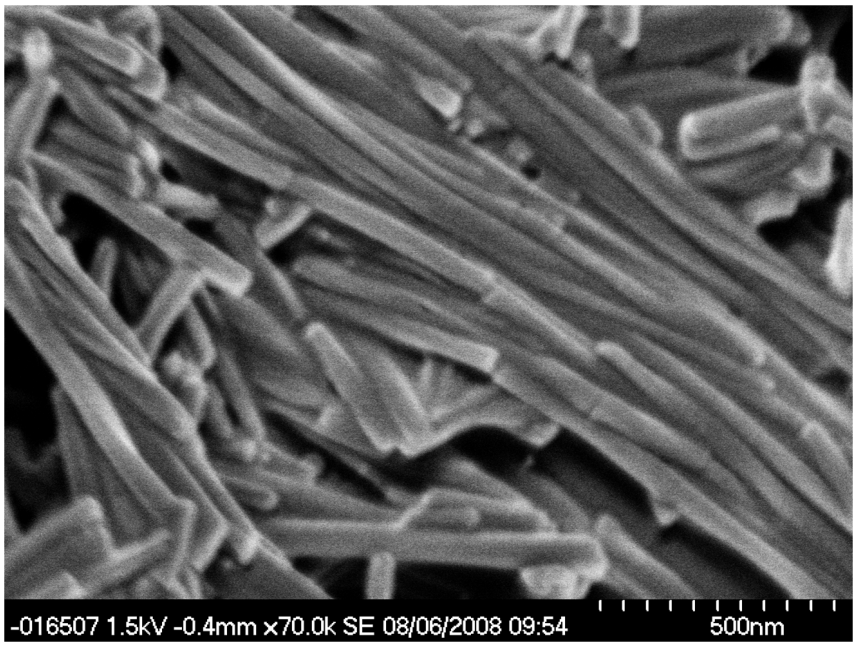

Figure 5.15: SEM micrograph of a xerogel of **5.15** and silver(I) tetrafluoroborate.

5.3.4 Metallogels from *N,N″*-methylenebisphenyl-4,1-diyl-bis(*N′*-pyridin-3-ylurea)

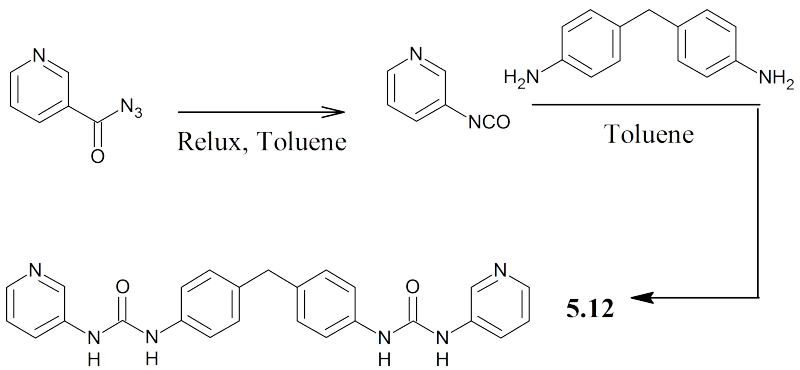

Compound **5.12**, *N,N″*-methylenebisphenyl-4,1-diylbis(*N′*-pyridin-3-ylurea), was synthesised using the same method as **2.1** but with 4,4′-methylenebisaniline as a spacer. When an equivalent of silver(I) nitrate is added to a solution of the ligand in water and THF (2:3), the solution turns into a clear, colourless gel, as shown in Figure 5.16. After twenty-four hours, the gel transforms into crystals. The crystal structure was partially solved and a proposed asymmetric unit is shown in Figures 5.17a and 5.17b. The crystal structure is a macrocycle formed from two molecules of **5.12** and two silver(I) atoms. The macrocycles are subsequently connected *via* nitrate anions that are hydrogen-bonded to the outward-facing urea NHs in two distinct modes that are overlaid. One chain of macrocycles is held together by single hydrogen-bonds between the nitrate and a urea NH, and the other by bifurcated interactions $R_2^2(8)$ and $R_2^1(6)$ hydrogen-bonds. The two chains are connected *via* a hydrogen-bond between the oxygen of the singly-bonded urea of the first chain with one of the NHs taking part in a $R_2^1(6)$ hydrogen-bonds to a nitrate in the second chain, as seen in 5.17b. Throughout the structure, there are channels of THF that lie in the spaces between the chains, as shown in Figure 5.18.

The crystallisation of the gel of 5.12 and silver(I) nitrate in THF and water is the same behaviour as that observed with **5.15**. As with **2.1**, while there is no evidence that the crystal structure obtained is identical to that of the fibres, it is not unreasonable to suggest they are related to some degree wherein the anion promotes the crystallisation along the direction of the fibre. Subsequent assembly would determine if a gel or crystal is formed.

Figure 5.16: Metallogel formed from **5.12** and silver(I) nitrate in water and THF (2:3).

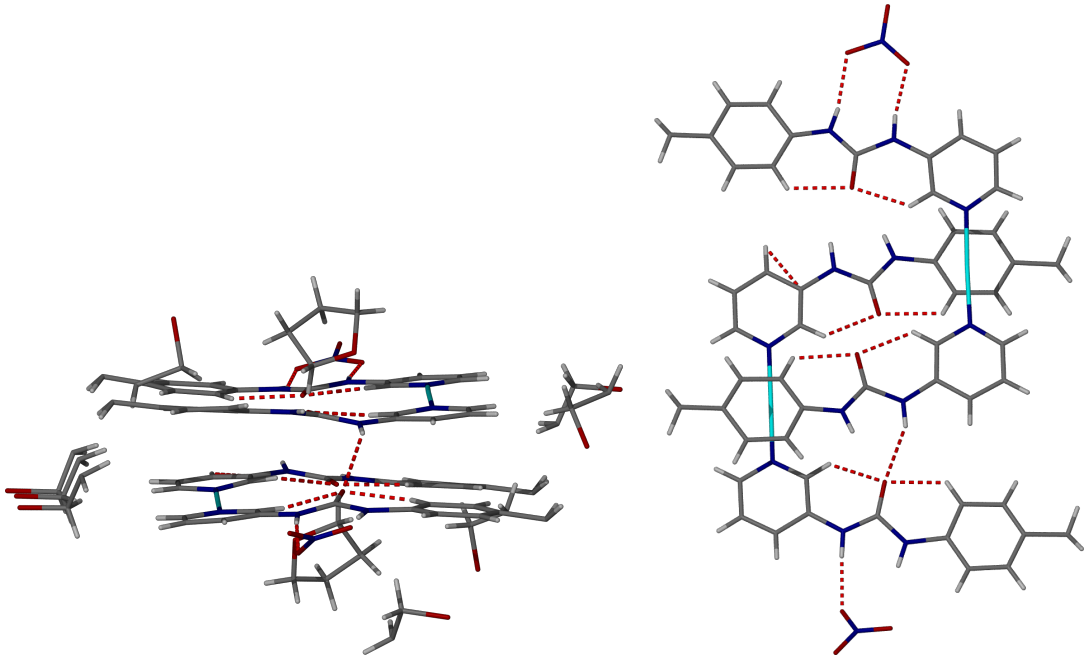

(a) THF included. (b) THF omitted.

Figure 5.17: Asymmetric unit of the crystal of the macrocycle formed between **5.12** and silver(I) nitrate with THF

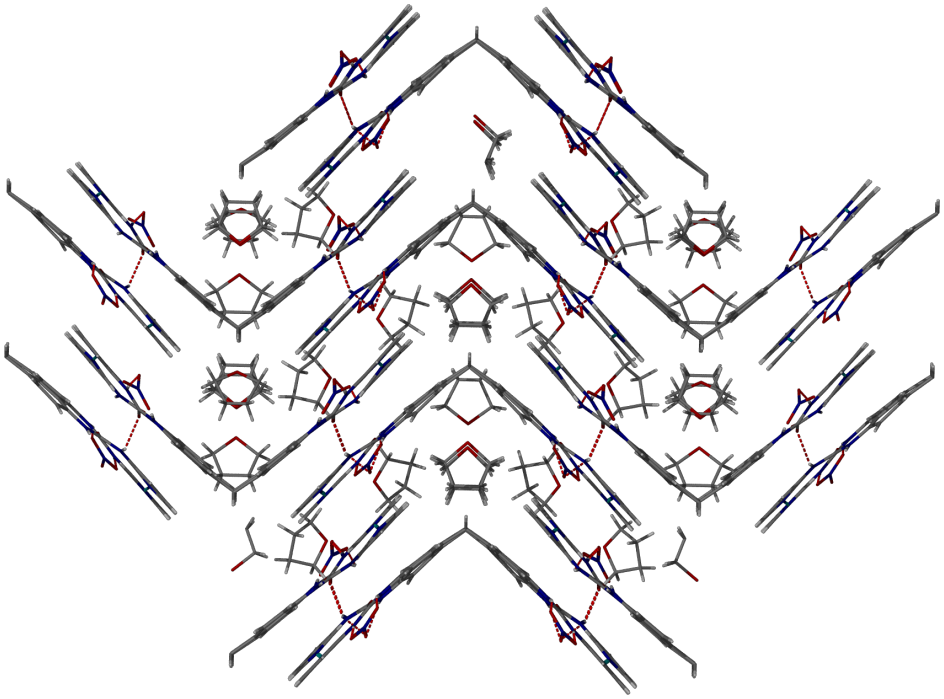

Figure 5.18: THF molecules lying between the chains of macrocycles formed between 5.12 and silver(I) nitrate.

5.4 Conclusions

Several bis(pyridylureas) have been shown to form both gels and crystals in the presence of silver(I) salts, predominantly silver(I) nitrate. While the exact structure of the gel fibres is unclear, the related systems in which crystallisation occurs may offer some hints as to how the molecules are aggregated.

Compounds **5.12**, **5.15**, and **2.1** all form macrocyclic structures with silver(I) with nitrate anions acting as bridges between adjacent urea groups. With **5.12** and **5.15**, these macrocylic structures are obtained as a result of the decomposition of a gel phase; with **2.1**, the structure is produced in a three-solvent mixture as opposed to the THF & water system for the gel, but in both instances, a more stable Borromean structure can be produced when the crystallisation is slowed.

Though further investigation is required, compounds **5.14** and **5.15** are related to similar organogelators in which the urea is appended with an alkyl chain: **5.14** on 2,6-di(3-(1-dodecyl)ureido)pyridine and **5.15** on cyclohexane based bis-ureas such as *trans*-1,2-bis(dodecylureido)cyclohexane and its functionalised counterpart *trans*-

1,2-bis[(5-aminohexyl)ureido]cyclohexane. It may be that the 3-pyridylurea group is a motif which can impart gelation by coordination of a silver salt by encouraging the aggregation of the ligands along the direction of the fibres.

Chapter 6

Conclusions

This thesis has explored the self-assembly of a set of bis(3-pyridylureas) in both how they aggregate in the solid-state and in the presence of various silver(I) salts to form both crystals and gels.

In chapter 2, the crystal structures of a series of bis(pyridylureas) were examined. When the spacer group was either a propylene, butylene or phenylene unit, the intermolecular hydrogen-bonding was shown to be a combination of both bifurcated hydrogen-bonding present in urea α-tapes, and a 'distrupted motif of a NH···O_{urea} and NH···$N_{pyridyl}$.This motif may be said to lie between the α-tape formed by *N,N′*-diphenylurea and the complexing behaviour of 1,3-bis(*m*-nitrophenyl)urea, caused by the lack of another electron-withdrawing pyridyl group on the remaining side of the urea group and the loss of one of the intramolecular CH···O_{urea} bonds. The urea tape formed by compound **2.11** and the lack of a bifurcated hydrogen-bonding motif in compound **2.1** illustrates that other factors can play a part in determining the intermolecular bonding mode which in this case is the nature of the spacer group. As these interactions become stronger, as with a napthylene spacer, either by greater van der Waals attraction in a longer oliomethylene chain or the greater π-π stacking interactions adjacent urea groups become closer and bind preferentially to form the α-tape.

In chapter 3, compound **2.1** was crystallised with various silver salts. With silver(I) nitrate, a set of five pseudopolymorphs of a Borromean-type structure which

could be classed into three categories when considering the way in which the pairs of Borromean weaves stacked in the crystal. The predominant stacking, present in three of the pseudopolymorphs was driven by alternate stacking of the solvent pockets and Ag_2 units, the remaining arrangements appeared to be driven by π-π stacking of the pyridyl units in one case, and in the other, by interactions between the solvent pockets of adjacent layers. Ultimately, however, the stacking was determined upon the occupancy of the solvent pocket and the presence of the nitrate group, as shown by the non-Borromean crystals produced from other silver(I) salts. Dependency of the final structure on the anion present was also shown in the structures of chapter 4. Here, compound **2.4** was shown to form a quintuple helix when re-crystallised in the presence of silve(I) tetrafluoroborate. Crystallisation with silver(I) acetate and silver(I) nitrate gave a single helix and planar crystal structure respectively.

Finally, in chapter 5, several bis(3-pyridylureas) were shown to form both gels and crystals in the presence of predominantly silver(I) nitrate. Three compounds, **5.12**, **5.15**, and **2.1** were shown to form macrocyclic structures with silver(I) nitrate and with **5.12** and **5.15**, these macrocylic structures came from the decomposition of a gel phase and with **2.1** a gel phase results by chainging the solvent conditions of the macrocycle crystallisation to THF & water. These crystal structures may offer an indication of the structure of the gel phase as promotion of the growth of the crystal in one direction by silver(I) nitrate would be consistent with the required conditions to grow gel fibres.

Chapter 7

Publications

Directly from this project:

1. "A "Compartmental" Borromean weave coordination polymer exhibiting saturated hydrogen-bonding to anions and water cluster inclusion." Peter Byrne, Gareth O. Lloyd, Nigel Clarke and Jonathan W. Steed, *Angew. Chem. Int. Ed.*, 2008, **47**, 5761–5764.

2. "Anion hydrogen-bond effects in the formation of planar or quintuple helical coordination polymers." Peter Byrne, Gareth O. Lloyd, Kirsty M. Anderson, Nigel Clarke and Jonathan W. Steed, *Chem. Comm.*, 2008, 3720–3722.

3. "Gradual transition from NH···pyridyl hydrogen-bonding to the NH···O tape synthon in pyridyl ureas." Peter Byrne., David R. Turner, Gareth O. Lloyd, Nigel Clarke and Jonathan W. Steed, *Cryst. Growth. Des.*, 2008, **8**, 3335–3344.

During this project:

4. "Helical or polar guest-dependent Z'=1.5 or Z'=2 forms of a sterically hindered bis(urea) clathrate." Adam M. Todd., Kirsty M. Anderson, Peter Byrne, Andres E. Goeta and Jonathan W. Steed, *Cryst. Growth Des.*, 2006, **6**, 1750–1752.

5. "Structure calculation of an elastic hydrogel from sonication of rigid small molecule components." Kirsty M. Anderson, Graeme M. Day, Martin J. Paterson, Nigel Clarke and Jonathan W. Steed, *Angew. Chem. Int. Ed.*, 2008, **47**, 1058–1062.

Chapter 8

Experimental

8.1 General

^{1}H and ^{13}C-{^{1}H} NMR spectra were measured with either a Bruker Avance NMR spectrometer operating at a proton frequency of 400 MHz or at 200 MHz with a Varian Mercury instrument. Chemical shifts are reported relative to residual solvent peaks.[182] Mass spectra were obtained with a Thermo LTQ FT spectrometer operating by electrospray positive ionization mode. IR spectra were measured with a Perkin-Elmer 100 FT-IR spectrometer, using a golden gate apparatus. Elemental Analysis for carbon, hydrogen and nitrogen was performed on an Exeter analytical E-400 elemental analyser. SEM of chromium-coated freeze-dried samples of gel was performed using an Hitachi S-5200 ultra-high field emission scanning electron microscope. Crystallographic measurements were carried out either with a Nonius KappaCCD or Bruker SMART 1000 diffractometer equipped with graphite monochromated Mo Kα radiation. Data collection temperature was 120 K, maintained by using an Oxford Cryosystem low temperature device. Integration was carried out by the Denzo-SMN package. Data sets were corrected for Lorentz and polarization effects and for the effects of absorption (Scalepack) and crystal decay where appropriate. Structures were solved using the direct methods option of SHELXS-97 and developed using conventional alternating cycles of least-squares refinement SHELXL-97 and difference Fourier synthesis with the aid of the pro-

gram X-Seed. In all cases non-hydrogen atoms were refined anisotropically except for some disordered, while C–H hydrogen atoms were fixed in idealized positions and allowed to ride on the atom to which they were attached. Hydrogen atom thermal parameters were tied to those of the atom to which they were attached. Where possible, non-C–H hydrogen atoms were located experimentally and their positional and isotropic displacement parameters refined. Otherwise a riding model was adopted. All calculations were carried out on an IBM-PC compatible personal computer. Specific issues relating to each refinement are detailed below.

8.2 Ligand Syntheses

8.2.1 Nicotinoyl Azide

Nicotinic acid (1.02 g, 8.29 mmol) was suspended in dry DMF (6 mL) and dissolved upon addition of triethylamine (0.89 g, 8.76 mmol). Diphenylphosphoryl azide (2.40 g, 8.70 mmol) was added and the solution warmed slightly. After stirring at room temperature for 1.5 h, the solution had become slightly yellow and was poured into water (30 mL) precipitating a colourless solid that was extracted with diethyl ether (3 × 15 mL). The organic layers were combined and washed with water (3 × 15 mL), dried over anhydrous magnesium sulfate, filtered and evaporated under reduced pressure to yield the product as colourless crystals. Yield: 0.79 g, 5.33 mmol (65%). M.p.: 45–46 °C; ^{1}H-NMR ($CDCl_3$, 200 MHz, δ / ppm, J / Hz): 9.21 (1H, d, J= 1.8, ArH), 8.83 (1H, dt, J= 1.8, 4.8, ArH), 8.29 (1H, dt, J= 1.8, 8.0, ArH), 7.42 (1H, dd, J= 4.8, 8.0, ArH); ^{13}C-{^{1}H} NMR ($CDCl_3$, 100 MHz, δ / ppm): 170.9 (C=O), 154.3 (CH), 150.3 (CH), 136.4 (CH), 126.2 (C), 123.3 (CH); EI-MS (m/z): 349 $[M+H]^+$; Analysis Calc. for $C_6H_4N_4O$: C 48.65, H 2.72, N 37.82 %, Found: C 48.17, H 2.78, N 35.72 %.; IR ($\tilde{\nu}$ / cm^{-1}): 2134 (strong, sharp, $–N_3$).

8.2.2 *N,N″*-ethylene-1,2-diylbis(*N′*-pyridin-3-ylurea), 2.1

Nicotinoyl azide (1.00 g, 6.75 mmol) was dissolved in dry toluene (50 mL) and stirred at reflux, and the evolution of nitrogen gas monitored. After 2 h, no more gas was

evolved and the solution was cooled to room temperature and 1,2-diaminoethylene (0.49 g, 3.40 mmol) was added, precipitating a colourless solid. The suspension was stirred for 15 min, filtered under suction and washed with acetone (2 × 15 mL) to give the product as a white solid. Yield: 0.42 g, 1.40 mmol (21%). Crystals for analysis by X-ray crystallography were grown by dissolving the final product (30 mg, 0.1 mmol) in a mixture of THF & water (2:3, 5 mL). Crystals formed upon evaporation of the solvent. M.p.: 210–211 °C; ^{1}H NMR (DMSO-d_6, 400 MHz, δ / ppm, J/ Hz): 8.76 (2H, s, NH), 8.53 (2H, d, J= 2.5, PyH), 8.10 (2H, dd, J= 1.4, 4.7, PyH), 7.88 (2H, dq, J= 1.4, 2.5, 8.3, PyH), 7.24 (2H, dd, J= 4.7, 8.3, PyH), 6.37 (2H, t, J= 5.4, NH), 3.21 (4H, m, J= 2.5, 5.4, CH_2); ^{13}C-{^{1}H} NMR (DMSO-d_6, 100 MHz, δ / ppm): 155.3 (C), 142.1 (CH), 139.6 (CH), 137.1 (C), 124.5 (CH), 123.4 (CH), 39.6 (CH_2); EI-MS (m/z): 121 [PyNHCO]$^+$, 151, 301 [M+H]$^+$, 323 [M+Na]$^+$, 623 [2M+Na]$^+$; Analysis Calc. for $C_{14}H_{16}N_6O_2$: C 55.99, H 5.37, N 27.98 %, Found: C 55.70, H 5.31, N 27.80 %; IR ($\tilde{\nu}$ / cm^{-1}): 3301 (m, $(N–H)_{str}$), 1640 (strong, sharp, $(C{=}O)_{str}$), 1549 (strong, sharp, $(N–H)_{def}$).

Crystallographic Data for $C_{14}H_{16}N_6O_2$: M = 300.33, colourless prism, 0.29 × 0.27 × 0.25 mm^3, monoclinic, space group $P2_1/c$ (No. 14), a = 8.4334(6), b = 8.8676(6), c = 9.8416(7) Å, β = 112.234(2)°, V = 681.27(8) Å^3, Z = 2, D_c = 1.464 g/cm^3, F_{000} = 316, Smart-6K, MoKα radiation, λ = 0.71073 Å, T = 120(2)K, $2\theta_{max}$ = 70.0°, 7672 reflections collected, 2814 unique (R_{int} = 0.0358). Final $GooF$ = 1.014, $R1$ = 0.0555, $wR2$ = 0.1460, R indices based on 1914 reflections with I >2Σ(I) (refinement on F^2), 100 parameters, 0 restraints. Lp and absorption corrections applied, μ = 0.104 mm^{-1}.

8.2.3 *N,N″*-propylene-1,3-diylbis(*N′*-pyridin-3-ylurea), 2.2

Prepared as *N,N″*-ethylene-1,2-diylbis(*N′*-pyridin-3-ylurea), using 1,3-diaminopropane. Yield: 0.19 g, 0.60 mmol (86%). Crystals suitable for X-ray crystallographic analysis were grown by dissolving the final product (30 mg, 0.1 mmol) in a mixture of THF & water (3:2, 3 mL). Crystals formed upon evaporation of the solvent. M.p.: 194–196 °C; ^{1}H NMR (DMSO-d_6, 400 MHz, δ / ppm, J/ Hz): 8.71 (2H, s, NH),

8.53 (2H, d, J= 2.6, PyH), 8.10 (2H, dd, J=1.4, 4.6, PyH), 7.88 (2H, dq, J= 1.4, 2.6, 8.3, PyH), 7.24 (2H, dd, J= 4.6, 8.3, PyH), 6.34 (2H, t, J= 5.7, NH), 3.14 (4H, q, J= 6.6, CH_2), 1.59 (2H, m, J= 6.6, CH_2); ^{13}C-{^{1}H} NMR (DMSO-d_6, 100 MHz, δ / ppm): 155.3 (C), 142.0 (CH), 139.5 (CH), 137.2 (C), 124.4 (CH), 123.4 (CH), 36.6 (CH_2), 30.5 (CH_2); EI-MS (m/z): 121 [PyNHCO]$^+$, 221, 315 [M+H]$^+$, 337 [M+Na]$^+$, 651 [2M+Na]$^+$; Analysis Calc. for $C_{15}H_{18}N_6O_2$: C 57.31, H 5.77, N 26.74 %, Found: C 56.94, H 5.79, N 26.13 %; IR ($\tilde{\nu}$ / cm^{-1}): 3319 (m, (N–H)$_{str}$), 1656 (strong, sharp, (C=O)$_{str}$), 1544 (strong, sharp, (N–H)$_{def}$).

Crystallographic Data for $C_{15}H_{18}N_6O_2$: $M = 314.35$, colourless plate, 0.45 × 0.38 × 0.12 mm^3, monoclinic, space group $2_1/c$ (No. 14), $a = 16.447(3)$, $b = 5.2902(11)$, $c = 18.364(4)$ Å, $\beta = 105.112(7)°$, $V = 1542.6(5)$ Å^3, $Z = 4$, $D_c = 1.354$ g/cm^3, F_{000} = 664, Smart-6K, MoKα radiation, λ = 0.71073 Å, T = 120(2)K, $2\theta_{max} = 52.0°$, 9467 reflections collected, 3032 unique (R_{int} = 0.0843). Final *GooF* = 0.864, *R1* = 0.0416, *wR2* = 0.0759, R indices based on 1741 reflections with I >2Σ(I) (refinement on F^2), 208 parameters, 0 restraints. Lp and absorption corrections applied, μ = 0.095 mm^{-1}.

8.2.4 *N,N″*-butylene-1,4-diylbis(*N′*-pyridin-3-ylurea), 2.3

Prepared as *N,N″*-ethylene-1,2-diylbis(*N′*-pyridin-3-ylurea), using 1,4-diaminobutane. The compound was re-crystallised by slow evaporation of a mixture of solution of the bis(urea) in acetonitrile and water (1:1), 10 mL. Yield: 4.16 g, 11.94 mmol (89%). M.p.: 208–210 °C; ^{1}H NMR (DMSO-d_6, 400 MHz, δ / ppm, J/ Hz): 8.60 (2H, s, NH), 8.52 (2H, s, ArH), 8.10 (2H, d, J= 4.6, ArH), 7.87 (2H, d, J= 8.1, ArH), 7.23 (2H, dd, J= 4.6, 8.1, ArH), 6.30 (2H, t, J= 5.2, NH), 3.11 (4H, d, J= 5.2, CH_2), 1.46 (4H, s, CH_2); ^{13}C-{^{1}H} NMR (DMSO-d_6, 100 MHz, δ / ppm): 155.6 (C), 142.5 (CH), 139.8 (CH), 137.7 (C), 124.9 (CH), 123.9 (CH), 39.4 (CH_2), 27.7 (CH_2); EI-MS (m/z): 165 [M+2H]$^{2+}$, 329 [M+H]$^+$, 351 [M+Na]$^+$, 657 [2M+H]$^+$, 679 [2M+Na]$^+$; Analysis Calc. for $C_{16}H_{20}N_6O_2$: C 58.52, H 6.14, N 25.59; Found: C 58.31, H 6.10, N 25.49 %; IR ($\tilde{\nu}$ / cm^{-1}): 3323 (m, (N–H)$_{str}$), 1643 (strong, sharp, (C=O)$_{str}$), 1552 (strong, sharp, (N–H)$_{def}$).

Crystallographic Data for $C_{16}H_{20}N_6O_2$: M = 328.38, colourless plate, 0.34 × 0.23 × 0.18 mm^3, triclinic, space group P-1 (No. 2), a = 6.251(5), b = 7.166(5), c = 17.535(13) Å, α = 79.034(11), β = 86.927(11), γ = 88.617(12)°, V = 769.9(10) Å^3, Z = 2, D_c = 1.417 g/cm^3, F_{000} = 348, MoKα radiation, λ = 0.71073 Å, T = 393(2)K, $2\theta_{max}$ = 46.5°, 1475 reflections collected, 1115 unique (R_{int} = 0.0348). Final *GooF* = 1.171, *R1* = 0.0506, *wR2* = 0.1277, R indices based on 1002 reflections with I >2Σ(I) (refinement on F^2), 217 parameters, 0 restraints. Lp and absorption corrections applied, μ = 0.098 mm^{-1}.

8.2.5 *N,N″*-pentylene-1,5-diylbis(*N′*-pyridin-3-ylurea), 2.4

Prepared as *N,N″*-ethylene-1,2-diylbis(*N′*-pyridin-3-ylurea), using 1,5-diaminopentane. Yield: 0.92 g, 2.69 mmol (46%). M.p.: 168–170 °C; ^{1}H NMR (DMSO-d_6, 400 MHz, δ / ppm, J/ Hz): 8.60 (2H, s, NH), 8.51 (2H, d, J= 2.7, PyH), 8.08 (2H, dd, J= 1.5, 4.6, PyH), 7.87 (2H, ddd, J= 1.5, 2.7, 8.3, PyH), 7.23 (2H, dd, J= 4.6, 8.3), 6.29 (2H, t, J= 6.5, NH), 3.09 (4H, q, J= 6.5, CH_2), 1.45 (4H, m, J= 7.4, CH_2), 1.31 (2H, m, CH_2); ^{13}C-{^{1}H} NMR (DMSO-d_6, 100 MHz, δ / ppm): 155.1 (C), 141.9 (CH), 139.5 (CH), 137.2 (C), 124.3 (CH), 123.4 (CH), 39.1 (CH_2), 29.4 (CH_2), 23.7 (CH_2); EI-MS (m/z): 121 [PyNHCO]$^+$, 223 [PyNHCONH$(CH_2)_5$NH+2H]$^+$, 343 [M+H]$^+$, 365 [M+Na]$^+$, 707 [2M+Na]$^+$; Analysis Calc. for $C_{17}H_{22}N_6O_2$: C 59.63, H 6.48, N 24.54 %, Found: C 59.55, H 6.47, N 24.57 %; IR ($\tilde{\nu}$ / cm^{-1}): 3332 (m, (N–H)$_{str}$), 1627 (strong, sharp, (C=O)$_{str}$), 1556 (strong, sharp, (N–H)$_{def}$).

8.2.6 *N,N″*-hexylene-1,6-diylbis(*N′*-pyridin-3-ylurea), 2.5

Prepared as *N,N″*-ethylene-1,2-diylbis(*N′*-pyridin-3-ylurea), using 1,6-diaminohexane. Yield: 0.84 g, 2.36 mmol (70%). M.p.: 186–188 °C; ^{1}H NMR (DMSO-d_6, 400 MHz, δ / ppm, J/ Hz): 8.59 (2H, s, NH), 8.51 (2H, s, ArH), 8.09 (2H, d, J= 4.8, ArH), 7.87 (2H, d, J= 7.6, ArH), 7.23 (2H, dd, J= 4.8, 8.3, ArH), 6.28 (2H, t, J= 5.3, NH), 3.08 (4H, q, J= 6.4, 12.6, CH_2), 1.46 (4H, br m, CH_2), 1.31 (4H, br m, CH_2); ^{13}C-{^{1}H} NMR (DMSO-d_6, 100 MHz, δ / ppm): 156.6 (C), 142.5 (CH), 139.8 (CH), 137.5 (C), 125.0 (CH), 124.0 (CH), 39.4 (CH_2), 30.0 (CH_2), 26.5 (CH_2); EI-MS

(m/z): 179 $[M+2H]^{2+}$, 357 $[M+H]^+$, 379 $[M+Na]^+$, 712 $[2M+H]^+$, 735 $[2M+Na]^+$; Analysis Calc. for $C_{18}H_{24}N_6O_2$: C 60.66, H 6.79, N 23.58 %, Found: C 60.10, H 6.84, N 23.47 %; IR ($\tilde{\nu}$ / cm^{-1}): 3329 ($(N–H)_{str}$), 1647 ($(C=O)_{str}$)

8.2.7 *N,N″*-heptylene-1,7-diylbis(*N′*-pyridin-3-ylurea), 2.6

Prepared as *N,N″*-ethylene-1,2-diylbis(*N′*-pyridin-3-ylurea), using 1,7-diaminoheptane. Yield: 0.89 g, 2.41 mmol (71%). M.p.: 155–157 °C; ^{1}H NMR (DMSO-d_6, 400 MHz, δ / ppm, J/ Hz): 8.58 (2H, s, NH), 8.51 (2H, d, J= 2.6, PyH), 8.09 (2H, dd, J= 1.5, 4.7, PyH), 7.87 (2H, ddd, J= 1.5, 2.6, 8.4, PyH), 7.23 (2H, dd, J= 4.7, 8.4, PyH), 6.27 (2H, t, J= 5.6, NH), 3.08 (4H, q, J= 6.5, CH_2), 1.43 (4H, m, J= 6.5, CH_2), 1.29 (6H, m, CH_2-CH_2-CH_2); ^{13}C-{^{1}H} NMR (DMSO-d_6, 100 MHz, δ / ppm): 155.1 (C), 141.9 (CH), 139.5 (CH), 137.2 (C), 124.3 (CH), 123.4 (CH), 39.1 (CH_2), 29.6 (CH_2), 28.5 (CH_2) 26.5 (CH_2); EI-MS (m/z): 121 $[PyNHCO]^+$, 131 $[NH(CH_2)_7NH+2H]^{2+}$, 251 $[PyNHCONH(CH_2)_7NH+2H]^{2+}$, 371 $[M+H]^+$, 393 $[M+Na]^+$, 741 $[2M+H]^+$, 763 $[2M+Na]^+$. Analysis Calc. for $C_{19}H_{26}N_6O_2$: C 61.60, H 7.07, N 21.69 %, Found: C 61.05, H 6.98, N 22.18 %; IR ($\tilde{\nu}$ / cm^{-1}): 3332 (m, $(N–H)_{str}$), 1627 (strong, sharp, $(C=O)_{str}$), 1557 (strong, sharp, $(N–H)_{def}$).

8.2.8 *N,N″*-octylene-1,8-diylbis(*N′*-pyridin-3-ylurea), 2.7

Prepared as *N,N″*-ethylene-1,2-diylbis(*N′*-pyridin-3-ylurea), using 1,8-diaminooctane. Yield: 1.04 g, 2.70 mmol (80%). M.p.: 180–182 °C; ^{1}H NMR (DMSO-d_6, 400 MHz, δ / ppm, J/ Hz): 8.58 (2H, s, NH), 8.51 (2H, d, J= 2.6, PyH), 8.10 (2H, dd, J= 1.4, 4.6, PyH), 7.87 (2H, ddd, J= 1.4, 2.6, 8.4, PyH), 7.24 (2H, dd, J= 4.6, 8.4, PyH), 6.27 (2H, t, J= 5.8) 3.08 (4H, q, J= 6.5, CH_2), 1.43 (4H, m, CH_2), 1.29 (6H, m, CH_2); ^{13}C-{^{1}H} NMR (DMSO-d_6, 100 MHz, δ / ppm): 155.1 (C), 142.0 (CH), 139.5 (CH), 137.2 (C), 124.3 (CH), 123.5 (CH), 39.6 (CH_2), 29.6 (CH_2), 28.6 (CH_2), 26.3 (CH_2); EI-MS (m/z): 145, 265, 385 $[M+H]^+$, 407 $[M+Na]^+$, 769 $[2M+H]^+$, 791 $[2M+Na]^+$; Analysis Calc. for $C_{20}H_{28}N_6O_2$: C 62.48, H 7.34, N 21.86 %, Found: C 62.12, H 7.28, N 21.36 %; IR ($\tilde{\nu}$ / cm^{-1}): 3336 (m, $(N–H)_{str}$), 1645 (strong, sharp, $(C=O)_{str}$) 1557 (strong, sharp, $(N–H)_{def}$).

8.2.9 *N,N″*-nonylene-1,9-diylbis(*N′*-pyridin-3-ylurea), 2.8

Prepared as *N,N″*-ethylene-1,2-diylbis(*N′*-pyridin-3-ylurea), using 1,9-diaminononane. Yield: 1.15 g, 2.88 mmol (85%). M.p.: 164–166 °C; ^{1}H NMR (DMSO-d_6, 400 MHz, δ / ppm, J/ Hz): 8.58 (2H, s, NH), 8.51 (2H, d, J= 2.6, PyH), 8.09 (2H, dd, J= 1.4, 4.7, PyH), 7.87 (2H, ddd, J= 1.4, 2.6, 8.3, PyH), 7.23 (2H, dd, J= 4.7, 8.3, PyH), 6.26 (2H, t, J= 5.5, NH), 3.07 (4H, q, J= 6.2, CH_2), 1.42 (4H, m, J= 6.7, CH_2), 1.28 (10H, s, CH_2); ^{13}C-{^{1}H} NMR (100 MHz, DMSO-d_6, 25 °C): 155.1 (C), 141.9 (CH), 139.5 (CH), 137.2 (C), 124.3 (CH), 123.6 (CH), 39.1 (CH_2), 29.6 (CH_2), 29.0 (CH_2), 28.7 (CH_2), 26.3 (CH_2) ppm; EI-MS (m/z): 399 $[M+H]^+$, 421 $[M+Na]^+$, 797 $[2M+H]^+$, 819 $[2M+Na]^+$; Analysis Calc. for $C_{21}H_{30}N_6O_2$: C 63.29, H 7.59, N 21.09 %, Found C 62.73, H 7.50, N 20.68 %; IR ($\tilde{\nu}$ / cm^{-1}): 3336 (m, $(N–H)_{str}$), 1632 (strong, sharp, $(C=O)_{str}$), 1557 (strong, sharp, $(N–H)_{def}$)

8.2.10 *N,N″*-decylene-1,10-diylbis(*N′*-pyridin-3-ylurea), 2.9

Prepared as *N,N″*-ethylene-1,2-diylbis(*N′*-pyridin-3-ylurea), using 1,10-diaminodecane. Yield: 1.31 g, 3.18 mmol (95%). M.p.: 176–178 °C; ^{1}H NMR (DMSO-d_6, 400 MHz, δ / ppm, J/ Hz): 8.57 (2H, s, NH), 8.51 (2H, d, J= 2.6, PyH), 8.09 (2H, dd, J= 1.4, 4.6, PyH), 7.87 (2H, ddd, J= 1.4, 2.6, 8.3, PyH), 7.23 (2H, dd, J= 4.6, 8.3, PyH), 6.26 (2H, t, J= 5.5, NH), 3.06 (4H, q, J= 6.8, CH_2), 1.41 (4H, m, J= 6.1, CH_2), 1.27 (12H, s, CH_2); ^{13}C-{^{1}H} NMR (DMSO-d_6, 100 MHz, δ / ppm): 155.1 (C), 141.9 (CH), 139.4 (CH), 137.2 (C), 124.3 (CH), 123.4 (CH), 39.1 (CH_2), 29.6 (CH_2), 29.0 (CH_2), 28.7 (CH_2), 26.3 (CH_2); EI-MS (m/z): 121 $[PyNHCO]^+$, 173, 293, 413 $[M+H]^+$, 435 $[M+Na]^+$, 847 $[2M+Na]^+$; Analysis Calc. for $C_{22}H_{32}N_6O_2$: C 64.05, H 7.82, N 20.37 %, Found: C 63.78, H 7.78, N 19.90 %; IR ($\tilde{\nu}$ / cm^{-1}): 3338 (m, $(N–H)_{str}$), 1648 (strong, sharp, $(C=O)_{str}$), 1562 (strong, sharp, $(N–H)_{def}$).

8.2.11 *N,N″*-phenylene-1,4-diybis(*N′*-pyridin-3-ylurea), 2.10

Prepared as *N,N″*-ethylene-1,2-diylbis(*N′*-pyridin-3-ylurea), using 1,4-diaminobenzene. Yield: 0.51 g, 1.46 mmol (43%). M.p.: Decomposes above 280 °C; ^{1}H NMR (DMSO-

d_6, 400 MHz, δ / ppm, J/ Hz): 8.79 (2H, s, NH), 8.69 (2H, s, NH), 8.59 (2H, s, PyH), 8.17 (2H, d, J= 4.7, PyH), 7.93 (2H, d, J= 8.4, PyH), 7.38 (4H, s, ArH), 7.30 (2H, dd, J= 4.7, 8.4, PyH); ^{13}C-{^{1}H} NMR (DMSO-d_6, 100 MHz, δ / ppm): 152.5 (C), 142.7 (CH), 139.8 (CH), 136.4 (C), 133.8 (C), 125.3 (CH), 123.6 (CH), 119.3 (CH); EI-MS (m/z): 175 $[M+2H]^{2+}$, 349 $[M+H]^+$, 670 $[2M+H]^+$; Analysis Calc. for $C_{18}H_{16}N_6O_2$: C 62.06, H 4.63, N 24.12 %, Found: C 61.79, H 4.65, N 24.01 %; IR ($\tilde{\nu}$ / cm^{-1}): 3279 (m, $(N–H)_{str}$), 1645 (strong, sharp, $(C=O)_{str}$), 1594 (strong, sharp, $(N–H)_{def}$).

Crystallographic Data for $C_{18}H_{16}N_6O_2$: M = 348.37, colourless plates, 0.21 × 0.13 × 0.06 mm^3, triclinic, space group P-1 (No. 2), a = 6.276(3), b = 7.316(4), c = 17.205(8) Å, α = 80.168(14), β = 83.754(15), γ = 85.013(13)°, V = 771.8(6) Å^3, Z = 2, D_c = 1.499 g/cm^3, F_{000} = 364, Smart-1K, MoKα radiation, λ = 0.71073 Å, T = 120(2)K, $2\theta_{max}$ = 52.0°, 4903 reflections collected, 3017 unique (R_{int} = 0.0445). Final *GooF* = 0.983, *R1* = 0.0661, *wR2* = 0.1496, R indices based on 1766 reflections with I >2Σ(I) (refinement on F^2), 235 parameters, 0 restraints. Lp and absorption corrections applied, μ = 0.104 mm^{-1}.

8.2.12 *N,N″*-naphthalene-1,5-diylbis(*N′*-pyridin-3-ylurea), 2.11

Prepared as *N,N″*-ethylene-1,2-diylbis(*N′*-pyridin-3-ylurea), using 1,5-diaminonaphthalene to give a pale brown solid. The solid was dissolved in DMSO and the product precipitated as a white powder upon addition of water. The product was isolated by filtration and washed with acetone. Yield: 0.05 g, 0.13 mmol (4%). M.p.: Decomposes above 280 °C; ^{1}H NMR (DMSO-d_6, 400 MHz, δ / ppm, J/ Hz): 9.23 (2H, s, NH), 8.90 (2H, s, NH), 8.65 (2H, s, PyH), 8.21 (2H, dt, J= 1.5, 4.7, PyH), 8.03 (2H, d, J= 7.6, ArH), 7.99 (2H, m, PyH), 7.88 (2H, d, J= 8.6, ArH), 7.58 (2H, t, J= 8.1, ArH), 7.34 (2H, dd, J= 4.7, 8.3, PyH); ^{13}C-{^{1}H} NMR (DMSO-d_6, 100 MHz, δ / ppm): 153.0 (C), 142.9 (CH), 140.0 (CH), 136.5 (C), 134.5 (C), 126.9 (C), 125.6 (CH), 125.1 (CH), 123.6 (CH), 118.1 (CH), 116.8 (CH); EI-MS (m/z) = 399 $[M+H]^+$, 421 $[M+Na]^+$, 797 $[2M+H]^+$; Analysis Calc. for $C_{22}H_{18}N_6O_2$: C 66.32, H 4.55, N 21.09 %, Found: C 66.45, H 4.78, N 20.37 %; IR ($\tilde{\nu}$ / cm^{-1}): 3275 (m,

$(N–H)_{str}$), 1635 (strong, sharp, $(C=O)_{str}$), 1542 (strong, sharp, $(N–H)_{def}$).

Crystallographic Data for $C_{22}H_{18}N_6O_2$: M = 398.42, colourless plate, 0.40 × 0.20 × 0.10 mm^3, monoclinic, space group $P2_1/c$ (No. 14), a = 18.2108(17), b = 4.5671(4), c = 11.3315(10) Å, β = 106.092(3)°, V = 905.52(14) Å^3, Z = 2, D_c = 1.461 g/cm^3, F_{000} = 416, SMART-6K, MoKα radiation, λ = 0.71073 Å, T = 120(2)K, $2\theta_{max}$ = 58.3°, 14787 reflections collected, 2442 unique (R_{int} = 0.0528). Final *GooF* = 1.057, *R1* = 0.0566, *wR2* = 0.1397, R indices based on 1662 reflections with I >2Σ(I) (refinement on F^2), 146 parameters, 0 restraints. Lp and absorption corrections applied, μ = 0.099 mm^{-1}.

8.2.13 *N,N″*-pyridine-2,6-diylbis(*N′*-pyridin-3-ylurea), 5.14

Prepared as *N,N″*-ethylene-1,2-diylbis(*N′*-pyridin-3-ylurea), using 2,6-diaminopyridine. Yield: 0.66. g, 1.88 mmol (56%). M.p.: 208–210 °C; ^{1}H NMR (DMSO-d_6, 400 MHz, δ / ppm, J/ Hz): 9.34 (2H, d, J= 2.8, NH), 8.63 (2H, t, J= 2.4, PyH), 8.08 (2H, dd, J= 1.5, 4.6, PyH), 7.87 (2H, ddd, J= 1.5, 2.7, 8.3, PyH), 7.23 (2H, dd, J= 4.6, 8.3), 6.29 (2H), t, J= 6.5, NH), 3.09 (4H, q, J= 6.5, CH_2), 1.45 (4H, m, J= 7.4, CH_2), 1.31 (2H, m, CH_2); ^{13}C-{^{1}H} NMR (DMSO-d_6, 100 MHz, δ / ppm): 115.1 (C), 141.9 (CH), 139.5 (CH), 137.2 (C), 124.3 (CH), 123.4 (CH), 39.1 (CH_2), 29.4 (CH_2), 23.7 (CH_2); EI-MS (m/z): 207 $[2M+Na]^+$; Analysis. Calc. for $C_{19}H_{28}N_6O_2$: C 59.63, H 6.48, N 24.54 %, Found: C 59.55, H 6.47, N 24.57 %; IR ($\tilde{\nu}$ / cm^{-1}): 3494 (m, $(N–H)_{str}$), 1698 (strong, sharp, $(C=O)_{str}$), 1547 (strong, sharp, $(N–H)_{def}$).

8.2.14 *N,N″*-cyclohexylene-1,2-diylbis(*N′*-pyridin-3-ylurea), 5.15

Prepared as *N,N″*-ethylene-1,2-diylbis(*N′*-pyridin-3-ylurea), using (±)-*trans*-1,2-diaminocyclohexane. Yield: 0.79 g, 0.22 mmol (66%). M.p.: 246–248 °C; ^{1}H NMR (DMSO-d_6, 400 MHz, δ / ppm, J/ Hz): 8.70 (2H, s, NH), 8.53 (2H, d, J= 2.6, PyH), 8.06 (2H, dd, J= 1.5, 4.7, PyH), 7.82 (2H, ddd, J= 1.5, 2.6, 8.3, PyH), 7.20 (2H, dd, J= 4.7, 8.3, PyH), 6.23 (2H, d, J= 7.4, NH), 3.44 (2H, m, CH), 1.95 (2H, d,

J= 10.5, CH_2), 1.66 (2H, m, CH_2), 1.26 (4H, m, CH_2); ^{13}C-{^{1}H} NMR (DMSO-d_6, 100 MHz, δ / ppm): 155.0 (C), 142.0 (CH), 139.5 (CH), 137.1 (C), 124.4 (CH), 123.3 (CH), 52.7 (CH), 32.7 (CH_2), 24.3 (CH_2); EI-MS (m/z): 178 $[M+2H]^{2+}$, 355 $[M+H]^+$; Analysis Calc. for $C_{18}H_{22}N_6O_2$: C 61.00, H 6.26, N 23.71 %, Found: C 60.90, H 6.24, N 23.76 %; IR ($\tilde{\nu}$ / cm^{-1}): 3348 (m, $(N–H)_{str}$), 1648 (strong, sharp, $(C=O)_{str}$), 1546 (strong, sharp, $(N–H)_{def}$).

8.2.15 *N,N″*-methylenebisphenyl-4,1-diylbis(*N′*-pyridin-3-ylurea), 5.16

Prepared as *N,N″*-ethylene-1,2-diylbis(*N′*-pyridin-3-ylurea), using 4,4-methylenebisaniline. Yield: 1.05g, 3.97 mmol (71%). M.p.: Decomposes above 250 °C; ^{1}H NMR (DMSO-d_6, 400 MHz, δ / ppm, J/ Hz): 8.80 (2H, s, NH), 8.73 (2H, s, NH), 8.58 (2H, d, J= 2.5, PyH), 8.17 (2H, d, J= 4.7, PyH), 7.93 (2H, d, J= 8.5, PyH), 7.36 (4H, d, J= 8.4, ArH), 7.30 (2H, dd, J= 4.7, 8.3, PyH), 7.13 (4H, d, J= 8.4, ArH), 3.82 (2H, s, -CH_2-); ^{13}C-{^{1}H} NMR (DMSO-d_6, 400 MHz, δ / ppm): 153.0 (C), 143.2 (CH), 140.3 (CH), 137.5 (C), 136.8 (C), 136.0 (C), 129.4 (CH), 125.8 (CH), 124.2 (CH), 119.2 (CH), 40.3 (CH_2); EI-MS (m/z): 220 $[M+2H]^{2+}$, 439 $[M+H]^+$, 877 $[2M+H]^+$; Analysis Calc. for $C_{25}H_{22}N_6O_2$: C 68.48, H 5.06, N 19.17 %, Found: C 68.43, H 5.03, N 18.88 %; IR ($\tilde{\nu}$ / cm^{-1}): 3300 (m, $(N–H)_{str}$), 1649 (strong, sharp, $(C=O)_{str}$), 1598 (strong, sharp, $(N–H)_{def}$).

8.3 Complex Syntheses

8.3.1 $[Cu(2.1)](NO_3)_2{\cdot}6H_2O$

N,N″-ethylene-1,2-diylbis(*N′*-pyridin-3-ylurea) (30 mg, 0.1 mmol) was dissolved in a mixture of THF & water (2:3, 5 mL) and added to copper(II) nitrate (23 mg, 0.1 mmol). Crystals formed upon evaporation of the solvent.

Crystallographic Data for $C_{14}H_{28}CuN_8O_{14}$: M = 595.98, blue block, 0.21 × 0.12 × 0.10 mm^3, triclinic, space group P-1 (No. 2), a = 7.4582(11), b = 9.4917(14), c

= 9.6997(14) Å, α = 113.399(4), β = 106.638(4), γ = 98.603(4)°, V = 576.10(15) Å^3, Z = 1, D_c = 1.718 g/cm^3, F_{000} = 309, Smart-6K, MoKα radiation, λ = 0.71073 Å, T = 120(2)K, $2\theta_{max}$ = 60.0°, 8766 reflections collected, 3371 unique (R_{int} = 0.0400). Final *GooF* = 1.024, *R1* = 0.0449, *wR2* = 0.1043, R indices based on 2609 reflections with I >2Σ(I) (refinement on F^2), 193 parameters, 6 restraints. Lp and absorption corrections applied, μ = 1.036 mm^{-1}.

8.3.2 [Ag(2.1)]NO_3·MeCN·$CHCl_3$

N,N″-ethylene-1,2-diylbis(*N′*-pyridin-3-ylurea) (30 mg, 0.10 mmol) was dissolved in a 1:1 mixture of MeCN and $CHCl_3$ (4.5 mL) which was then added to solution of silver(I) nitrate (17.0 mg, 0.10 mmol) in MeOH (3 mL) Crystals formed upon standing which were analysed using X-ray crystallography. Yield: 30.3 mg, 0.05 mmol (48%). Analysis Calc. for $C_{43}H_{62}Ag_2N_{20}O_{18}$: C 32.38, H 3.20, N 17.77 %, Found: C 32.42, H 3.21, N 18.03 %; IR ($\tilde{\nu}$ / cm^{-1}): 3311 (w, (N–H)$_{str}$), 1681 (strong, sharp, (C=O)$_{str}$), 1547 (strong, sharp, (N–H)$_{def}$).

Crystallographic Data for $C_{17}H_{20}AgCl_3N_8O_5$: M = 630.63, colourless flat needles, 0.39 × 0.32 × 0.19 mm^3, triclinic, space group *P*-1 (No. 2), a = 5.5449(16), b = 13.819(4), c = 15.927(5) Å, α = 85.794(8), β = 84.557(8), γ = 87.260(7)°, V = 1210.6(6) Å^3, Z = 2, D_c = 1.730 g/cm^3, F_{000} = 632, Smart-6K, MoKα radiation, λ = 0.71073 Å, T = 120(2)K, $2\theta_{max}$ = 65.1°, 21797 reflections collected, 8123 unique (Rint = 0.0410). Final *GooF* = 1.038, *R1* = 0.0515, *wR2* = 0.1132, R indices based on 5974 reflections with I >2Σ(I) (refinement on F^2), 308 parameters, 0 restraints. Lp and absorption corrections applied, μ = 1.210 mm^{-1}.

8.3.3 [Ag(2.1)]$C_4H_3O_2$·4H_2O

N,N″-ethylene-1,2-diylbis(*N′*-pyridin-3-ylurea) (15 mg, 0.05 mmol) was dissolved in a 1:1 mixture of EtOH and water (3 mL) which was then added to silver(I) acetate (8.3 mg, 0.05 mmol). Upon slow evaporation of the solvent, crystals formed which were analysed using X-ray crystallography. Yield: 10.4 mg, 0.02 mmol (39%). Analysis Calc. for $C_{16}H_{27}AgN_6O_8$: C 35.60, H 5.05, N 15.60 %, Found: C 35.19, H

4.82, N 13.13 %; IR ($\tilde{\nu}$ / cm^{-1}): 3328 (m, $(N–H)_{str}$), 1669 (strong, sharp, $(C=O)_{str}$), 1549 (strong, sharp, $(N–H)_{def}$).

Crystallographic Data for $C_{16}H_{27}AgN_6O_8$: M = 539.31, colourless flat needle, 0.21 × 0.16 × 0.10 mm^3, triclinic, space group P-1 (No. 2), a = 6.8864(5), b = 12.0430(10), c = 13.2699(10) Å, α = 78.535(3), β = 77.905(3), γ = 78.335(3)°, V = 1039.71(14) $Å^3$, Z = 2, D_c = 1.723 g/cm^3, F_{000} = 552, Smart-6K, MoKα radiation, λ = 0.71073 Å, T = 120(2)K, $2\theta_{max}$ = 65.0°, 15692 reflections collected, 7102 unique (R_{int} = 0.0452). Final *GooF* = 0.928, *R1* = 0.0407, *wR2* = 0.0775, R indices based on 5317 reflections with I >2Σ(I) (refinement on F^2), 312 parameters, 8 restraints. Lp and absorption corrections applied, μ = 1.027 mm^{-1}.

8.3.4 2[Ag(2.1)]PF_6·2C_3H_7NO

N,N″-ethylene-1,2-diylbis(*N′*-pyridin-3-ylurea) (15 mg, 0.05 mmol) was dissolved in a 1:1 mixture of MeCN and DMF (3 mL) which was then added to silver(I) acetate (9.7 mg, 0.05 mmol). Upon slow evaporation of the solvent, crystals formed which were analysed using X-ray crystallography.

Crystallographic Data for $C_{17}H_{23}AgF_3N_7O_3P_{0.50}$, M = 553.78, colourless prism, 0.15 × 0.13 × 0.09 mm^3, monoclinic, space group $P2_1/c$ (No. 14), a = 9.0260(8), b = 16.3903(17), c = 14.0277(14) Å, β = 97.969(3)°, V = 2055.2(3) $Å^3$, Z = 4, D_c = 1.790 g/cm^3, F_{000} = 1118, Smart 6K, MoKα radiation, λ = 0.71073 Å, T = 120(2)K, $2\theta_{max}$ = 55.0°, 15292 reflections collected, 4722 unique (R_{int} = 0.0714). Final *GooF* = 0.839, *R1* = 0.0411, *wR2* = 0.0700, R indices based on 2915 reflections with I >2Σ(I) (refinement on F^2), 286 parameters, 0 restraints. Lp and absorption corrections applied, μ = 1.083 mm^{-1}.

8.3.5 [Ag(2.1)]BF_4·MeOH

N,N″-ethylene-1,2-diylbis(*N′*-pyridin-3-ylurea) (15 mg, 0.05 mmol) was dissolved in 1:1 mixture of MeOH and water (3 mL) which was then added to silver(I) tetrafluoroborate (9.7 mg, 0.05 mmol). Upon slow evaporation of the solvent, crystals formed which were analysed using X-ray crystallography. Yield: 9.3 mg, 0.02 mmol (35%).

IR ($\tilde{\nu}$ / cm^{-1}): 3361 (m, $(N–H)_{str}$), 1675 (strong, sharp, $(C=O)_{str}$), 1539 (strong, sharp, $(N–H)_{def}$).

Crystallographic Data for $C_{15}H_{20}AgBF_4N_6O_3$: M = 527.05, colourless needle, 0.18 × 0.12 × 0.11 mm^3, triclinic, space group P-1 (No. 2), a = 9.1412(13), b = 9.2472(12), c = 11.3257(15) Å, α = 84.346(4), β = 84.501(4), γ = 87.385(4)°, V = 947.7(2) $Å^3$, Z = 2, D_c = 1.847 g/cm^3, F_{000} = 528, Smart-6K, MoKα radiation, λ = 0.71073 Å, T = 120(2)K, $2\theta_{max}$ = 65.9°, 18399 reflections collected, 6538 unique ($Rint$ = 0.0375). Final $GooF$ = 0.916, $R1$ = 0.0324, $wR2$ = 0.0589, R indices based on 5073 reflections with I >2Σ(I) (refinement on F^2), 273 parameters, 0 restraints. Lp and absorption corrections applied, μ = 1.134 mm^{-1}.

8.3.6 $[Ag_2(2.1)_3](NO_3)_2 \cdot 7H_2O$

N,N″-ethylene-1,2-diylbis(*N′*-pyridin-3-ylurea) (30 mg, 0.10 mmol) was dissolved in a mixture of DMF & water (1:1, 6 mL) and added to silver(I) nitrate (17 mg, 0.10 mmol). Crystals formed upon evaporation of the solvent. Yield: 18.0 mg, 0.01 mmol (40%). Analysis. Calc. for $C_{42}H_{62}N_{20}O_{19}Ag_2$: C 36.91, H 4.57, N 20.50 %, Found: C 36.86, H 4.22, N 20.54 %; IR ($\tilde{\nu}$ / cm^{-1}): 3337 (m, $(N–H)_{str}$), 1687 (strong, sharp, $(C=O)_{str}$), 1549 (strong, sharp, $(N–H)_{def}$).

Crystallographic Data for $C_{42}H_{62}Ag_2N_{20}O_{19}$: M = 1366.86, colourless prism, 0.28 × 0.24 × 0.23 mm^3, monoclinic, space group $P2_1/c$ (No. 14), a = 15.683(4), b = 27.326(6), c = 12.807(3) Å, β = 96.982(7)°, V = 5448(2) $Å^3$, Z = 4, D_c = 1.666 g/cm^3, F_{000} = 2800, Smart-6K, MoKα radiation, λ = 0.71073 Å, T = 120(2)K, $2\theta_{max}$ = 52.0°, 68674 reflections collected, 10697 unique (R_{int} = 0.0985). Final $GooF$ = 1.160, $R1$ = 0.0698, $wR2$ = 0.1525, R indices based on 7662 reflections with I >2Σ(I) (refinement on F^2), 804 parameters, 21 restraints. Lp and absorption corrections applied, μ = 0.811 mm^{-1}.

8.3.7 $3[Ag(2.1)_{1.5}]NO_3 \cdot 3MeCN \cdot 2CHCl_3 \cdot MeOH$

N,N″-ethylene-1,2-diylbis(*N′*-pyridin-3-ylurea) (30 mg, 0.10 mmol) was dissolved in a mixture of acetonitrile, chloroform and methanol (3:3:4, 15 mL) and added to

silver(I) nitrate (17 mg, 0.10 mmol). Crystals formed upon slow evaporation of the solvent. Yield: 18.0 mg, 0.01 mmol (40%). Analysis. Calc. for $C_{72}H_{87}N_{33}O_{19}Ag_3Cl_6$: C 38.35, H 3.89, N 20.50 %, Found: C 38.30, H 3.94, N 20.56 %.

Crystallographic Data for $C_{25}H_{30}AgN_{12}O_6$: $M = 702.46$, colourless prism needles, $0.43 \times 0.24 \times 0.23\,mm^3$, monoclinic, space group $C2/c$ (No. 15), $a = 15.727(2)$, $b = 27.878(4)$, $c = 12.9629(18)$ Å, $\beta = 103.922(6)°$, $V = 5516.6(13)$ Å^3, $Z = 8$, $D_c = 1.593$ g/cm^3, $F_{000} = 2696$, Smart-6K, MoKα radiation, $\lambda = 0.71073$ Å, $T = 120(2)$K, $2\theta_{max} = 70.1°$, 31608 reflections collected, 11136 unique ($R_{int} = 0.0419$). Final *GooF* = 1.024, *R1* = 0.0639, *wR2* = 0.2020, *R* indices based on 5993 reflections with I >2Σ(I) (refinement on F^2), 372 parameters, 0 restraints. Lp and absorption corrections applied, $\mu = 0.791$ mm^{-1}.

8.3.8 $[Ag_2(2.1)_3](NO_3)_2 \cdot 7H_2O \cdot 2MeCN$

N,N″-ethylene-1,2-diylbis(*N′*-pyridin-3-ylurea) (30 mg, 0.10 mmol) was dissolved in a mixture of MeCN and $CHCl_3$ (1:1, 9 mL) and added to a solution of silver(I) nitrate (17 mg, 0.10 mmol) in MeOH (6 mL). Crystals formed upon evaporation of the solvent. Yield: 7.2 mg, 0.01 mmol (15%). Analysis. Calc. for $Ag_2C_{42}H_{48}N_{20}O_{12}(H_2O)_7(CH_3CN)_2$: C 38.13, H 4.73, N 21.27 %; Found: C 38.03, H 4.20, N 21.18 %.

8.3.9 $[Ag_2(2.1)_3](NO_3)_2 \cdot MeOH \cdot 5H_2O$

N,N″-ethylene-1,2-diylbis(*N′*-pyridin-3-ylurea) (15 mg, 0.05 mmol) was dissolved in a 1:1 mixture of MeOH and water (6 mL) which was then added to silver(I) nitrate (8.5 mg, 0.05 mmol). Upon slow evaporation of the solvent, crystals formed which were analysed using X-ray crystallography. Yield: 19.7 mg, 0.01 mmol (87%). Analysis Calc. for $C_{43}H_{62}Ag_2N_{20}O_{18}$: C 37.90, H 4.59, N 20.56 %, Found: C 37.31, H 4.18, N 20.58 %; IR ($\tilde{\nu}$ / cm^{-1}): 3338 (w, $(N–H)_{str}$), 1686 (strong, sharp, $(C=O)_{str}$), 1547 (strong, sharp, $(N–H)_{def}$).

Crystallographic Data for $C_{43}H_{62}Ag_2N_{20}O_{18}$: $M = 1362.87$, $0.20 \times 0.12 \times 0.10$ mm^3, monoclinic, space group $P2_1/c$ (No. 14), $a = 16.0110(3)$, $b = 26.9940(5)$,

c = 12.6123(3) Å, β = 91.3200(10)°, V = 5449.60(19) Å^3, Z = 4, D_c = 1.661 g/cm^3, F_{000} = 2792, MoKα radiation, β = 0.71073 Å, T = 120(2)K, $2\theta_{max}$ = 52.0°, 37442 reflections collected, 10717 unique (R_{int} = 0.0907). Final *GooF* = 1.063, *R1* = 0.0677, *wR2* = 0.1563, R indices based on 5853 reflections with I >2Σ(I) (refinement on F^2), 745 parameters, 0 restraints. Lp and absorption corrections applied, μ = 0.810 mm^{-1}.

8.3.10 $[Ag_2(2.1)_3](NO_3)_2{\cdot}5H_2O{\cdot}MeCN$

N,N″-ethylene-1,2-diylbis(*N′*-pyridin-3-ylurea) (30 mg, 0.10 mmol) was dissolved in a mixture of MeCN & water (1:1, 6 mL) and added to silver(I) nitrate (17 mg, 0.10 mmol). Crystals formed upon evaporation of the solvent.

Crystallographic Data for $C_{20}H_{25}AgN_6O_4$, M = 521.33, 0.23 × 0.34 × 0.21 mm^3, triclinic, space group *P*-1 (No. 2), a = 15.4333(12), b = 15.5503(12), c = 15.6241(12) Å, α = 113.907(2), β = 118.481(2), γ = 95.751(2)°, V = 2805.0(4) Å^3, Z = 5, D_c = 1.543 g/cm^3, F_{000} = 1330, MoKα radiation, λ = 0.71073 Å, T = 120(2)K, $2\theta_{max}$ = 60.0°, 30537 reflections collected, 16342 unique (R_{int} = 0.0468). Final *GooF* = 0.999, *R1* = 0.0575, *wR2* = 0.1305, R indices based on 8680 reflections with I >2Σ(I) (refinement on F^2), 766 parameters, 2 restraints. Lp and absorption corrections applied, μ = 0.936 mm^{-1}.

8.3.11 $[Ag(2.4)]NO_3{\cdot}2H_2O{\cdot}MeCN$

N,N″-pentylene-1,5-diylbis(*N′*-pyridin-3-ylurea) (90 mg, 0.26 mmol) was dissolved in a 1:1:1 mixture of MeOH, $CHCl_3$ and MeCN (4.5 mL) and added to silver(I) nitrate (45 mg, 0.26 mmol). Crystals formed upon evaporation of the solvent which were analysed using X-ray crystallography. Samples for elemental analysis were dried in air resulting in some loss of water. Samples dried under high vacuum proved to absorb moisture from the atmosphere upon exposure. Yield: 79 mg, 0.14 mmol (55%). Calc. for $C_{17}H_{22}N_7O_5Ag(MeCN)(H_2O)_{1.25}$: C 39.53, H 4.83, N 19.41 %, Found: C 39.44, H 4.39, N 18.93 %; IR ($\tilde{\nu}$ / cm^{-1}): 3309 (w, $(N–H)_{str}$), 1674 (strong, sharp, $(C{=}O)_{str}$), 1549 (strong, sharp, $(N–H)_{def}$).

Crystallographic Data for $C_{19}H_{29}AgN_8O_7$: M = 589.37, plate colourless, 0.32 × 0.27 × 0.14 mm^3, orthorhombic, space group $Pna2_1$ (No. 33), a = 34.975(3), b = 12.5607(11), c = 5.7537(5) Å, V = 2527.7(4) Å^3, Z = 4, D_c = 1.549 g/cm^3, F_{000} = 1208, Smart-6K, MoKα radiation, λ = 0.71073 Å, T = 120(2)K, $2\theta_{max}$ = 66.4°, 19731 reflections collected, 8425 unique (R_{int} = 0.0393). Final *GooF* = 1.029, *R1* = 0.0460, *wR2* = 0.0984, R indices based on 6401 reflections with I >2Σ(I) (refinement on F^2), 333 parameters, 7 restraints. Lp and absorption corrections applied, μ = 0.852 mm^{-1}. Absolute structure parameter = -0.03(2) (Flack, H. D. Acta Cryst. 1983, A39, 876-881).

8.3.12 [Ag(2.4)]BF_4·THF

N,N″-pentylene-1,5-diylbis(*N′*-pyridin-3-ylurea) (90 mg, 0.26 mmol) was dissolved in a 3:2 mixture of THF and water (6 mL) and added to silver(I) tetrafluoroborate (51 mg, 0.26 mmol). Crystals formed upon slow evaporation of the solvent. The material proved highly unstable in the atmosphere rapidly losing solvent and as a result samples for elemental analysis were dried under high vacuum however varying amounts of solvent remained. Two separate crystals were analysed by X-ray crystallography at low temperature under nitrogen and both gave the same structure. Yield: 29 mg, 0.05 mmol (19 %). Analysis Calc. for $C_{17}H_{22}BN_6O_2F_4Ag(C_4H_8O)_{0.25}$: C 38.94, H 4.36, N 15.14 %, Found: C 38.00, H 4.45, N 14.81 %; IR ($\tilde{\nu}$ / cm^{-1}): 3402 (w, $(N–H)_{str}$), 1683 (strong, sharp, $(C=O)_{str}$), 1544 (strong, sharp, $(N–H)_{def}$).

Crystallographic Data for $C_{21}H_{22}AgBF_4N_6O_3$: M = 601.13, 0.22 × 0.37 × 0.26 mm^3, monoclinic, space group $P2_1/c$ (No. 14), a = 15.4795(17), b = 7.3939(8), c = 23.842(3) Å, β = 122.153(3)°, V = 2310.3(4) Å^3, Z = 4, D_c = 1.728 g/cm^3, F_{000} = 1208, MoKα radiation, λ = 0.71073 Å, T = 273(2)K, $2\theta_{max}$ = 50.0°, 21914 reflections collected, 4077 unique (R_{int} = 0.0592). Final *GooF* = 1.252, *R1* = 0.1462, *wR2* = 0.3479, R indices based on 3670 reflections with I >2Σ(I) (refinement on F^2), 296 parameters, 7 restraints. Lp and absorption corrections applied, μ = 0.942 mm^{-1}.

8.3.13 $[Ag(2.4)]CH_3CO_2 \cdot 7H_2O$

N,N″-pentylene-1,5-diylbis(*N′*-pyridin-3-ylurea) (30 mg, 0 .09 mmol) was dissolved in a 1:1 mixture of THF and water (6 mL) and added to silver(I) acetate (14.6 mg, 0.09 mmol). Crystals formed upon evaporation of the solvent

Crystallographic Data for $C_{19}H_{32}AgN_6O_{11}$: M = 628.38, colourless triangular plate, 0.30 × 0.10 × 0.05 mm^3, monoclinic, space group $C2/c$ (No. 15), a = 5.7459(2), b = 21.9616(7), c = 22.1388(8) Å, β = 92.730(2)°, V = 2790.51(17) Å^3, Z = 4, D_c = 1.496 g/cm^3, F_{000} = 1292, SMART 6k, MoKα radiation, λ = 0.71073 Å, T = 120(2)K, $2\theta_{max}$ = 58.3°, 23587 reflections collected, 3770 unique (R_{int} = 0.0873). Final *GooF* = 0.972, *R1* = 0.0517, *wR2* = 0.1173, R indices based on 2120 reflections with I >2Σ(I) (refinement on F^2), 212 parameters, 0 restraints. Lp and absorption corrections applied, μ = 0.785 mm^{-1}.

8.3.14 $[Ag(5.15)]NO_3 \cdot 1.5H_2O$

N,N″-cyclohexane-1,2-diylbis(*N′*-pyridin-3-ylurea) (30 mg, 0.08 mmol) was dissolved in a 1:1 mixture of THF and water (3 mL) which was then added to silver(I) nitrate (16.5 mg, 0.08 mmol). Upon slow evaporation of the solvent, crystals formed which were analysed using X-ray crystallography. Yield: 22.2 mg, 0.02 mmol (46%). Analysis Calc. for $C_{18}H_{25}AgN_7O_{6.5}$: C 39.22, H 4.57, N 17.78 %, Found: C 39.33, H 4.46, N 17.58 %; IR ($\tilde{\nu}$ / cm^{-1}): 3324 (m, $(N–H)_{str}$), 1667 (strong, sharp, $(C=O)_{str}$), 1547 (strong, sharp, $(N–H)_{def}$).

Crystallographic Data for $C_{18}H_{25}AgN_7O_{6.5}$: M = 551.32, Prism colourless, 0.21 × 0.20 × 0.18 mm^3, monoclinic, space group $C2/c$ (No. 15), a = 24.965(3), b = 8.6312(9), c = 21.090(3) Å, β = 105.509(3)°, V = 4378.9(8) Å^3, Z = 8, D_c = 1.673 g/cm^3, F_{000} = 2248, Smart-6K, MoKα radiation, λ = 0.71073 Å, T = 120(2)K, 2θmax = 56.0°, 16078 reflections collected, 5275 unique (R_{int} = 0.0492). Final *GooF* = 0.945, *R1* = 0.0374, *wR2* = 0.0797, R indices based on 3762 reflections with I >2Σ(I) (refinement on F^2), 306 parameters, 3 restraints. Lp and absorption corrections applied, μ = 0.974 mm^{-1}.

8.3.15 [Ag(5.12)]NO_3·nTHF

N,N″-methylenebisphenyl-4,1-diylbis(*N′*-pyridin-3-ylurea) was dissolved in a mixture of THF & water (1:1) and added to a solution of silver(I) nitrate in THF & water. Upon standing, the solution turned into a clear gel which crystallised. Analysis Calc. for $(C_{25}H_{22}AgN_7O_5)_2(H_2O)_3$: C 47.30, H 3.97, N, 15.40 %, Found: C 47.41, H 3.96, N 14.40 %.

Crystallographic Data for $C_{25}H_{22}AgN_7O_3$: $M = 576.37$, $0.23 \times 0.22 \times 0.18$ mm^3, triclinic, space group $P1$ (No. 1), $a = 17.348(2)$, $b = 24.906(3)$, $c = 17.2274(18)$ Å, $\alpha = 90.00$, $\beta = 90.00$, $\gamma = 90.00°$, $V = 7443.4(14)$ Å^3, $Z = 12$, $D_c = 1.543$ g/cm^3, $F_{000} = 3504$, MoKα radiation, $\lambda = 0.71073$ Å, $T = 273(2)$K, $2\theta_{max} = 46.6°$, 50382 reflections collected, 36355 unique ($R_{int} = 0.0906$). Final *GooF* = 3.265, *R1* = 0.2366, *wR2* = 0.5117, *R* indices based on 24098 reflections with I >2Σ(I) (refinement on F^2), 1073 parameters, 3 restraints. Lp and absorption corrections applied, $\mu = 0.854$ mm^{-1}. Absolute structure parameter = 0.41(10) (Flack, H. D. Acta Cryst. 1983, A39, 876-881).

8.4 Gel Syntheses

8.4.1 *N,N″*-ethylene-1,2-diylbis(*N′*-pyridin-3-ylurea) and copper(II) chloride

N,N″-ethylene-1,2-diylbis(*N′*-pyridin-3-ylurea) (15 mg, 0.05 mmol) was dissolved in THF & water (1:1) (1.5mL) and added to $CuCl_2{\cdot}2H_2O$ (8.5 mg, 0.05 mmol) to yield a clear blue gel Samples for IR spectroscopic analysis were dried in air. IR ($\tilde{\nu}$ / cm^{-1}): 1616 (medium, sharp, $(C{=}O)_{str}$), 1554 (strong, sharp, $(N{-}H)_{def}$).

8.4.2 *N,N″*-ethylene-1,2-diylbis(*N′*-pyridin-3-ylurea) and copper(II) bromide

N,N″-ethylene-1,2-diylbis(*N′*-pyridin-3-ylurea) (15 mg, 0.05 mmol) was dissolved in THF & water (1:1) (1.5mL) and added to $CuBr_2$ (11.2 mg, 0.05 mmol) to yield a

opaque green viscous liquid. Samples for IR spectroscopic analysis were dried in air. IR ($\tilde{\nu}$ / cm^{-1}): 1614 (medium, sharp, $(C{=}O)_{str}$), 1555 (strong, sharp, $(N{-}H)_{def}$).

8.4.3 *N,N″*-ethylene-1,2-diylbis(*N′*-pyridin-3-ylurea) and silver(I) nitrate

N,N″-ethylene-1,2-diylbis(*N′*-pyridin-3-ylurea) (15 mg, 0.05 mmol) was dissolved in THF & water (1:1) (1.5mL) and added to solid $AgNO_3$. Upon sonication, the silver nitrate dissolved, and further sonication led to the formation of a clear colourless gel. Samples for IR spectroscopic analysis were dried in air. IR ($\tilde{\nu}$ / cm^{-1}): 1614 (medium, sharp, $(C{=}O)_{str}$), 1557 (strong, sharp, $(N{-}H)_{def}$).

8.4.4 *N,N″*-pyridine-2,6-diylbis(*N′*-pyridin-3-ylurea) and silver(I) nitrate

N,N″-pyridine-2,6-diylbis(*N′*-pyridin-3-ylurea) (30 mg, 0.09 mmol) was dissolved in THF & water (3:2) (1.5mL) and added to solid $AgNO_3$ (14.6 mg, 0.09 mmol). Upon standing after the silver nitrate dissolved, an opaque colourless gel formed. Samples for IR spectroscopic analysis were dried in air. IR ($\tilde{\nu}$ / cm^{-1}): 1616 (v. weak, $(C{=}O)_{str}$), 1559 (strong, sharp, $(N{-}H)_{def}$).

8.4.5 *N,N″*-cyclohexylene-1,2-diylbis(*N′*-pyridin-3-ylurea) and silver(I) tetrafluoroborate

N,N″-cyclohexylene-1,2-diylbis(*N′*-pyridin-3-ylurea) (30 mg, 0.08 mmol) was dissolved in THF & water (3:2) (1.5mL) and added to solid $AgBF_4$ (16.5 mg, 0.08 mmol). Upon standing after the silver nitrate dissolved, an opaque colourless gel formed. Samples for IR spectroscopic analysis were dried in air. IR ($\tilde{\nu}$ / cm^{-1}): 1637 (medium, sharp, $(C{=}O)_{str}$), 1577 (strong, sharp, $(N{-}H)_{def}$).

8.4.6 *N,N″*-methylenebisphenyl-4,1-diylbis(*N′*-pyridin-3-ylurea) and silver(I) nitrate

N,N″-methylenebisphenyl-4,1-diylbis(*N′*-pyridin-3-ylurea) (30 mg, 0.09 mmol) was dissolved in THF & water (3:2) (1.5mL) and added to solid $AgBF_4$ (14.6 mg, 0.09 mmol). Upon standing, the opaque solution transforms into a clear, colourless gel, and after twenty-four hours, the gel decomposes into crystals. Samples of gel for IR spectroscopic analysis were dried in air. IR ($\tilde{\nu}$ / cm^{-1}): 1603 (medium, sharp, $(C{=}O)_{str}$), 1543 (strong, sharp, $(N{-}H)_{def}$).

References

1. T. Graham, *Philos. Trans. R. Soc.*, 1861, **151**, 183–224.

2. T. Graham, *J. Chem. Soc.*, 1864, **17**, 318–327.

3. D. Jordon Lloyd, *Colloid Chemistry*, The Chemical Catalog Co., New York, 1926.

4. P. J. Flory, *Discuss. Faraday Soc.*, 1974, **57**, 7–18.

5. A. A. Karim and R. Bhat, *Trends Food Sci. Tech.*, 2008, **19**, 644–656.

6. F. Fages, *Angew. Chem. Int. Ed.*, 2006, **45**, 1680–1682.

7. N. M. Sangeetha and U. Maitra, *Chem. Soc. Rev.*, 2005, **34**, 821–836.

8. K. Tsuchiya, Y. Orihara, Y. Kondo, N. Yoshino, T. Ohkubo, H. Sakai and M. Abe, *J. Am. Chem. Soc.*, 2004, **126**, 12282–12283.

9. S. A. Ahmed, X. Sallenave, F. Fages, G. Mieden-Gundert, W. M. Mller, U. Müller, F. Vgtle and J. Pozzo, *Langmuir*, 2002, **18**, 7096–7101.

10. L. Frkaneć, M. Jokić, J. Makarević, K. Wolsperger and M. Zinić, *J. Am. Chem. Soc.*, 2002, **124**, 9716–9717.

11. T. Noata and H. Koori, *J. Am. Chem. Soc.*, 2005, **127**, 9324–9325.

12. H. Kim, J. Lee and M. Lee, *Angew. Chem. Int. Ed.*, 2005, **44**, 5810–5814.

13. J. M. J. Paulusse and R. P. Sijbesma, *Angew. Chem. Int. Ed.*, 2006, **45**, 2334–2337.

14. K. Murata, M. Aoki, T. Suzuki, T. Harada, H. Kawabat, T. Komori, F. Ohseto, K. Ueda and S. Shinkai, *J. Am. Chem. Soc.*, 1994, **116**, 6664–6676.

15. J. B. Beck and S. J. Rowan, *J. Am. Chem. Soc.*, 2003, **125**, 13922–13923.

16. S. Kawano, N. Fujita and S. Shinkai, *J. Am. Chem. Soc.*, 2004, **126**, 8592–8593.

17. A. Kishimura, T. Yamashita and T. Aida, *J. Am. Chem. Soc.*, 2005, **127**, 179–183.

18. S. Rieth, C. Baddeley and J. D. Badjić, *Soft Matter*, 2007, **3**, 137–154.

19. M. Dukh, D. Šaman, J. Kroulík, I. Černý, V. Pouzar, V. Král and P. Drašar, *Tetrahedron*, 2003, **59**, 4069–4076.

20. H. Maeda, *Chem. Eur. J.*, 2008, **14**, 11274–11282.

21. S. Wang, S. W., Y. Feng and H. Tian, *Chem. Commun.*, 2006, 1497–1499.

22. O. Roubeau, A. Colin, V. Schmitt and R. Clérac, *Angew. Chem. Int. Ed.*, 2004, **43**, 3283–3286.

23. J. Wu, T. Yi, Q. Xia, Y. Zou, F. Liu, J. Dong, T. Shu, F. Li and C. Huang, *Chem. Eur. J.*, 2009, **15**, 6234–6243.

24. H. Kim, W. Zin and M. Lee, *J. Am. Chem. Soc.*, 2004, **126**, 7009–7014.

25. S. Kume, K. Kuroiwa and N. Kimizuka, *Chem. Commun.*, 2006, 2442–2444.

26. O. J. Dautel, M. Robitzer, J.-P. Lère-Porte, F. Serein-Spirau and J. J. E. Moreau, *J. Am. Chem. Soc.*, 2006, **128**, 16213–16223.

27. J. H. van Esch and B. L. Feringa, *Angew. Chem. Int. Ed.*, 2000, **39**, 2263–2266.

28. M. George and R. G. Weiss, *Acc. Chem. Res.*, 2006, **39**, 489–497.

29. R. G. Weiss and D. J. Abdallah, *Adv. Mater.*, 2000, **12**, 1237–1247.

30. P. Dastidar, *Chem. Soc. Rev.*, 2008, **37**, 2699–2715.

31. M. de Loos, B. L. Feringa and J. H. van Esch, *Eur. J. Org. Chem.*, 2005, 3615–3631.

32. P. Terech and R. G. Weiss, *Chem. Rev.*, 1997, **97**, 3133–3159.

33. L. A. Estroff and A. D. Hamilton, *Chem. Rev.*, 2004, **104**, 1201–1218.

34. O. Gronwald, E. Snip and S. Shinkai, *Curr. Opin. Colloid Interface Sci.*, 2002, **7**, 148–156.

35. K. Yoza, Y. Ono, K. Yoshihara, T. Akao, H. Shinmori, M. Takeuchi, S. Shinkai and D. N. Reinhoudt, *Chem. Commun.*, 1998, 907–908.

36. K. Yoza, N. Amanokura, Y. Ono, T. Akao, H. Shinmori, M. Takeuchi, S. Shinkai and D. N. Reinhoudt, *Chem. Eur. J.*, 1999, **5**, 2722–2729.

37. N. Amanokura, Y. Kanekiyo, S. Shinkai and D. N. Reinhoudt, *J. Chem. Soc., Perkin Trans. 2*, 1999, **2**, 1995–2000.

38. O. Gronwald and S. Shinkai, *Chem. Eur. J.*, 2001, **7**, 4328–4334.

39. R. Luboradzki, O. Gronwald, A. Ikeda and S. Shinkai, *Chem. Lett.*, 2000, **29**, 1148–1149.

40. R. Luboradzki, O. Gronwald, M. Ikeda, S. Shinkai and D. N. Reinhoudt, *Tetrahedron*, 2000, **56**, 9595–9599.

41. R. Wang, C. Geiger, L. Chen, B. Swanson and D. G. Whitten, *J. Am. Chem. Soc.*, 2000, **122**, 2399–2400.

42. P. Terech, R. Ramasseul and F. Volino, *J. Colloid Interface Sci.*, 1983, **91**, 280–282.

43. Y. Lin and R. G. Weiss, *Macromolecules*, 1987, **20**, 414–417.

44. T. Ishi-i, R. Iguchi, E. Snip, M. Ikeda and S. Shinkai, *Langmuir*, 2001, **17**, 5825–5833.

45. R. Mukkamala and R. G. Weiss, *Langmuir*, 1996, **12**, 1474–1482.

46. Y. Lin, B. Kachar and R. G. Weiss, *J. Am. Chem. Soc.*, 1989, **111**, 5542–5551.

47. K. Murata, M. Aoki, T. Nishi, A. Ikeda and S. Shinkai, *J. Chem. Soc., Chem. Commun.*, 1991, 1715–1718.

48. J. H. Jung, O. Yoshiyuka and S. Shinkai, *Tetrahedron Lett.*, 1999, **40**, 8395–8399.

49. M. de Loos, J. H. van Esch, R. M. Kellogg and B. L. Feringa, *Tetrahedron*, 2007, **63**, 7285–7301.

50. K. J. C. van Bommel, C. van der Pol, I. Muizebelt, A. Friggeri, A. Heeres, A. Meetsma, B. L. Feringa and J. H. van Esch, *Angew. Chem. Int. Ed.*, 2004, **43**, 1663–1667.

51. J. F. Miravet and B. Escuder, *Org. Lett.*, 2005, **7**, 4791–4794.

52. K. Hanabusa, H. Fukui, M. Suzuki and H. Shirai, *Langmuir*, 2005, **21**, 10383–10390.

53. K. Hanabusa, Y. Matsumoto, T. Miki, T. Koyama and H. Shirai, *J. Chem. Soc., Chem. Commun.*, 1994, 1401–1402.

54. E. J. de Vries and R. M. Kellogg, *J. Chem. Soc., Chem. Commun.*, 1993, 238–240.

55. D. Ranganathan, C. Lakshmi, V. Haridas and M. Gopikumar, *Pure Appl. Chem.*, 2000, **72**, 365–372.

56. M. George, G. Tan, V. T. John and R. G. Weiss, *Chem. Eur. J.*, 2005, **11**, 3243–3254.

57. J. van Esch, F. Schoonbeek, M. de Loos, H. Kooijman, A. L. Spek, R. M. Kellogg and B. L. Feringa, *Chem. Eur. J.*, 1999, **5**, 937–950.

58. M. de Loos, J. H. van Esch, R. M. Kellogg and B. L. Feringa, *Angew. Chem. Int. Ed.*, 2001, **40**, 613–616.

59. Y. Jeong, K. Hanabusa, H. Masunaga, I. Akiba, K. Miyoshi, S. Sakurai and K. Sakurai, *Langmuir*, 2005, **21**, 586–594.

60. J. Brinksma, B. L. Feringa, R. M. Kellogg, R. Vreeker and J. H. van Esch, *Langmuir*, 2000, **16**, 9249–9255.

61. M. de Loos, A. Friggeri, J. van Esch, R. M. Kellogg and B. L. Feringa, *Org. Biomol. Chem.*, 2005, **3**, 1631–1639.

62. F. S. Schoonbeek, J. H. van Esch, R. Hulst, R. M. Kellogg and B. L. Feringa, *Chem. Eur. J.*, 2000, **6**, 2633–2643.

63. J. H. van Esch, R. M. Kellogg and B. L. Feringa, *Tetrahedron Lett.*, 1997, **38**, 281–284.

64. R. A. Koevoets, R. M. Versteegen, H. Kooijman, S. A. L., R. P. Sijbesma and E. W. Meijer, *J. Am. Chem. Soc.*, 2005, **127**, 2999–3003.

65. S. van der Laan, B. L. Feringa, R. M. Kellogg and J. van Esch, *Langmuir*, 2002, **18**, 7136–7140.

66. K. Yabuuchi, E. Marfo-Owusa and T. Kato, *Org. Biomol. Chem.*, 2003, **1**, 3464–3469.

67. O. Colombani and L. Bouteiller, *New J. Chem.*, 2004, **28**, 1373–1382.

68. Q. Wei and S. L. James, *Chem. Commun.*, 2005, 1555–1556.

69. B. Xing, M. Choi, Z. Zhou and B. Xu, *Langmuir*, 2002, **18**, 9654–9658.

70. B. G. Xing, M. F. Choi and B. Xu, *Chem. Commun.*, 2002, 362–363.

71. T. Becker, C. Y. Goh, F. Jones, M. J. McIldowie, M. Mocerino and M. I. Ogden, *Chem. Commun.*, 2008, 3900–3902.

72. A. R. Hirst and D. K. Smith, *Chem. Eur. J.*, 2005, **11**, 5496–5508.

73. H. Maeda, Y. Haketa and K. Nakashima, *J. Am. Chem. Soc.*, 2007, **129**, 13661–13674.

74. K. Hanabusa, Y. Maesaka, M. Suzuki, M. Kimura and H. Shirai, *Chem. Lett.*, 2000, 1168–1169.

75. P. C. Andrews, P. C. Junk, M. Massi and M. Silberstein, *Chem. Commun.*, 2006, 3317–3319.

76. K. Kuroiwa, T. Shibata, A. Takada, N. Nemoto and N. NKimizuka, *J. Am. Chem. Soc.*, 2004, **126**, 2016–2021.

77. G. Mieden-Gundert, L. Klein, M. Fisher, F. Vögtle, K. Heuzé, J. Pozzo, M. Vallier and F. Fages, *Angew. Chem. Int. Ed.*, 2001, **40**, 3164–3166.

78. N. Pilpel, *Chem. Rev.*, 1963, **63**, 221–234.

79. P. Terech, D. Pasquier, V. Bordas and C. Rossat, *Langmuir*, 2000, **16**, 4485–4494.

80. P. Terech, V. Rodriguez, J. D. Barnes and G. B. McKenna, *Langmuir*, 1994, **10**, 3406–3418.

81. L. Marton, J. W. McBain and R. D. Vold, *J. Am. Chem. Soc.*, 1941, **63**, 1990–1993.

82. M. G. Page and G. G. Warr, *J. Phys. Chem. B*, 2004, **108**, 16983–16989.

83. M. George, G. P. Funkhouser and R. G. Weiss, *Langmuir*, 2008, **24**, 3537–3544.

84. Z. Zhou, Y. Georgalis, W. Lian, J. Li, R. Xu and B. Chu, *J. Colloid Interface Sci.*, 1987, **116**, 473–484.

85. S. A. Joshi and N. D. Kulkarni, *Chem. Commun.*, 2009, 2341–2343.

86. M. Aoki, K. Murata and S. Shinkai, *Chem. Lett.*, 1991, **20**, 1715–1718.

87. M. Aoki, K. Nakashima, H. Kawabata, S. Tsutsui and S. Shinkai, *J. Chem. Soc., Perkin Trans. 2*, 1993, 347–354.

88. S. Shinkai, *Tetrahedron*, 1993, **49**, 8933–8968.

89. B. Xing, M. Choi and B. Xu, *Chem. Eur. J.*, 2002, **8**, 5028–5032.

90. I. Odriozola, I. Loinaz, J. A. Pomposo and H. J. Grande, *J. Mater. Chem.*, 2007, 4843–4845.

91. M. Enomoto, A. Kishimura and T. Aida, *J. Am. Chem. Soc.*, 2001, **123**, 5608–5609.

92. M. Shirakawa, N. Fujita, T. Tani, K. Kaneko and S. Shinkai, *Chem. Commun.*, 2005, 4149–4151.

93. A. Y. Tam, K. M. Wong, G. Wang and V. W. Yam, *Chem. Commun.*, 2007, 2028–2030.

94. Y. Zhao, J. B. Beck, S. J. Rowan and A. M. Jamieson, *Macromolecules*, 2004, **37**, 3529–3531.

95. W. Weng, J. B. Beck, A. M. Jamieson and S. J. Rowan, *J. Am. Chem. Soc.*, 2006, **128**, 11663–11672.

96. S. J. Rowan and J. B. Beck, *Faraday Discuss.*, 2005, **128**, 43–53.

97. P. Terech, C. Rossat and F. Volino, *J. Colloid Interface Sci.*, 2000, **227**, 363–370.

98. F. M. Menger and K. L. Caran, *J. Am. Chem. Soc.*, 2000, **122**, 11679–11691.

99. D. J. Pochan, Z. Chen, H. Cui, K. Hales, K. Qi and K. L. Wooley, *Science*, 2004, **306**, 94–97.

100. E. Davies, *Chem. World*, 2006, **3**, 46–50.

101. A. R. Hirst, B. Escuder, J. F. Miravet and D. K. Smith, *Angew. Chem. Int. Ed.*, 2008, **47**, 8002–8018.

102. Z. M. Yang, K. M. Xu, L. Wang, H. W. Gu, H. Wei, M. J. Zhang and B. Xu, *Chem. Commun.*, 2005, 4414–4416.

103. J. F. Miravet and B. Escuder, *Chem. Commun.*, 2005, 5796–5798.

104. Z. Yang, H. Gu, Y. Zhang, L. Wang and B. Xu, *Chem. Commun.*, 2004, 208–209.

105. E. Carretti, L. Dei and R. G. Weiss, *Soft Matter*, 2005, **1**, 17–22.

106. B. Adhikari, G. Palui and A. Banerjee, *Soft Matter*, 2009, **5**, 3452–3460.

107. M. C. Etter, *Acc. Chem. Res.*, 1990, **23**, 120–126.

108. J. Bernstein, R. E. Davis, L. Shimoni and N.-L. Chang, *Angew. Chem. Int. Ed. Engl.*, 1995, **34**, 1555–1573.

109. M. C. Etter and J. C. MacDonald, *Acta Cryst. B.*, 1990, **46**, 256–262.

110. M. J. Kamlet, J. L. M. Abboud, M. H. Abraham and R. W. Taft, *J. Org. Chem.*, 1983, **48**, 2877–2887.

111. M. C. Etter and T. W. Panunto, *J. Am. Chem. Soc.*, 1988, **110**, 5896–5897.

112. M. C. Etter, Z. Urbañczyk Lipkowska, M. Zia-Ebrahimi and T. W. Panunto, *J. Am. Chem. Soc.*, 1990, **112**, 8415–8426.

113. L. S. Reddy, S. K. Chandran, S. George, N. J. Babu and A. Nangia, *Cryst. Growth. Des.*, 2007, **7**, 2675–2690.

114. L. S. Reddy, S. Basavoju, V. R. Vangala and A. Nangia, *Cryst. Growth. Des.*, 2006, **6**, 161–173.

115. A. A. Caraculacu and S. Coseri, *Prog. Polym. Sci.*, 2001, **26**, 799–851.

116. D. P. N. Satchell and R. S. Satchell, *Chem. Soc. Rev.*, 1975, **4**, 231–250.

117. S. Ozaki, *Chem. Rev.*, 1972, **72**, 457–496.

118. J. H. Saunders and R. J. Slocombe, *Chem. Rev.*, 1948, **43**, 203–218.

119. H. Eckert and B. Forster, *Angew. Chem. Int. Ed. Engl.*, 1987, **26**, 894–895.

120. H. J. Twitchett, *Chem. Soc. Rev.*, 1974, **3**, 209–230.

121. K. Ninomiya, T. Shioiri and S. Yamada, *Tetrahedron*, 1974, **30**, 2151–2157.

122. R. Custelcean, P. Remy, P. V. Bonnesen, D. Jiang and B. A. Moyer, *Angew. Chem. Int. Ed.*, 2008, **47**, 1866–1870.

123. C. R. Bondy, P. A. Gale and S. J. Loeb, *J. Am. Chem. Soc.*, 2004, **126**, 5030–5031.

124. L. S. Evans, P. A. Gale, M. E. Light and R. Quesada, *New J. Chem.*, 2006, **30**, 1019–1025.

125. B. Schazmann and D. Diamond, *New J. Chem.*, 2007, **31**, 587–592.

126. D. R. Turner, E. C. Spencer, J. A. K. Howard, D. A. Tocher and J. W. Steed, *Chem. Commun.*, 2004, 1352–1353.

127. V. Amendola, D. Esteban-Gmez, L. Fabbrizzi and M. Licchelli, *Acc. Chem. Res.*, 2006, 343–353.

128. L. Applegarth, A. E. Goeta and J. W. Steed, *Chem. Commun.*, 2005, 2405–2406.

129. R. Custelcean, B. A. Moyer and B. P. Hay, *Chem. Commun.*, 2005, 5971–5973.

130. B. Wu, J. Liang, J. Yang, C. Jia, X.-J. Yang, H. Zhang, N. Tang and C. Janiak, *Chem. Commun.*, 2008, 1762–1764.

131. R. Custelcean, V. Sellin and B. A. Moyer, *Chem. Commun.*, 2007, 1541–1543.

132. R. Custelcean and B. A. Moyer, *Eur. J. Inorg. Chem.*, 2007, 1321–1340.

133. M. Alajarín, A. López-Lázaro, A. Pastor, P. D. Prince, J. W. Steed and R. Arakawa, *Chem. Commun.*, 2001, 169–170.

134. M. Alajarín, A. Pastor, R. Orenes and J. W. Steed, *J. Org. Chem.*, 2002, **67**, 7091–7095.

135. M. Alajarín, A. Pastor, R. Orenes, J. W. Steed and R. Arakawa, *Chem. Eur. J.*, 2004, **10**, 1383–1397.

136. Y. L. Cho, D. M. Rudkevich and J. Rebek Jr., *J. Am. Chem. Soc.*, 2000, **122**, 9868–9869.

137. J. Rebek Jr. and R. K. Castellano, *J. Am. Chem. Soc.*, 1998, **120**, 3657–3663.

138. C. E. Stanley, N. Clarke, K. M. Anderson, J. A. Elder, J. T. Lenthall and J. W. Steed, *Chem. Commun.*, 2006, 3199–3201.

139. M. de Loos, A. G. J. Ligtenbarg, J. H. van Esch, H. Kooijman, A. L. Spek, R. Hage, R. M. Kellogg and B. L. Feringa, *Eur. J. Org. Chem.*, 2000, 3675–3678.

140. G. R. Desiraju, *Angew. Chem. Int. Ed.*, 1995, **34**, 2311–2327.

141. M.-O. M. Piepenbrock, G. O. Lloyd, N. Clarke and J. W. Steed, *Chem. Commun.*, 2008, 2644–2646.

142. L. Carlucci, G. Ciani and D. M. Proserpo, *Cryst. Eng. Comm.*, 2003, **5**, 269–279.

143. S. J. Cantrill, K. S. Chichak, A. J. Peters and J. F. Stoddart, *Acc. Chem. Res.*, 2005, **38**, 1–9.

144. K. S. Chichak, S. J. Cantrill and J. F. Stoddart, *Chem. Commun.*, 2005, 3391–3393.

145. C. D. Meyer, C. S. Joiner and J. F. Stoddart, *Chem. Soc. Rev.*, 2007, **36**, 1705–1723.

146. A. J. Peters, K. S. Chichak, S. J. Cantrill and J. F. Stoddart, *Chem. Commun.*, 2005, 3394–3396.

147. K. S. Chichak, A. J. Peters, S. J. Cantrill and J. F. Stoddart, *J. Org. Chem.*, 2005, **70**, 7956–7962.

148. J. Li, L. Song and S. Du, *Inorg. Chem. Commun.*, 2007, **10**, 358–361.

149. R. Liantonio, P. Metrangolo, F. Meyer, T. Pilati, W. Navarrini and G. Resnati, *Chem. Commun.*, 2006, 1819–1821.

150. X. Lin, J. Jia, X. Zhao, K. M. Thomas, A. J. Blake, G. S. Walker, N. R. Champness, P. Hubberstey and M. Schrder, *Angew. Chem. Int. Ed. Engl.*, 2006, **45**, 7358–7364.

151. J. L. C. Rowsell and O. M. Yaghi, *Angew. Chem. Int. Ed.*, 2005, **44**, 4670–4679.

152. S. L. James, *Chem. Soc. Rev.*, 2003, **32**, 276–288.

153. E. J. Cussen, J. B. Claridge, M. J. Rosseinsky and C. J. Kepert, *J. Am. Chem. Soc.*, 2002, **124**, 9574–9581.

154. W. J. Belcher, C. A. Longstaff, M. R. Neckenig and J. W. Steed, *Chem. Commun.*, 2002, 1602–1603.

155. L. Applegarth, N. Clark, A. C. Richardson, A. D. M. Parker, I. Radosavljevic-Evans, A. E. Goeta, J. A. K. Howard and J. W. Steed, *Chem. Commun.*, 2005, 5423–5425.

156. L. Dobrzańska, H. G. Raubenheimer and L. J. Barbour, *Chem. Commun.*, 2005, 5050–5052.

157. X. Zhang, C. Guo, Q. Yang, W. Wang, W. Liu, B. Kang and C. Su, *Chem. Commun.*, 2007, 4242–4244.

158. X. Zhang, C. Guo, Q. Yang, T. Lu, Y. Tong and C. Su, *Chem. Mater.*, 2007, **19**, 4630–4632.

159. Z. Lu, L. Wen, J. Yao, H. Zhu and Q. Meng, *Cryst. Eng. Comm.*, 2006, **8**, 847–853.

160. L. Dobrzańska, G. O. Lloyd, T. Jacobs, I. Rootman, C. L. Oliver, M. W. Bredenkamp and L. J. Barbour, *J. Mol. Struct.*, 2006, **796**, 107–113.

161. D. R. Turner, B. Smith, E. C. Spencer, A. E. Goeta, I. Radosavljevic-Evans, D. A. Tocher, J. A. K. Howard and J. W. Steed, *New J. Chem.*, 2005, **29**, 90–98.

162. W. Jaunky, M. W. Hosseini, J. M. Planeix, A. D. Cian, N. Kyritsakas and J. Fischer, *Chem. Commun.*, 1999, 2313–2314.

163. Y. Cui, S. J. Lee and W. Lin, *J. Am. Chem. Soc.*, 2003, **125**, 6014–6015.

164. L. Han and M. Hong, *Inorg. Chem. Commun.*, 2005, **8**, 406–419.

165. L. Carlucci, G. Ciani, D. M. Proserpo and S. Rizzato, *Chem. Commun.*, 2000, 1319–1320.

166. D. Xiao, Y. Li, E. Wang, L. Fan, H. An, Z. Su and L. Xu, *Inorg. Chem.*, 2007, **46**, 4158–4166.

167. C. J. Kepert, T. J. Prior and M. J. Rosseinsky, *J. Am. Chem. Soc.*, 2000, **122**, 5158–5168.

168. A. Jouaiti, M. W. Hosseini and N. Kyritsakas, *Chem. Commun.*, 2003, 472–473.

169. M. Barboiu, G. Vaughan, R. Graff and J. Lehn, *J. Am. Chem. Soc.*, 2003, **125**, 10257–10265.

170. B. Moulton and M. J. Zaworotko, *Chem. Rev.*, 2001, **101**, 1629–1658.

171. J. L. Atwood, L. J. Barbour, M. J. Hardie and C. L. Raston, *Coord. Chem. Rev.*, 2001, **222**, 3–32.

172. G. O. Lloyd, J. L. Atwood and L. J. Barbour, *Chem. Commun.*, 2005, 1845–1847.

173. J. M. Russell, A. D. M. Parker, I. Radosavljevic-Evans, J. A. K. Howard and J. W. Steed, *Cryst. Eng. Comm.*, 2006, **8**, 119–122.

174. D. R. Turner, B. Smith, A. E. Goeta, I. Radosavljevic-Evans, D. A. Tocher, J. A. K. Howard and J. W. Steed, *Cryst. Eng. Comm.*, 2004, **6**, 633–641.

175. D. K. Kumar, D. A. Jose, A. Das and P. Dastidar, *Chem. Commun.*, 2005, 4059–4061.

176. N. N. Adarsh, D. K. Kumar and P. Dastidar, *Tetrahedron*, 2007, **63**, 7386–7396.

177. M. Tiliakos, P. Cordopatis, A. Terzis, C. P. Raptopoulou, S. P. Perlepes and E. Manessi-Zoupa, *Polyhedron*, 2001, **20**, 2203–2214.

178. F. Kyriakidou, A. Panagiotopoulos, S. P. Perlepes and E. Manessi-Zoupa, *Polyhedron*, 1996, **15**, 1031–1034.

179. S. Kawano, N. Fujita, K. J. C. van Bommel and S. Shinkai, *Chem. Lett.*, 2003, **32**, 12–13.

180. M. M. Coleman, K. H. Lee, D. J. Skrovanek and P. C. Painter, *Macromolecules*, 1986, **19**, 2149–2157.

181. M. M. Coleman, M. Sobkowiak, G. J. Pehlert and P. C. Painter, *Macromol. Chem. Phys.*, 1997, **198**, 117–136.

182. H. E. Gottlieb, V. Kotlyar and A. Nudelman, *J. Org. Chem.*, 1997, **62**, 7512–7515.